SYNTHESIS AND SURFACE MODIFICATION STUDIES OF BIOMEDICAL POLYURETHANES TO IMPROVE LONG TERM BIOCOMPATIBILITY

A THESIS SUBMITTED TO
THE GRADUATE SCHOOL OF NATURAL AND APPLIED SCIENCES
OF
MIDDLE EAST TECHNICAL UNIVERSITY

BY

EDA AYŞE AKSOY

IN PARTIAL FULFILLMENT OF THE REQUIREMENTS
FOR
THE DEGREE OF DOCTOR OF PHILOSOPHY
IN
POLYMER SCIENCE AND TECHNOLOGY

JULY 2008

Approval of the thesis:

SYNTHESIS AND SURFACE MODIFICATION STUDIES OF BIOMEDICAL POLYURETHANES TO IMPROVE LONG TERM BIOCOMPATIBILITY

submitted by **EDA AYŞE AKSOY** in partial fulfillment of the requirements for the degree of **Doctor of Philosophy in Polymer Science and Technology Department, Middle East Technical University** by,

Prof. Dr. Canan Özgen _____
Dean, Graduate School of **Natural and Applied Sciences**

Prof. Dr. Cevdet Kaynak _____
Head of Department, **Metallurgical and Materials Engineering Dept.**

Prof. Dr. Nesrin Hasırcı _____
Supervisor, **Chemistry Dept., METU**

Examining Committee Members:

Prof. Dr. Duygu Kısakürek _____
Chemistry Dept., METU

Prof. Dr. Nesrin Hasırcı _____
Chemistry Dept., METU

Prof. Dr. Erdal Bayramlı _____
Chemistry Dept., METU

Prof. Dr. Kezban Ulubayram _____
Faculty of Pharmacy, Hacettepe University

Assoc. Prof. Dr. Göknur Bayram _____
Chemical Engineering Dept., METU

Date: 4.07.2008

I hereby declare that all information in this document has been obtained and presented in accordance with academic rules and ethical conduct. I also declare that, as required by these rules and conduct, I have fully cited and referenced all material and results that are not original to this work.

Name, Last name: Eda Ayşe Aksoy

Signature:

ABSTRACT

SYNTHESIS AND SURFACE MODIFICATION STUDIES OF BIOMEDICAL POLYURETHANES TO IMPROVE LONG TERM BIOCOMPATIBILITY

Aksoy, Eda Ayşe

Ph.D., Department of Polymer Science and Technology

Supervisor: Prof. Dr. Nesrin Hasırcı

July 2008, 167 pages

Thrombus formation and blood coagulation is a major problem associated with blood contacting products such as catheters, vascular grafts and artificial hearts. An intense research is being conducted towards the synthesis of new hemocompatible materials and modifications of surfaces with biological molecules. In this study, polyurethane (PU) films were synthesized in medical purity from diisocyanate and polyol without using any other ingredients and the chemical, thermal and mechanical properties were characterized by solid state NMR, FTIR, GPC, mechanical tests, DMA and TGA. The surfaces of PU films were modified by covalent immobilization of different molecular weight heparins; low molecular weight heparin (LMWH) and unfractionated heparin (UFH) and these surfaces were examined by ESCA, ATR-FTIR, AFM and contact angle goniometer. Cell adhesion studies were conducted with whole human blood and examined by SEM. The effects of different types of heparins on blood protein adsorption and on platelet adhesion were analyzed by electrophoresis and SEM, respectively. The surfaces of the UFH immobilized polyurethane films (PU-UFH)

resulted in lesser red blood cell adhesion in comparison to LMWH immobilized polyurethane film surfaces (PU-LMWH). When the PU films were treated with blood plasma, the surfaces modified with two different heparin types showed a clearly different protein adsorption behavior especially in the early stage of blood plasma interaction. PU-LMWH samples showed about three times less protein adsorption compared to PU-UFH samples. The morphologies of platelets adhered on material surfaces demonstrated differences; such as PU-UFH had clusters with some pseudopodia extensions, while PU-LMWH had round shaped platelets with little clustering. PU surfaces modified by immobilization of LMWH and UFH, demonstrated promising results for the improvement of non-thrombogenic devices and surfaces.

Keywords: Polyurethane, Surface Modification, Heparin Immobilization, Protein Adsorption.

ÖZ

UZUN SÜRELİ BİYOUYUMLULUĞUN GELİŞTİRİLMESİ AMACIYLA BİYOMEDİKAL POLİÜRETANLARIN SENTEZİ VE YÜZEY MODİFİKASYONU ÇALIŞMALARI

Aksoy, Eda Ayşe

Doktora, Polimer Bilimi ve Teknolojisi Bölümü

Tez Yöneticisi: Prof. Dr. Nesrin Hasırcı

Temmuz 2008, 167 sayfa

Trombi oluşumu ve kan pıhtılaşması kanla temas eden katater, damar ve yapay kalp gibi ürünlerde karşılaşılan en büyük problemdir. Kan ile uyumlu yeni malzemelerin sentezi ve yüzeylerinin biyolojik moleküller ile modifiye edilmesi konularında yoğun araştırmalar yapılmaktadır. Bu çalışmada medikal saflıkta poliüretan (PU) filmler diizosiyanat ve poliolden başka hiçbir katkı maddesi kullanılmadan sentezlenmiş ve bu filmlerin kimyasal, termal ve mekanik özellikleri katı NMR, FTIR, GPC, mekanik test cihazı, DMA ve TGA ile karakterize edilmiştir. PU filmlerin yüzeyi farklı molekül ağırlığındaki heparinler; düşük molekül ağırlıklı heparin (LMWH) ve fraksiyonlanmamış heparin (UFH) kullanılarak kovalent immobilizasyon ile modifiye edilmiş ve bu yüzeyler ESCA, ATR-FTIR, AFM ve temas açısı gonyometresi ile incelenmiştir. Hücre yapışması çalışmaları total insan kanı ile yapılmış ve SEM ile görüntülenmiştir. Farklı türdeki heparinli yüzeylere kan proteini adsorpsiyonu ve platelet yapışması sırasıyla elektroforez ve SEM ile incelenmiştir. UFH immobilize

edilmiş poliüretan filmlerin yüzeylerinde (PU-UFH), LMWH immobilize edilmiş poliüretan film yüzeylerine (PU-LMWH) göre daha az sayıda kırmızı kan hücresi yapışması görülmüştür. PU filmler kan plazması ile temas ettirildiğinde iki farklı heparin türü ile modifiye edilmiş yüzeyler arasında özellikle temasın erken basamağında protein yapışması yönünden belirgin fark gözlenmiştir. PU-LMWH örneklerinde, PU-UFH örneklerine göre üç kat az protein adsorplanması gözlenmiştir. Malzeme yüzeylerine yapışan plateletler farklı morfolojiler göstermiştir. PU-UFH kümelenmiş ve yayılmış platelet morfolojilerine sahipken, PU-LMWH de az kümelenme ve yuvarlak, yayılmamış plateletler olmuştur. LMWH ve UFH immobilize edilerek modifiye edilen PU yüzeyleri, trombi oluşturmayan cihazların ve yüzeylerin geliştirilmesi için olumlu sonuçlar göstermiştir.

Anahtar Kelimeler: Poliüretan, Yüzey Modifikasyonu, Heparin İmmobilizasyonu, Protein Adsorpsiyonu.

To my family...

ACKNOWLEDGEMENTS

I would like to express my special thanks to my supervisor Prof. Dr. Nesrin Hasırcı for her continuous guidance, encouragement, motivation and support during all the stages of my thesis. I sincerely appreciate the time and effort she has spent to improve my experience during my graduate years.

I am also deeply thankful to Prof. Dr. Vasıf Hasırcı for his support, leadership and guidance in our METU-BIOMAT Biomaterials and Tissue Engineering Research Group.

My sincere acknowledgements go to my thesis progress committee members, Prof. Dr. Erdal Bayramlı and Prof. Dr. Kezban Ulubayram for their helpful comments and suggestions throughout this thesis.

I am thankful for their support and understanding of Prof. Dr. Çiğdem Erçelebi and Prof. Dr. Hayrettin Yücel through out all the stages of my graduate years.

I am grateful to Prof. Dr. Claudio Migliaresi and Prof. Dr. Antonella Motta for their guidance during the stage of blood compatibility studies at Trento University, Italy. Also, I am thankful to Dr. Mariangela Fedel for her help and friendship during the experiments at Trento University.

I would like to thank to METU Central Laboratory for DMA, TGA, GPC, ESCA and Solid State NMR analysis and the Central Laboratory staff for their support provided during these characterization studies. I am also thankful to Pınar Zorlutuna and Erkin Aydın for their help during AFM analysis, İsmail Doğan Günbaş and Tuğba

Endoğan for SFE analysis. Assoc. Prof. Necati Özkan and Prof. Dr. İskender Yılgör are acknowledged for their suggestions in DMA examinations and polyurethane characterizations.

I deeply thank all the members of METU-BIOMAT group and my special lab mates Tuğba Endoğan, Aysel Kızıltay, Cantürk Özcan, İsmail Doğan Günbaş and Taylan Özerkan, for the good memories, continuous help and support during my experiments.

I would like to thank to two kind people, Assist. Prof. Dr. Burcu Akata Kurç and Kübra Kamışoğlu for being my good friends and perfect research partners.

My special friends Leyla Molu, Elif Kemeröz, Bengi Aran, Serap Tekin, Elif Vargün are kindly acknowledged for their continuous motivation and support.

This study was supported by METU-BAP 2005-07-02-00-92 and FP6 European Network of Excellence project EXPERTISSUES and these grants are gratefully acknowledged.

Finally, I would like to thank to my mother Prof. Dr. Serpil Aksoy, my father Atila Aksoy and my brother Salih Can Aksoy and my grandmother Hatice Coşkun, for the love and patience they have shown through out all my life.

TABLE OF CONTENTS

LIST OF TABLES

TABLES

LIST OF FIGURES

FIGURES

ABBREVIATIONS

AA	Acrylic Acid
AB	Acid-Base
AFM	Atomic Force Microscopy
Apo-A1, Apo-E	Apolipoprotein E A1, Apolipoprotein E
AT-III	Antitrombin III
ATR	Attenuated Total Reflectance
CHDI	Cyclohexane Diisocyanate
CPMAS	Cross Polarization Magic Angle Spinning
DMA	Dynamic Mechanical Analysis
E	Young's Modulus
E′	Storage Modulus
E″	Loss Modulus
EAB	Elongation at Break
EDC	Ethyl carbodiimide hydrochloride
ESCA	Electron Spectroscopy for Chemical Analysis
ESEM	Environmental Scanning Electron Microscope
Fn	Fibronectin
Fng	Fibrinogen
FTIR	Fourier Transform Infrared Spectroscopy
GPC	Gel Permeation Chromatography
GPIb, GPIIb, GPIIIa	Glycoproteins
HDI	Hexamethylene Diisocyanate
HI	Heterogeneity index
HSA	Human Serum Albumin

IPDI	Isophorone Diisocyanate
LMWH	Low Molecular Weight Heparin
MDI	Methylene Diphenyl Diisocyanate
Mn	Number Average Molecular Weight
Mw	Weight Average Molecular Weight
MW	Molecular Weight
NDI	Naphthalene-1,5-diisocyanate
NMR	Nuclear Magnetic Resonance
OWRK	Owens, Wendt, Rabel and Kaelble
PBS	Phosphate Buffer Saline
PDI	Phenylene Diisocyanate
PPP	Platelets Poor Plasma
PRP	Platelets Rich Plasma
PU	Polyurethane
PU-AA	Acrylic Acid Grafted Polyurethane
PU-PLASMA	Oxygen Plasma Treated Polyurethane
PU-LMWH	Low Molecular Weight Heparin Immobilized Polyurethane
PU-UFH	Unfractionated Heparin Immobilized Polyurethane
SDS	Sodium Dodecyl Sulfate
SEM	Scanning Electron Microscope
TDI	Toluene Diisocyanate
Tg	Glass Transition Temperature
TMXDI	Tetramethylxylene diisocyanate
UTS	Ultimate Tensile Strength
Vn	Vitronectin
vWF	von Willebrand Factor
XDI	Xylene diisocyanate

CHAPTER 1

INTRODUCTION

1.1 Polyurethanes

Polyurethanes were discovered in 1937 by Bayer and the research on the synthesis of polyurethanes has gained great importance since the World War II [1]. They are the class of polymers that contain urethane groups in their backbone structures (Figure 1).

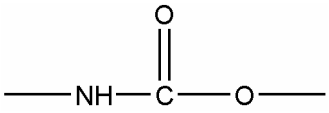

Figure 1 Urethane group

Polyurethanes are a very diverse family of polymers capable of exhibiting a wide range of properties changing from smooth elastomeric membranes to rigid bulk structures depending on their molecular composition. They can be prepared in different forms, including foam, fiber, film, tube, resin, elastomer etc. and therefore have found applications in various areas [2].

1.1.1 Basic Polyurethane Synthesis

Polyurethanes are generally obtained by condensation reaction of diisocyanates and polyhydroxy compounds (polyols) as shown in Figure 2 [3].

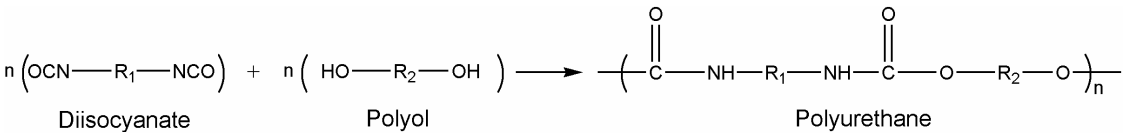

Figure 2 Condensation reaction of diisocyanate and polyol.

In the preparation of polyurethanes, the compounds containing amino and carboxyl groups or organic halides and metal cyanides may also be used [3]. These reactions are summarized in Figure 3.

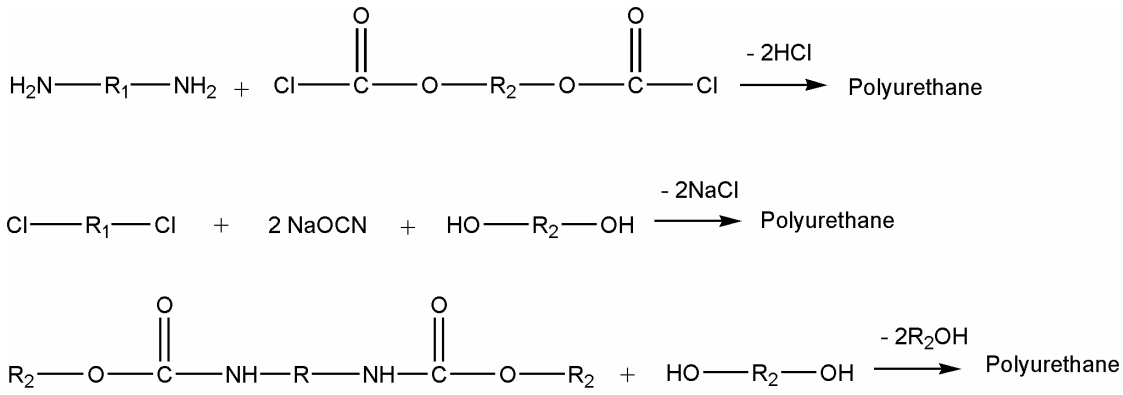

Figure 3 Various reactions for polyurethane synthesis.

1.1.2 Raw Materials for Polyurethanes

Polyurethanes are usually produced by the reaction of a di or polyfunctional isocyanates, with di or polyhyroxyl compounds. Since the chemistry and functionality of the hydroxyl containing reactant (polyol) or the isocyanate can be varied, a wide range of branched or crosslinked polymers with different properties can be obtained.

1.1.3 Isocyanates

The most common commercial method used to produce isocyanates is the phosgene-based process. Free amines are reacted with excess phosgene in an inert organic solvent at low temperature; the resulting slurry of carbamoyl chlorides and amine hydrochloride is then heated at elevated temperature in the presence of excess phosgene to give the desired isocyanates [4]. The overall reaction scheme is shown in Figure 4.

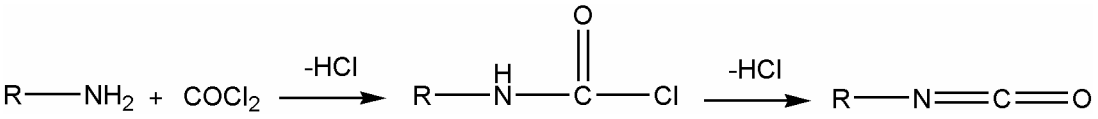

Figure 4 Isocyanate synthesis reaction.

Isocyanates have very reactive N=C=O groups and undergo addition reaction across the carbon-nitrogen double bond. These groups react with a large number of compounds such as amines, alcohols, carboxylic acids and even with themselves [3, 5]. Isocyanate components can have aromatic and aliphatic groups.

Aromatic isocyanates are most widely used in the production of both flexible and rigid polyurethane foam coatings, adhesives, elastomers and fibers. Polyurethanes obtained from aromatic diisocyanates undergo slow oxidation in the presence of air and light, causing discoloration. Reactivity of isocyanates depends on their chemical structures and aromatic isocyanates are more reactive than aliphatic ones. The presence of electron withdrawing substituents on the isocyanate molecule increases the partial positive charge on the isocyanate carbon atom and moves the negative charge farther away from the site of reaction. This makes the transfer of the electron from the donor substance to the carbon easier, thus causing a faster reaction. On the other hand, the presence of electron-donating substituents on isocyanate compounds can cause slower

reactions. Bulky groups in the ortho positions of aromatic isocyanates, and bulky and branched groups in the aliphatic isocyanates retard the reaction because of steric hindrance. In the reactions of diisocyanates, the reactivity of the second isocyanate decreases significantly after the first has been reacted. The difference in the reactivities is less if the two isocyanates belong to different aromatic rings or are separated with an aliphatic chain [3, 6]. Commonly used aromatic isocyanates are listed in Table 1.

Toluene diisocyanate (TDI) and 4,4′-methylene diphenyl diisocyanate (MDI) are the most widely used isocyanates in the manufacture of polyurethanes. TDI, which is colorless liquid, is almost always used as a mixture of 2,4 and 2,6 isomers, usually as a 80:20 mixture and obtained by phosgenation of aniline-formaldehyde-derived polyamines. Boiling point of TDI is around 120°C at 10mmHg and the vapor pressure of it is $2{,}3 \times 10^{-3}$ mmHg at 25°C. MDI is solid, melting at 37°C, has a tendency to dimerize at room temperature. MDI has a lower vapor pressure (10^{-5}mmHg at 25°C) than TDI. MDI is generally used in elastomer and rigid foam production. Naphthalene-1,5-diisocyanate (NDI) is commonly used in the production of high grade elastomers.

Aliphatic diisocyanates are used in the production of color stable polyurethanes, although it is necessary to add antioxidants and UV-stabilizers to formulation to maintain the physical properties by time. The least costly aliphatic diisocyanate is 1,6-hexamethylene diisocyanate (HDI), which is a colorless liquid and less reactive than both TDI and MDI. The use of HDI leads to urethane polymers with better resistance to discoloration, hydrolysis and heat degredation than TDI. Hexamethylene diisocyanate (HDI), tetramethylxylene diisocyanate (TMXDI) and isophorone diisocyanate (IPDI) are used for aliphatic polyurethane synthesis. Tetramethylxylene diisocyanate (TMXDI) and dicyclohexylmethane diisocyanate (H_{12}MDI) are important in the production of non-discoloring polyurethanes, used in industry for surface coating [3, 6]. The most widely used aliphatic diisocyanates are listed in Table 2.

Table 1 List of aromatic diisocyanates.

Name	Structure
Toluene 2,4-diisocyanate (TDI)	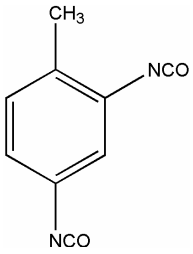
Toluene 2,6-diisocyanate (TDI)	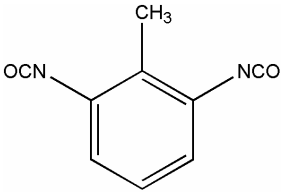
4,4'-methylene diphenyl diisocyanate (MDI)	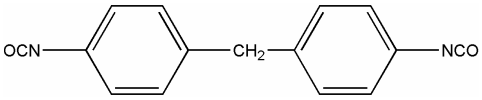
2,4'-methylene diphenyl diisocyanate	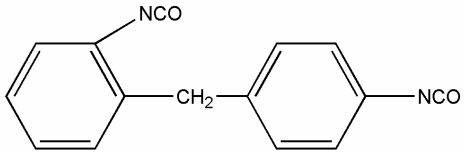
p-phenylene diisocyanate (PDI)	
Naphthalene-1,5-diisoyanate (NDI)	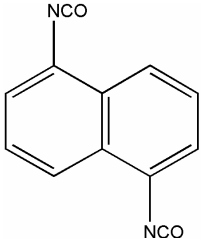

Table 2 List of aliphatic diisocyanates.

Name	Structure
1,6-hexamethylene diisocyanate (HDI)	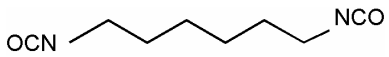
m-tetramethylxylene diisocyanate (m-TMXDI)	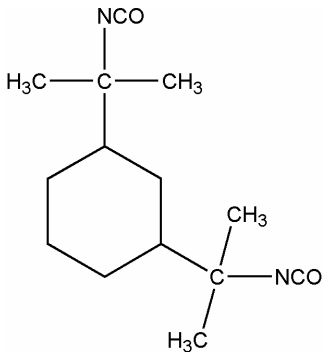
Isophorone diisocyanate (IPDI)	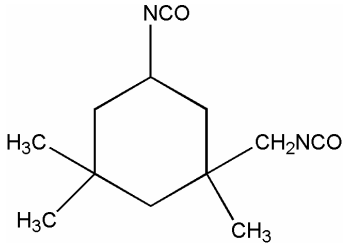
4,4'-dicyclohexylmethane diisocyanate (H_{12}MDI)	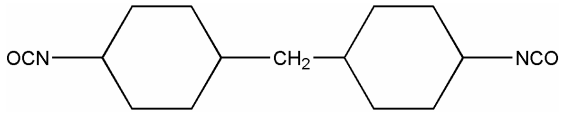
1,4-cyclohexane diisocyanate (CHDI)	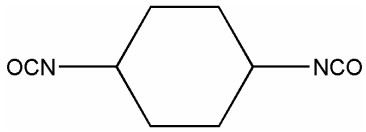
Bis(isocyanatomethyl)cyclo-hexane (H_6XDI, DDI)	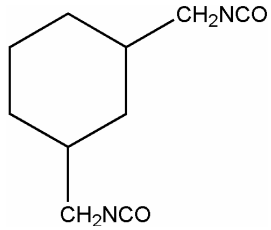

1.1.4 Reactions of Isocyanates

Isocyanates have highly unsaturated -N=C=O groups and react with both electron donor and electron acceptor functional groups due to cumulative double bonds. They react vigorously with hydroxyl, amino, carboxyl groups and water at low temperatures. Isocyanates react more easily with primary hydroxyl groups than secondary hydroxyl groups to form urethanes. They also react with amino groups to form substituted urea and in these reactions primary amino groups have higher reactivity than secondary ones. Reactions of isocyanates with carboxylic acids form amide linkages while fast reactions with water form amines [3]. These reactions are known as primary reactions of isocyanates and given in Figure 5.

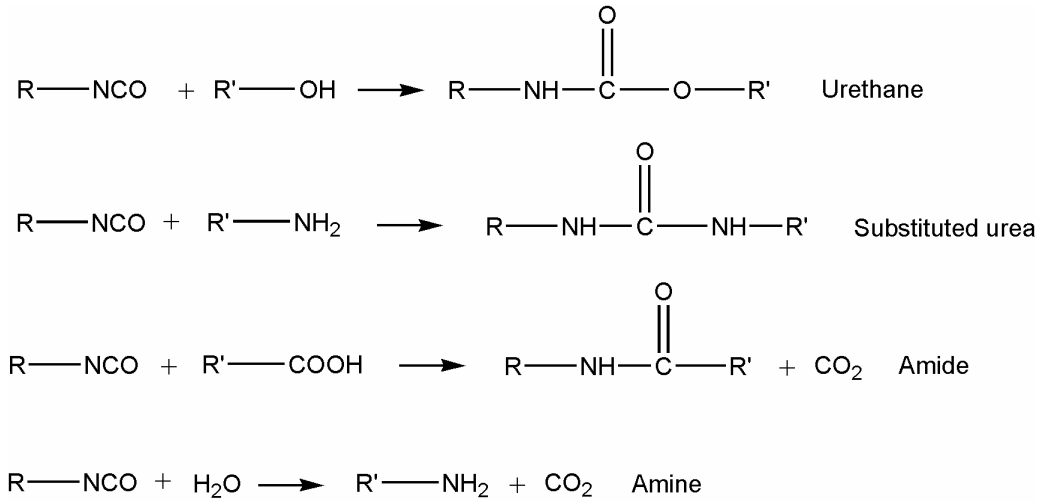

Figure 5 The primary reactions of isocyanates.

Reactions of isocyanates with carboxylic acid and water produce carbon dioxide gas and this cause foaming. In elastomer synthesis, foaming is undesirable and therefore all the reactants and the systems used in polyurethane synthesis need to be dried throughly.

Isocyanates can go further reactions with urethanes, ureas, amides or with themselves forming allophanates, substituted biureates, acryl ureas and isocyanurates respectively. These are known as secondary reactions and are shown in Figure 6 [3].

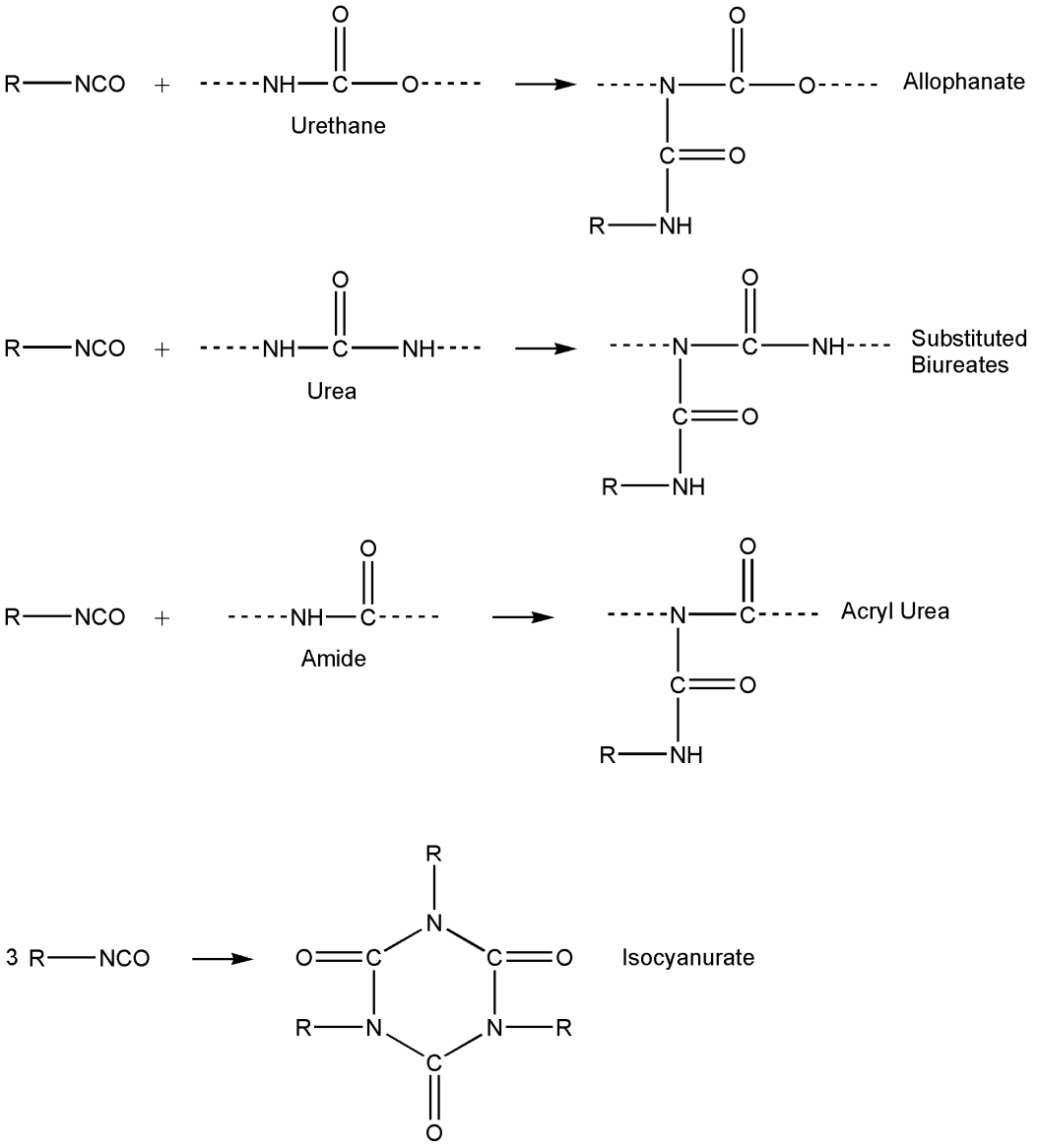

Figure 6 The secondary reactions of isocyanates.

These secondary reactions of isocyanate lead to crosslinking, and the resulting polyurethane becomes insoluble and infusible. Thus the temperature control during polyurethane synthesis is critical to control secondary reactions and crosslinking.

At ordinary temperatures up to 50°C isocyanates reacts with hydroxyl groups to produce urethanes, but at higher temperatures up to 150°C, secondary reactions to give allophanates, substituted biureates, isocyanurates takes place at a significant rates. If linear polyurethane is desired, then the application of the lowest temperature is required. If high crosslinking and branching through secondary reactions is needed higher temperatures (50-150°C) should be applied. At about 150°C phenolic polyurethanes start to decompose and around 220°C aliphatic polyurethanes decompose [2, 7]. Decomposition yields free isocyanates, alcohols, free amines, olefins and carbondioxide.

Polyisocyanates are also very reactive substances. As a result, the reaction between polyisocyanates and polyhydroxyl compounds is complicated by presence of moisture. The presence of water first causes formation of unstable carbamic acid, which then disintegrates into amine and carbon dioxide. The formation of gas gives rise to foam production. Further reaction between amine and isocyanate leads to the formation of urea and substituted biureate groups as shown in Figure 6.

1.1.5 Polyols

The most widely used polyhydroxy compounds (polyols) in polyurethane synthesis are hydroxyl-terminated polyether or polyester glycols with molecular weights in the range of 400-5000. Polyether polyols are addition products derived from cyclic ethers and are easily designed when the polarity of backbone is important. They are high molecular weight polymers that range from viscous liquids to waxy solids, depending on structure and molecular weight. The most commercial polyether polyols are based on less expensive ethylene or propylene oxide or on combination of the two. Polyurethanes

prepared with polyether polyols can be hydrophilic or hydrophobic or react to water at all levels and in general they are hydrolytically more stable compared to polyester polyols. Therefore polyethers are used in the design and the development of biocompatible and hemocompatible devices in which biodegradation is not a desired property. The most commonly used polyols are polyethylene glycol and polypropylene glycol. Their structures are given in Figure 7 [7, 8].

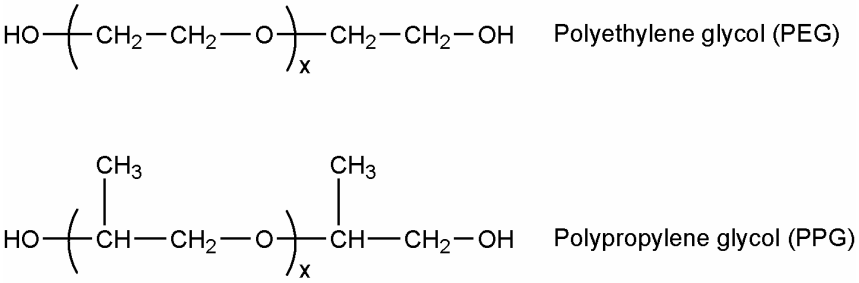

Figure 7 Chemical structures of polyethylene glycol and polypropylene glycol.

Polyester polyols are based on saturated aliphatic or aromatic carboxylic acids and diols or mixtures of diols. For elastomers, linear polyester polyols of molecular weight 2000 are prefered. Branched polyester polyols, formulated from higher functional glycols, are used for foam and coating applications. Polyester based polyurethanes undergo rapid hydrolysis when implanted in the human body, so they are most widely used in tissue engineering applications in the preperation of biodegradable materials. [7, 8]. Polyester polyol structure is shown in Figure 8.

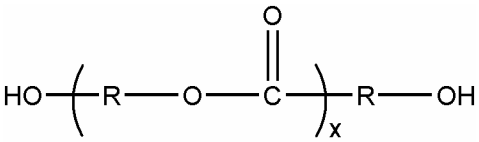

Figure 8 Chemical structure of polyester polyol.

1.1.6 Polyurethane Elastomers

Polyurethane elastomers cover a very wide range of polyurethanes, classified according to the method of manufacture. The main types are, beside milliable polyurethane elastomers, cast polyurethane elastomers and thermoplastic polyurethane elastomers. Other types are the relatively high density elastomeric foams and the elastomeric spandex fibres [7, 9].

In some cases the elastomeric properties derive from the crosslinking of rubbery polymer chains with low Tg values and in conventional elastomers usually physical crosslinks are important. These arise from the two phase nature of most polyurethane elastomers, which consist of block copolymer molecules consisting elastomeric, or soft block of aliphatic ester units or of aliphatic ether units; and more rigid, or hard blocks containing a high urethane content, such as those formed by reaction of TDI or MDI with an active diol [7, 9].

The development of necessary cross-linking in elastomers also depends on the reaction of some isocyanate groups with atmospheric moisture to form urea groups, which react with other isocyanate groups to form biuret crosslinks. In order to obtain the required amount of crosslinking, formulations with at least one component having more than two reactive end groups are necessary [3, 7, 9].

1.1.7 Segmented Structure of Polyurethane Elastomers

Polyurethane elastomers are block polymers composed of flexible glycol ‘soft segments’ and rigid urethane ‘hard segments’. The soft segments (~1500 nm) are most often comprised of polyester or polyether macroglycols and the hard segments (~150 nm) are formed from the chain extension of diisocyanate linkages with low molecular weight diols. The hard and soft segments are combined end-to-end through covalent urethane bonds, therefore polyurethanes are classified as multiblock copolymers. The

differences in polarity between the hard and soft segments render these regions incompatible and the result is that they do not mix on a molecular level, producing a microphase separated structure. The hard segment domains are generally semi-crystalline and provide stiffness, reinforcement to the polyurethane. The soft segment domains are responsible for elastic behavior and are usually amorphous with a Tg below room temperature [7, 10]. The chemical and physical segregation of segments in polyurethane structure is shown in Figure 9.

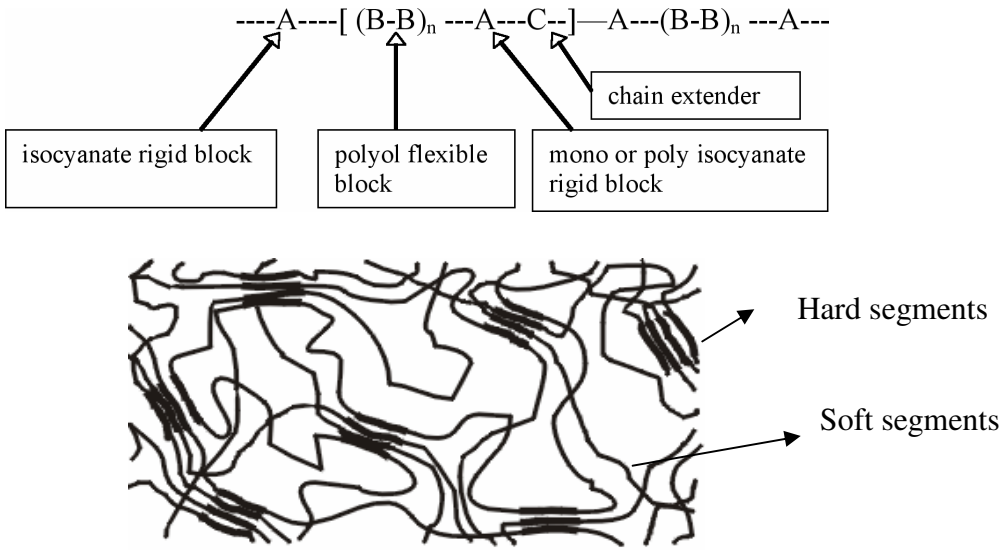

Figure 9 Chemical and physical segregation of segments in polyurethane structure.

There are large numbers of chemical and structural factors which play important roles in microphase separation or phase mixing. Important factors that influence morphology of polyurethanes include [11]:

1. Chemical structure, number average molecular weight and molecular weight distribution of soft segments.
2. Chemical structure and symmetry of the diisocyanate compound.
3. Chemical structure of the chain extender.

4. Average chain length and length distribution of hard segments.
5. Hard/soft segment ratio in the copolymer.
6. Crystallizability of hard and soft segments.
7. Extent of competitive hydrogen bonding between hard–hard and hard–soft segments.
8. Inherent solubility between hard and soft segments.
9. Method/polymerization procedure used during the synthesis (can be a one-step or two-step prepolymer formation methods).
10. The nature of the interfacial region between the soft segment matrix and hard segment domains.

In general longer block lengths lead to higher degrees of phase segregation and more perfect hard segment domains. Higher hard segment content result in more hard segments mixed into soft phase. Polyester soft segments are usually more compatible with urethane hard segments, then with polyether soft segments. This due to the fact that the strength and degree of hard segment-soft segment hydrogen binding is greater for the ester carbonyl group than the ether oxygen.

Polyurethanes based on aromatic reactants show generally better phase segregation than those synthesized from aliphatic ones. Phase segregation in polyurethanes is strongly affected by temperature. Raising the temperature of a polymer system induces phase mixing. Subsequent cooling causes phase segregation, leading to the original morphology.

1.1.8 Polyurethane Production Processes

Polyurethanes can be prepared by two processes: prepolymer method and one-shot method. In prepolymer method, a linear polyhydroxy compound reacts with excess isocyanate to form an intermediate polymer called "prepolymer". The prepolymer is viscous liquid or low-melting solid. It is then converted into final high molecular

weight polymer by further reaction with a small molecular weight diol or diamine chain extender. The process is two steps. In the first step, a prepolymer with an isocyanate end group of moderate molecular weight is prepared. In the second step, the prepolymer is reacted with active hydrogen containing groups in the polymer chain to give allophanate branch points. If the polymer chain contains urea groups, it will form biureate branch points. When both urea and urethane groups are present, biureate branch points are predominant. Thus, a great variety of structures in the polymer chain are exist depending on the nature, the molecular weight and the proportion of diols and diisocyanates [3].

The 'one-shot' method, is simplest method by simultaneous reaction of polyol, isocyanate and chain extender. The mixture when it is still liquid is taken in to molds for casting. In order to obtain rubber elasticity, the reactants should be chosen with proper functionality and proper amounts to produce cross-linked network structure. Relatively simple linear polymers may be obtained by using compounds with two active groups; diisocyanates and diols. In each polymerization reaction, secondary reactions can take place to a certain extent. Polyurethanes, in addition to urethane groups, contain urea, ester and ether groups with aromatic rings. These groups affect the properties of the resultant polymer [3].

1.1.9 Structure – Mechanical Property Relation of Polyurethanes

Mechanical properties of polyurethane elastomers are directly related to the extent of hard and soft segment domain segregations. Depending on the chain length of these diols or glycols the properties of the polyurethanes change. Polyol gives the high flexibility to the backbone of network chains. On the other hand, isocyanate and chain extender components give rigidity to the chain. Since the functionality of the macroglycol, or the isocyanate can be changed, a wide variety of branched or cross-linked polymers can be formed. Generally, elastomers are synthesized from long chain,

high molecular weight polyols. Physical and mechanical properties of polyurethanes can be explained in terms of their morphological structures [3, 12].

Soft segment chemical composition, molecular weight, degree of phase mixing affect elongation, modulus and tensile strength. Increasing the soft segment molecular weight at fixed hard segment length, creates polyurethanes with lower tensile strength, lower modulus, higher elongation and causes a decrease in Tg due to decreased tendency of the soft segment to crystallize and increased tendency for the hard segment to be isolated in the soft segment matrix. Increasing hard segment content at constant soft segment content with constant molecular weight, results increase in crystallinity, increase in hard segment crystalline melting temperature, increase in tensile strength and modulus, decrease in ultimate elongation and enhanced mixing of the continuous and dispersed phase leading increase in Tg. The structure-property behavior of polyurethanes are mostly determined by diisocyanate symmetry and hydrogen bond strength [12].

1.1.10 Applications of Polyurethanes

Polyurethanes have very wide diversity in industrial applications due to wide range of polyurethane types from flexible and rigid polyurethane foams to elastomers and fibers. As rigid polyurethane foams, applications can be given as; thermal insulation of buildings, refrigerators, deep freeze equipment, pipelines and storage tanks, packaging, furniture, house appliances, etc. The flexible foam applications in industry are; household furniture, automotive seating, textile laminates. Semi-rigid and low density structural foam applications are; steering wheels, headrests and other automotive interior trim components, furniture elements, sports goods such as skis and surf boards. Industrial applications of polyurethane elastomers are; shoe soles, vehicle body panels, rollers and gear wheels, conveyors, sealants for the construction and automotive industries. Although polyurethanes are used in a very wide area, the ones obtained from aromatic diisocyanates undergo slow oxidation in the presence of air and light, causing

discoloration. Aliphatic diisocyanates have growing application in thermoplastic polyurethanes [2, 3].

1.2 Biomaterials

Devices made of synthetic or natural materials have been used in medical area and introduced into human body since the early 1950s at an increasing rate. Synthetic polymers are the most widely used ones since they have significant contribution to the effectiveness of health care. They are used in a variety of implants or other supporting materials (e.g. vascular grafts, artificial hearts, intraocular lenses, joints, mammary prostheses, sutures); in utilization of extracorporeal therapeutics and other supporting devices (e.g. hemodialysis, hemoperfusion, blood oxygenation, intravenous lines, needle catheters, blood-bags), in controlled release systems (e.g. transdermal drug delivery patches, microspheres, microcapsules for targeted drug-delivery devices for different routes of administration), and clinical diagnostic assays (mainly as carriers and supporting materials) [13]. When any material is implanted into the body or used in contact with the body fluids, it should be compatible with the biological environment, so that it should be 'biomaterial'.

Biomaterial is defined as; any substance (other than a drug) or combination of substances, synthetic or natural in origin that is used in contact with living tissue and biological fluids for prosthetic, diagnostic, therapeutic applications, and storage of blood and its components, without adversely affecting the biological constituents of the entire living organism [14]. The biocompatibility of a material with tissue include both local biological compatibility which is seen over various time periods following implantation and systemic compatibility which implies no propogated effect to tissue remote from the site implantation [15].

It is important to stress that the biocompatibility requirements a biomaterial has to fulfill depend strictly on the specific host environment. In the case of devices for blood

contacting applications, such as vascular grafts, artificial heart valves, total artificial heart, haemodialysis equipment, stents, etc., biocompatibility is related to the reciprocal interactions between the materials and complex body fluid such as blood. On the otherhand compatibility of a contact lens mostly depend on the host reactions taking place between the material and cornea cells or proteins exist in the tear.

1.2.1 Polyurethanes as Biomaterials

The polyurethanes are among the best choices for biomedical applications because of their desired mechanical properties due to their segmented polymeric character, their availability in wide range of physical properties and their excellent blood and tissue compatibility. These materials played an important role in the development of many medical devices ranging from catheters to total artificial hearts. Table 3 gives some current biomedical applications of polyurethanes [8].

Table 3 Current biomedical application areas of polyurethanes.

Blood bags, closures, fittings	Leaflet heart valves
Blood oxygenation tubing	Mechanical heart valve coatings
Breast prostheses	Orthopedic splints, bone adhesives
Cardiac assist pump bladders, tubing, coatings	Percutaneous shunts
Catheters	Reconstructive surgery materials
Dental cavity liners	Skin dressing and tapes
Endotracheal tubes	Surgical drapes
Heart pacemaker connectors, coatings	Suture materials
Hemodialysis tubing, membranes, connectors	Synthetic bile ducts
Lead insulators, fixation devices	Vascular grafts and patches

Due to exhibiting high flexure endurance, high strength, and inherent non-thrombogenic characteristics, segmented polyurethane elastomers, have a maximum impact in medical prostheses and appear to have promising applications in the cardiovascular area, where chronic, non-thrombogenic interfacing with blood is the main importance.

The first biomedical grade polyether polyurethane was synthesized by Boretos and Pierce [16]. It was reported that the material composed of urea hard segments and polyether soft segments sustained high modulus of elasticity, biocompatibility, resistance to flex-fatigue and excellent stability over long implantation periods. In 1970s and 1980s, polyurethanes recognized as the blood contacting materials of cardiovascular devices and their long term applications were accepted. Nylias synthesized a blood compatible polyurethane-co-polydimethyl siloxane and used this copolymer in heart assist balloon pumps [17].

The research and discussions on blood compatible materials had contradictory results. Lelah et. al. reported that materials having higher surface soft segment concentration are more thromboresistant [18], while in contrast Hanson et. al reported that platelet consumption decreased as the percentage of surface carbon atoms forming hydrocarbon bonds increased [19]. Research on the artificial heart, carried out at Termedics, Inc., U.S.A., has focused on the segmented polyurethane elastomers. Various types of artificial hearts; fibrillated total artificial heart, hybrid total artificial heart, and total replacement artificial hearts were studied since the years of 1960s. The research was carried to reduce the size of artificial heart. In the year of 1998 two types of artificial hearts; undulation pump total artificial heart and flow transformed pulsatile artificial heart were designed and to prevent ring thrombus, a jellfish polyurethane membrane valve was developed [20]. Polyurethane blood veins have still not found a common use because of the unsolved lack of long–term resistance to degradation.

An intense research is still going on the development of new designs and production methods of different kinds of catheters as well as improvement of their surface compatibilities through different modification techniques. There are studies on polyurethane vascular catheters coated with antithrombin (ATH) complex [21] or grafted with zwitterionic sulfobetaine monomer [22] for the targets of thrombogenicity or therapeutic purposes. Stent designs and stent coatings are also studied by researchers for the same reason. Polyurethaneurea films were synthesized on vascular stents by different methods. Solvent evaporation, plasma application are commonly used techniques. It was reported that good adhesion of polyurethane films on the stent surfaces were achieved by using a combination of plasma and toluene diisocyanate treatment [23]. Different surface alterations methods (heparin, aluminium and polyurethane coatings as well as mechanical polishing, passivation and electropolishing techniques) were applied to nitinol stents by Tepe and Schmehl [24]. They reported that sandblasting, electropolishing and aluminium covering decreased activation of the coagulation cascade after 120 min of blood contact and the lowest thrombogenic potential was found in the polyurethane-coated stent group.

A double-layered NiTi-S stent which consists of inner polyurethane layer and outer uncovered nitinol wire tube was developed by Verschuur et al. [25]. The NiTi-S stent provides symptomatic relief of malignant dysphagia. Low-profile valved self-expanding stent made of polyurethane was designed to circumvent size restrictions of percutaneous heart valves and modified for the treatment of abdominal and thoracic aortic aneurysms served as delivery device [26].

Application of polyurethanes as wound dressing materials or porous scaffolds for tissue engineering in the forms biodegradable or injectable structures leads to new developments. Biodegradable polyurethane synthesis is also gained importance in the last decades especially for scaffold design. Biodegradation properties and biological mechanisms were reported for in vivo applications [27, 28]. Polyurethanes are

frequently used as wound dressing materials because of their good barrier properties and high oxygen permeabilities. The electrospun nanofibrous PU membranes were prepared by Khil et.al as possible candidates for wound dressings [29]. Immediate adherence to wet wound surface, fast epithelization and well organized dermis formation was reported when these membranes were applied [30]. The effect of bovine collagen dressing TissueFascie^{R} and polyurethane film dressing OpSite^{R} were compared on burn wounds and it was reported that both dressings did not cause any significant risk of infection but the collagen membrane attached directly to the wound surface functions as a collagen substrate to promote epidermal-dermal regeneration, and it may therefore be more effective in promoting wound healing than polyurethane film dressing. To clarify the efficiency of polyurethane wound dressings, they were compared with a hydrogel wound dressing and it was given that PU dressings were better in the wound healing time, amount of exudates, and frequency of dressing changes [31].

Polyurethanes also used as coverage for silicone gel breast implants. The first use was in 1970's and some contradictory results were reported [32, 33]. It was also reported that these prosthesis represented a great advance in avoiding capsular contracture after studying over a thousand polyurethane-covered implants [34]. Smahel [35] and Barone et al. [36] described the histological aspects of polyurethane-covered breast implants and they reported that polyurethane surface was effective creating capsules in the implants and polyurethane cause a body reaction most probably by degrading and producing some undesired side effects. Researchers mostly work on the enhancement of bio-stability of polyurethanes for in vivo long term applications [37 - 39].

There is intense research in the production of biodegradable and bioresorbable polyurethanes for in tissue engineering applications. Linear poly(ester-ether urethane)s with different hydrophilic characters were synthesized from L-lysine diisocyanate and block copolymers of poly(ε-caprolactone)-poly(ethyleneoxide)-poly(ε-caprolactone)

macrodiols, for tissue engineering applications [40]. Polycaprolactone-polyurethane composite scaffolds for vascular tissue engineering were synthesized by Williamson et.al [41]. These scaffolds were produced by electrospinning of polyurethane onto the back of the wet spinned polycaprolactone fibres. Marcos-Fernandez et. al synthesized and characterized a series of biodegradable non-toxic poly(urethane-urea)s based on polycaprolactone diols of different molecular weights and two different amino acid chain extenders, namely ethyl ester of L-lysine or L-ornithine which are good candidates for the biodegradability of scaffolds [42]. In the recent years biodegradable lysine based polyurethanes have an important platform as bone cements for bone tissue engineering implants. Muh et. al synthesized lysine-urethanedimethacrylate monomer from addition of hydroxyethylmethacrylate to lysinediisocyanate [43]. They observed good adhesion of osteoblasts on polymerized cement. Bonzani et al. synthesised a polyurethane-based injectable, in situ curable polymer to determine its potential uses as bone cements [44]. Films of the polymers were prepared by reacting pentaerythritol-based DL-lactic acid/ethyl lysine diisocyanate and pentaerythritol-based glycolic acid prepolymers where β-tricalcium phosphate was incorporated to improve mechanical properties. These injectable polymers showed appropriate bonding strength and mechanical support to be used as bone cements and provided a favorable in vitro environment for initial cell adhesion, maintained cell viability, and normal rates of proliferation of human osteoblasts. Investigation of the viability of elastomeric polyurethanes for total-joint arthroplasty devices was carried out by Schwartz and Bahadur [45]. Elastomeric polyurethane Pellethane^{TM}, which is currently used in non-orthopedic biomedical applications, was tested for wear and and it was reported that its wear rate was much lower than that of ultra high molecular weight polyethylene (UHMWPE), likely due to its ability to conform to the counterface and thus reduce the contact pressure.

In different applications, antibacterial PU is obtained by either coating the polyurethane with silver [46, 47] or by silver particle impregnation [48]. Using silver ion loaded

zeolites as antibacterial agents offer an advantage over the other methods since silver ions are more effective than metallic silver atoms. For this purpose, different types of zeolite micro particles were synthesized and Ag^+ was added by ion-exchange process. These antibacterial zeolite particles were incorporated into PU prepolymer which was prepared from its main components of toluene diisocyanate and polypropylene-ethylene glycol in medical purity. Microbiological tests revealed that the composites, either prepared by adding Ag^+ containing zeolite Beta or zeolite A in PU matrix, had antibacterial property [49].

Polyurethanes and polyurethane composites can be used in many different areas of the body to support or heal the desired region. Properties of the materials such as durability, elasticity, elastomer-like character, fatigue resistance, compliance, and acceptance or tolerance in the body during healing are associated with the chemical composition and the production and modification techniques of polyurethanes.

1.3 Surface Modification of Biomaterials

There are various chemical (oxidation), physical (patterning), biological (heparinization), electromagnetic radiation (plasma glow discharge) techniques used to modify surfaces of materials to create more biocompatible and hemocompatible devices. Therefore, it is more economical to modify the materials with satisfying mechanical properties rather than the development of new materials.

The human body's acceptance of synthetic polymers is highly complex, and most polymers have a tendency to form surface thrombus. The thromboresistancy of the elastomeric polyurethanes is subject to many complex factors such as polymer surface composition, device configuration, and blood flow characteristics. Polyurethanes have shown as materials with high blood compatibility in numerous devices, but still their blood compatibility needs to be examined, controlled and improved. The capacity of

polyurethanes to undergo modifications increases their suitability for biomedical applications [8, 50].

1.3.1 Plasma Surface Modification

Surface modification of vascular and cardiac implants as well as other medical devices by use of glow discharge plasma application is a concept studied in the last decades. The process has many consequent steps and depends on various factors including the geometrical shape of the reaction chamber, type and power of electrical discharge, type and flow rate of gas used, properties of substrate, etc. Generally radiofrequency energy is applied at low pressures for the surface modifications. The generated plasma contains free electrons, radicals, excited atoms and neutral particles. Constant bombardment of the substrate surface with these active particles leads to breaking some bonds of the surface molecules, and react with them by forming new bonds. Therefore, a chemical change on the surface about 30 Å occurs while the bulk structure of the substrate stays intact. Depending on the type the gas used, it becomes possible to change hydrophilicity of the surface or create a coat having completely different than the bulk structure. Most generally used gases are oxygen, nitrogen, argon, or various monomeric substances [8].

1.4 Blood Compatibility

Blood compatibility is a special case of biocompatibility, and comprehends many interlinked aspects as thrombogenicity, complement activation, leukocytes activation and changes in plasma proteins [51]. Blood compatibility (hemocompatibility) is defined as the ability of an artificial substrate not to activate the intrinsic blood coagulation system or not to attract or alter platelets or leucocytes [8].

1.4.1 Biomaterial - Blood Interaction

Thrombus formation is major and unresolved problem associated with blood contacting devices such as catheters, grafts, and artificial hearts [8, 21]. When these devices come in contact with blood the first event which takes place in the first few seconds is the adsorption of blood proteins at the solid-liquid interface. Composition of the adsorbed protein layer usually changes with a complex process as a function of exposure time [52]. In this process; the adsorbed proteins can change their tertiary structure, and the proteins with stronger adsorption activity subsequently can replace with the first adsorbed proteins [53]. Depending on the composition and the conformation of this residing protein layer, the interaction of platelets, the activation of intrinsic coagulation, the adhesion and aggregation of platelets and the activation of complement system can take place [52]. More specifically, the adsorbed fibrinogen and other platelet adhesion-stimulating proteins support irreversible platelet adhesion and activation, which promotes the formation of white thrombus. In addition to platelet adhesion, a self-amplifying cascade of molecular reactions between mutually activating blood coagulation factors is triggered at the material surface or at the surface of the adhered platelets. Final steps in the coagulation cascade include formation of thrombin, which converts fibrinogen into insoluble fibrin, from which a fibrin network and thrombi is produced [53, 54].

1.4.2 Blood Coagulation Cascade in Material Interaction

Thrombosis is the major and the most frequent complication related to cardiovascular applications. Under the physiological conditions blood contacts the endothelium, that represents a natural nonthrombogenic surface. When a lesion is produced to the vascular endothelium a thrombogenic reaction is triggered: blood components come in contact with the negatively charged sub-endothelium and, as a consequence, platelets are stimulated to adhere to the lesion area to form the so-called ‘white plug’. At the same time, the ‘tissue factor’ expressed on damaged endothelial cells at the site of

vascular injury, triggers the coagulation cascade via the 'extrinsic pathway', that finally leads to formation of a clot of mesh-organized fibrin [55].

Blood contact with a foreign surface can induce a thrombogenic reaction as well by organizing platelet adhesion and triggering the coagulation cascade through the 'intrinsic pathway' (Figure 10).

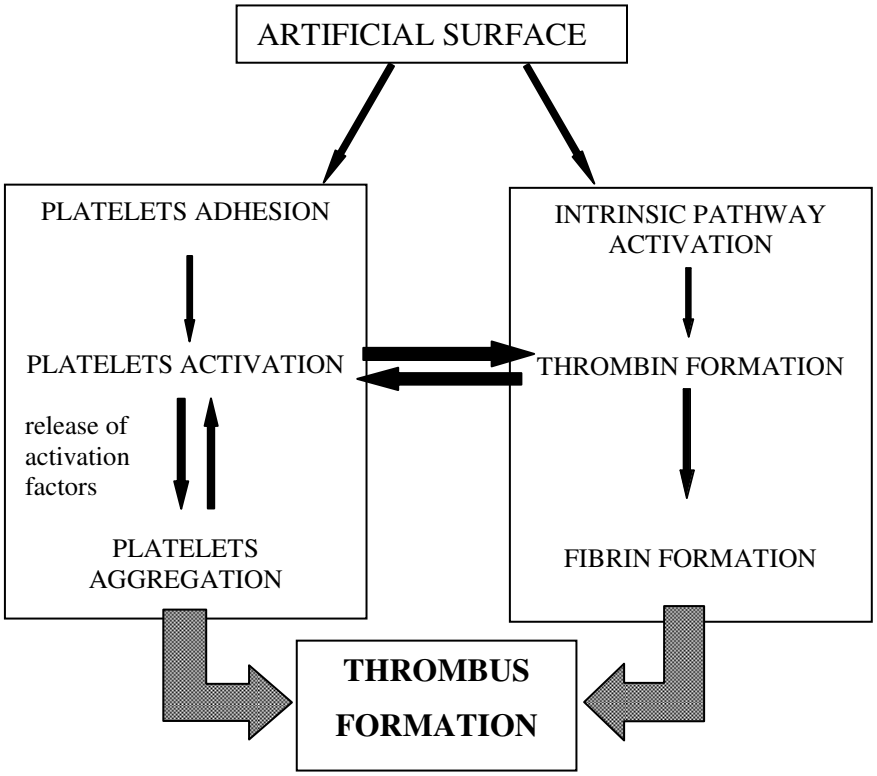

Figure 10 Events occurring after blood-material contact.

If stimulated by contact with a biomaterial, or to be more correct, by contact with the protein layer adsorbed on the biomaterial itself, platelets will adhere to the surface and become gradually activated. Upon activation, platelets change their shape, spread

around surface, release the content of their granules (ADP, platelet factor 4, thrombospondin, serotonin, fibrinogen, and other), and contribute to the generation of thromboxane A_2 and to the formation of small amounts of thrombin, that constitutes an important agonist for platelet aggregation. Activated platelets can thus bind one another trough fibrinogen bridging creating highly organized thrombi that can grow on the surface, or can detach and originate thromboembolic particles according to surface adhesiveness [56].

Following platelet activation, in parallel with platelet adhesion and activation, the coagulation cascade is initiated through the intrinsic pathway (Figure 11). The intrinsic pathway, initiated by blood-material contact activation, is triggered by activation of factors FXII (Hageman Factor), FXI, Prekallikrein and High Molecular Weight Kininogen (HMWK). At least 12 factors are involved in the coagulation process; most of them are serine protease, pro-enzymes usually circulating in plasma in an inactive form, that following surface contact or after proteolytic cleavage by other enzymes, can explicit their enzymatic action. Activation of clotting factors lead to the formation of fibrin by activation of thrombin on fibrinogen molecules. The final product of coagulation cascade is stable, insoluble fibrin polymer, produced from precursor fibrinogen by the activation of thrombin. The result is achieved through the sequential activation of a series of coagulation factors present in plasma [55].

Platelets activation/aggregation and coagulation are highly interconnected processes. Platelet phospholipidic membrane represents, in fact, an essential element where the formation of active complexes takes place during coagulation (e.g. the assembly of the prothrombinase complex, which converts prothrombin to thrombin). On the other side, the generation of thrombin itself activates platelets, which then catalyze the production of more thrombin [51]. Moreover, thrombin leads to the formation of fibrin, which stabilizes the platelet thrombus.

A schematic representation of the sequential steps involved in the coagulation cascade, inclusive of intrinsic, extrinsic and common pathways is depicted in Figure 11 [51].

It worth to stress blood contacting artificial materials can lead to not only to the formation of localized thrombi which can cause occlusion, malfunctioning of the device or other complication. If the surface of the biomaterial is thrombogenic but non-adherent, in fact, thrombi can rapidly shed from the surface where they have formed, particularly in conditions of high flow rates [51], thus causing high potentially dangerous emboli [56].

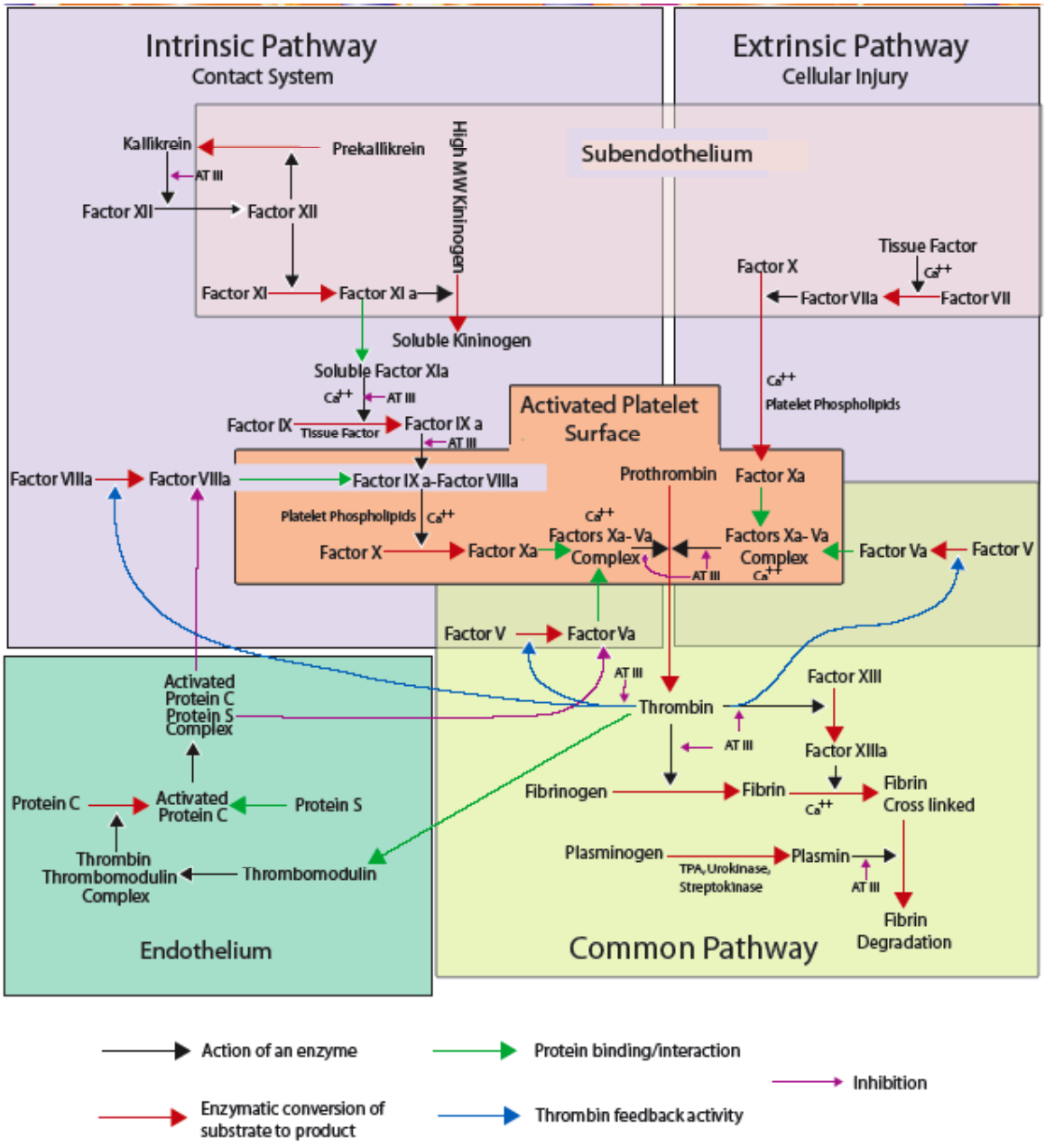

Figure 11 Schematic representation of the coagulation cascade.

1.4.3 Protein Adsorption

When a biomaterial is inserted into cardiovascular system, the first event that takes place is the adsorption of plasma proteins. With in seconds of blood-material contact the surface is covered by a layer of proteins, whose composition, relative concentration, conformation and orientation guide the subsequent host response and play a key role in determining the fate of the material. A series of biological reactions, such as platelets adhesion/activation, triggering of coagulation and complement systems, activation of leukocytes, etc., are strongly dependent upon protein adsorption. Thus, for example, adsorption of the contact phase proteins may be responsible for the activation of the intrinsic coagulation system, while adsorbed plasma proteins (fibrinogen, fibronectin, vitronectin) plays an important role on platelet activation [55, 57].

Protein absorption onto biomaterial surface from multi component solutions is dynamic multi-step process, that can be divided into different phases, as schematized in Figure 12. The process includes proteins transport (by diffusion, convection or gravity) from the bulk of the solution towards the surface, their first reversible adsorption and competition among different species through exchange phenomena. With increasing residence time, modifications of the three dimensional structure of the adsorbed proteins may take place. When adsorbed proteins experience conformational changes in their structure (time dependent molecular spreading and unfolding) their functionality may be altered. According to their structural conformation and orientation on the surface, in the fact, proteins can expose functional groups and biological active regions to the surrounding environment, promoting subsequent biological reactions (e.g. platelets or cell adhesion and activation, initiation of the coagulation cascade, activation of complement, inflammation, etc.) [58]. The stages of protein adsorption on biomaterial surface is summarized in Table 4 and schematic representation is given in Figure 12.

Table 4 The phases of protein adsorption on biomaterial surface.

Phase 1 TRANSPORT	Phase 2 ADSORPTION	Phase 3 EXCHANGE	Phase 4 DENATURATION	Phase 5 CONTINUOUS ADSORPTION
Transport of soluble protein molecules towards the surface.	Reversible binding of molecules to the surfaces.	Modification in the composition of the adsorbed layer, until a pseudo-steady state is reached.	Adsorbed proteins undergo progressive conformational changes in their three-dimensional structure.	Formation of multiple protein layers.
The process of transport is ruled by diffusion constants and concentration of the different species.	The proteins interact with the surface via intermolecular interactions (hydrophobic, electrostatic, charge-transfer)	The most rapid and concentrated species may be partially replaced with proteins with higher MW and greater surface affinity.	With increasing residence time the protein may unfold and spread on the surface. The adhesion gets strengthened and the original functionality of the proteins can be altered.	The adsorbed protein layer forms a kind of coat on the surface of biomaterial.

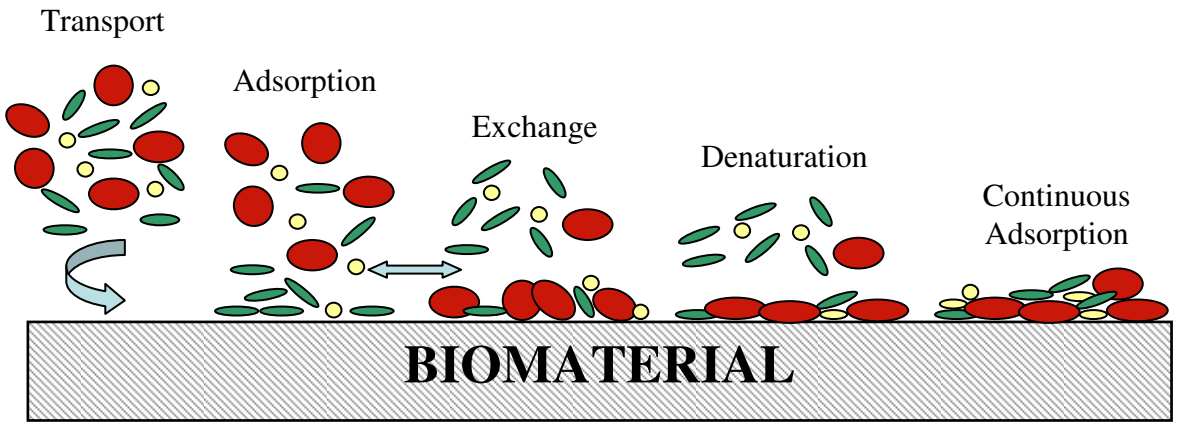

Figure 12 Different phases of protein adsorption on biomaterial surface.

Biological fluids represent highly complex examples of real multicomponent solutions. Blood plasma, in particular, contains hundreds of molecular species and more than 150 proteins, in a wide range of molecular weights, charge, structure and concentrations. Some simplifications are often required, in order to understand some functional concenpts of the protein-biomaterial interaction.

As suggested by Andrade and Hlady, about a dozen proteins ('the big twelve') is considered to dominate plasma protein adsorption, including albumin (HAS), immunoglubulins (IgG, IgA, IgM), C3 complement component, fibrinogen (Fng), haptoglobin, α1-antitrypsin, α2-macroglobulin, as well as low and high density lipoproteins. Among these, albumin, fibrinogen and to a less extent fibronectin, are assumed to have prominent role in leading blood-material interactions [59].

Human Serum Albumin (HSA) (66 kDa) is the most abundant plasma protein (35-50 mg/mL). It is a globular protein composed of three structurally similar globular domains, each of which contains two sub domains and has a net negative charge. Owing to its high concentration in plasma and to its relatively small size, HAS is usually the dominating protein at the initial stage of adsorption. Even if HAS is not involved in coagulation or platelet adhesion processes, once adsorbed it is often referred as a passivating agent, able to reduce the thrombogenic potential of the surface [60].

Fibrinogen (Fng) is a 340 kDa glycoprotein. Its structure is made up of two symmetric molecules, each formed by three polypeptide chains: Aα (63,5 kDa), Bβ (56 kDa), γ (47kDa). In physiological conditions Fng is present in human plasma with a concentration about 2.0–4.5 mg/mL. It plays a certain role in thrombogenic processes as it is converted in fibrin during coagulation and mediates the adhesion of platelets to the surfaces on which is adsorped [61, 62].

1.4.4 Platelet Biology

Platelets are anuclear, disc-shaped cells, about 2-4 μm in diameter in testing conditions. Their physiological concentration in human blood ranges from 150-400x10^6 cells/mL. Platelets are produced by megakaryocytes in the bone marrow; their mean life time is about 5–6 days. In the resting time, platelet shape is discoid and controlled by cytoskeleton. Platelets membrane plays an important role in platelet physiology. The external surface coat contains the receptors (e.g. glycoproteins GPIb and GPIIb/IIIa) that, by binding specific proteins, mediate the process of adhesion, activation and aggregation [63].

The main physiological function of platelets is to arrest blood flow injured vessels by formation of a temporary haemostatic plug, but platelet thrombotic activity can be initiated by interaction of platelets with an artificial surface as proven by frequent complications associated with cardiovascular devices. The process of platelet thrombus formation, both due to vessel injury or contact with a foreign surface, can be described as consisting three events: the first is the initial adhesion of platelets to the surface, the second is platelet spreading on the surface and the third consists in the aggregation of the platelets to form a three-dimensional thrombus [55].

1.4.5 Platelet Adhesion, Activation and Aggregation

Platelets are extremely sensitive cells that become activated by contact with any thrombogenic surface such as injured blood vessels implants and biomaterials. Platelets possess specific adhesion receptors that allow them to bind to surface. Platelet adhesion to biomaterial surfaces may be mentioned by interaction of GPIb receptor with vWF protein and GPIIb/IIIa receptor with Fng. GPIIb/IIIa is the dominant platelet receptor with 40,000-80,000 molecules per platelet, and represents the receptor for plasma proteins which support cell attachment, including Fng, Fn, Vn and vWF. Binding of platelet receptors to such adhesive proteins requires that either receptors are activated

by conformational changes, or proteins adsorped on the surface are denaturated and expose specific binding sites (Figure 13) [55, 63].

Due to its concentration in plasma and its greater adsorption rate with respect to other adhesive proteins, fibrinogen plays a key role in the process of platelets adhesion to biomaterials [61, 62]. Also its conformation and orientation upon adsorption on biomaterial affects the platelet binging sites [62, 64].

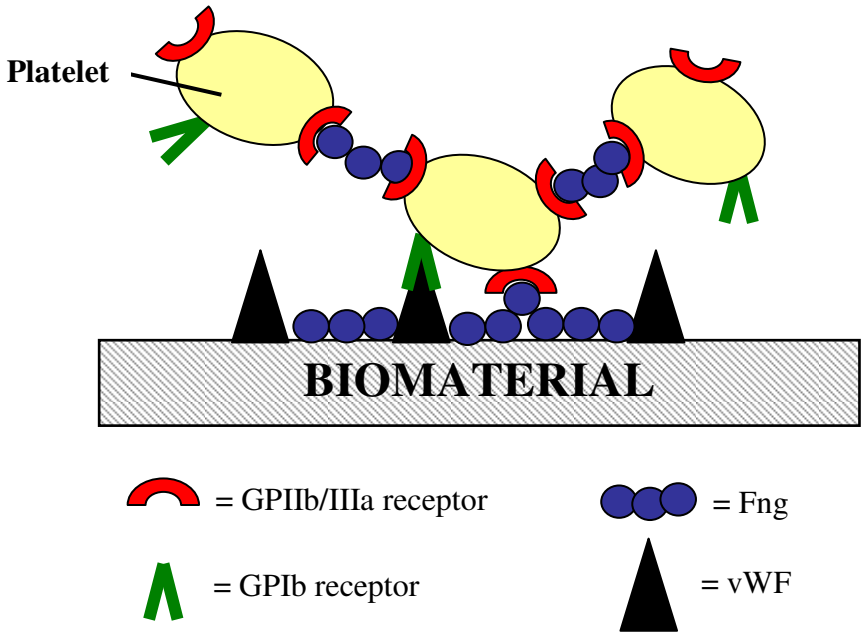

Figure 13 Platelet adhesion on biomaterial surface by binding of platelet membrane receptors to the relative adhesive protein: GPIIb/IIIa-Fng and GPIb-vWF. Fng molecule acts as bridge between activated GPIIb/IIIa receptors of adjacent platelets inducing aggregation.

The adhesion to the surface follows generation of biochemical signals, that rapidly initiates platelet activation, change of shape and degranulation. Activation causes platelets to gradually spread on the surface, changing from classical resting discoid

shape to a 'spiny sphere' shape. This process involves the contraction of cytoskeleton molecules and the polymerization of actin filaments, and implies the reorganization of plasma membrane, that will assume important procoagulant properties. The change of shape is accompanied by platelets secretion. The formation of small amounts of thrombin takes place. Activated platelets expose glycoprotein complexes GPIIb/IIIa that work as receptors for fibrinogen. Fibrinogen acts as a bridge binding adjacent platelets together and allowing the formation of thrombus-like aggregates. Formation of temporary white plug, adhered platelets and circulating platelet micro-particles contribute to the amplification of the coagulation cascade (Figure 13) [55, 61, 64].

1.4.6 Surface Properties of Materials Affecting Blood Compatibility

The severity of the host response to the implantation a cardiovascular device is strictly related to the surface properties of the biomaterial employed, as the surface is the first part that communicates with the surrounding environment.

The main responsible bodies for the initiation of biomaterial-induced thrombotic events are platelet and coagulation factors circulating in plasma. Since platelet adhesion/activation and coagulation activity are mediated by the protein layer that rapidly adsorbed onto a surface following the blood contact, it is accepted that protein adsorption plays a certain role in guiding the biological response of a biomaterial.

The adsorption phenomena that take place at the blood-material interface depend both on the properties of the protein solution and on the physico-chemical characteristics of the surface. Size, structure, concentration, charge, stability and unfolding rate are the main properties of proteins that affect their surface activity. On the other side, material physico-chemical surface characteristics such as wettability, chemical composition, charge, topography and heterogeneity are believed to highly influence adhesion, composition and conformation of the adsorbed protein layer. All these properties

contribute to some extent of the definition of the behavior of proteins at the interface and, finally, to the fate of a blood-contacting implant.

During the past three decades many attempts have been carried out to correlate the biological performance of materials with their surface characteristics. Due to the complexity of the blood-material system, absolute criteria to predict materials biological response from their surface properties can not be fixed. Protein adsorption onto various kinds of materials and in particular on polymers with different surface characteristics (wettability, surface energy, charge, chemistry, etc.) has been examined, in order to try to answer the question: 'how do proteins interact with material surfaces?' [61, 65, 66].

The surface energetic properties of a biomaterial seem to be the dominant characteristic driving protein adsorption. As a general rule, hydrophobic surfaces are usually reported to induce higher and more rapid adsorption and conformational changes on plasma proteins with respect to hydrophilic surfaces [66, 67]. This behavior is dedicated by thermodynamic laws. In fact, in an aqueous environment, a protein tends to adopt a conformation with its polar groups turned externally, facing water environment, and non- polar groups internally. As a protein comes in contact with a hydrophobic surface, it will dehydrate and release surface-bound water originating a net entropy gain. The protein will thus adsorb on the substrate with the hydrophobic regions located at the material-protein interface and the hydrophilic regions located at the protein-water interface as shown in Figure 14 [65].

On contrary, in the case of a hydrophilic surface, water desorption from the solid is not energetically favorable, therefore, the proteins remain surrounded by their solvation shell, and adsorption occurs through a strong bound hydration layer. Therefore, protein adsorption to hydrophilic surface is generally weak and reversible and does not originate changes in protein conformation [65, 66].

In contrast, in the case of contact with an hydrophobic surface, a rearrangement of protein structure takes place, causing a tight mainly irreversible binding. As a consequence, denaturation may cause proteins to lose their original biological activity. This is the reason why surfaces that present low water-wettability are often considered to have a low procoagulant activity [65, 66].

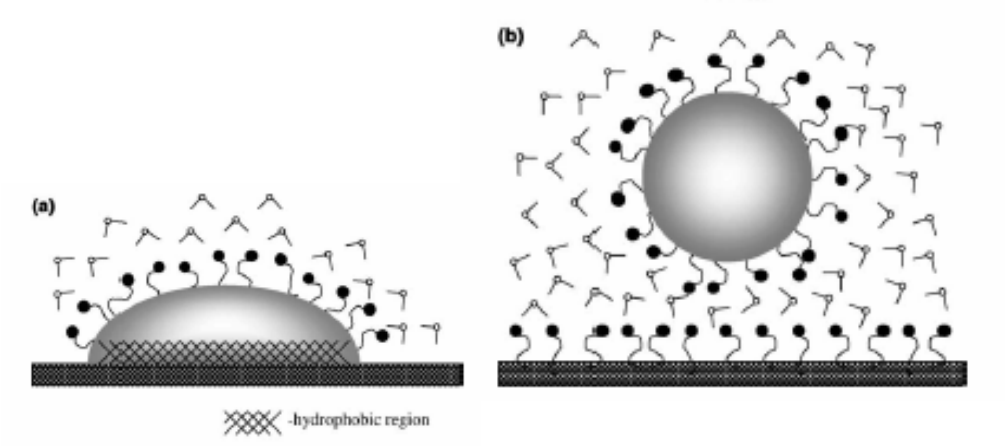

Figure 14 Schematic representation of protein adsorption to a) hydrophobic surface b) hydrophilic surface. The distribution of polar functional groups and water molecules surrounding surface-protein complexes is shown [65].

Surface wettability may also modulate platelet-binding epitose expression in Fng through molecule unfolding, thus affecting platelet inclination to adhesion and aggregation [62]. High hydrophilic materials have been reported to induce low conformational changes on Fng and consequently, a low degree of platelets adhesion. Besides hydrophobic interaction, the adsorption of molecules from a solution to the surface of a material is ruled by intermolecular interactions, such as ionic bonding, and charge transfer interactions (dipole-dipole, induced dipole-dipole, induced dipole-induced dipole). The types of intermolecular forces governing the interaction with proteins are determined by the surface chemical composition of a material, by the charge properties of both the surface and the molecules, pH and ionic strength of the

solution, etc. Moreover, the presence of the surface heterogeneity, resulting in the presence of domains with different characteristics, can lead to differentiated preferential adsorption and influence the protein orientation on the surface [61, 62].

Material properties and features on a microscopic scale may also affect adsorption. The surface topography and roughness contribute to influence protein adsorption, by increasing the surface area exposed to plasma and making it available for protein attachment and exchange. Surface topography may also address protein pattering and promote specific stimuli for cells [68].

1.4.7 Surface Modifications for Blood Compatibility

In surface modifications for blood compatibility, the basic approaches are summarized in three categories:

- the control of the surface properties of a polymer;
- the use of an antithrombogenic substance in combination with a polymer;
- the utilization of assimilation and repairing properties of living tissue such as pseudoendothelialization.

Altering of the surface properties can be achieved in different ways such as creating minimum interfacial free energy, optimum hydrophilic/ hydrophobic balance, optimum critical surface tension, a negatively charged surface, a hydrogel layer, a micro-phase-separated structure, and so on [69].

New surface modification techniques include immobilization of specific biological molecules mostly heparin and albumin on the materials surface [70]. The use of these antithrombogenic substances in combination with a polymer or as coating enhances blood compatibility. Most commonly used antithrombogenic substances are; heparin (inhibits the activation of blood clotting factors), urokinase (activates fibrinolysis), and prostacyclin (suppresses the aggregation of platelets) [69].

1.5 Heparin

Heparin, often-used as anticoagulant, is classified as an anionic, highly sulfated mucopolysaccharide or glycosaminoglycan. It is biosynthesized and stored in mast cells of various mammalian tissues, particularly liver, lung and mucosa. Commercial heparin is chiefly isolated from beef lung or pork intestinal mucosa [71].

It does not have a uniform molecular structure and composed of alternating units of sulfated d-glucosamine and d-glucuronic acid (Figure 15). The esterified sulfuric acid component gives acidic property to unfractionated heparin. The strong electronegative charges on the unfractionated heparin molecule attract and bind to electropositive charges on clotting factors and are an important step in their inactivation.

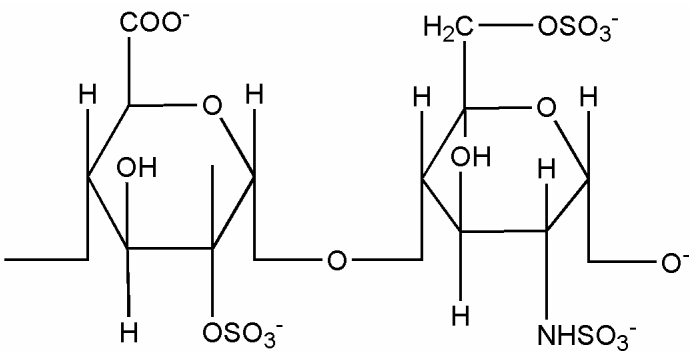

Figure 15 Chemical structure of a single unit of heparin molecule.

Heparin can catalytically increase the antithrombin III (AT III) activity which inhibit thrombin or some other coagulating proteases and inhibit the formation of the fibrin network [72]. Unfortunately, the large dose of heparin needed for anticoagulation can lead to uncontrolled bleeding that can be dangerous and fatal.

1.5.1 Biological Activity of Heparin and Its Molecular Weight Ranges

Heparin has been used for years as an anticoagulant. It binds to antithrombin III (AT III), a naturally occurring plasma protease inhibitor, accelerating significantly the rate at which AT-III inhibits coagulation proteases (factor Xa and thrombin).

The activity of heparin as an anticoagulant has been shown to be related to the molecular weight; because heparin apparently binds to AT-III in a 1:1 stoichiometry. Heparin is a mixture of polyanion chains in a wide range of molecular weights. Therefore, heparins are classified according to their molecular weight ranges; the unfractionated heparin (UFH) and low molecular weight heparin (LMWH). Molecular weight of unfractionated heparin ranges from as low as 6,000 to as high as 30,000 Da. The commercial heparin (a product of Sigma H3393) have most chains in the range 17,000-19,000 Da. LMWHs have a mean molecular weight of 4,000 to 5,000 Da, with a molecular weight distribution of 1,000 to 10,000 Da and showing different anticoagulant activities compared with unfractionated heparin [73].

1.5.2 Limitations of Unfractionated Heparin

Unfractionated heparin (UFH) has some pharmacokinetic, biophysical, and biologic limitations. The pharmacokinetic limitations of UFH are the result of its nonspecific binding to proteins and cells. Because UFH is highly negatively charged, it binds to a variety of plasma proteins (including histidine-rich glycoproteins, vitronectin, lipoproteins, fibronectin, and fibrinogen) as well as to proteins secreted by platelets (platelet factor 4, PF4, and high-molecular-weight von Willebrand factor) and endothelial cells (high-molecular- weight von Willebrand factor). This causes variability in plasma levels of heparin-binding proteins in patients and results in thromboembolic disease and unpredictable anticoagulant response. Biologic limitations of UFH apart from the well-known complication of bleeding, which is common to all anticoagulants, UFH can produce thrombocytopenia and osteoporosis [72-74].

1.5.3 Low Molecular Weight Heparins

Low molecular weight heparins (LMWHs) are flagments of unfractionated heparin (UFH) and are produced by chemical or enzymatic depolymerization. LMWHs have been introduced in clinical practice in the last years with good antithrombotic results and with a lower rate of bleeding complications compared to UFH [75]. LMWH fragments are approximately one third of the size of UFH. Like UFH, LMWHs are heterogeneous with respect to molecular size and anticoagulant activity. LMWHs have a mean molecular weight of 4,000 to 5,000 Da, with a molecular weight distribution of 1,000 to 10,000 Da [73].

1.5.4 Differences of Anticoagulant Effects of LMWH and UFH

Like UFH, LMWHs produce their major anticoagulant effect by activating antithrombin. Their interaction with antithrombin is mediated by a unique pentasaccharide sequence found on fewer than one third of LMWH molecules. A minimum chain length of 18 saccharides (including the pentasaccharide sequence) is required for ternary complex formation of heparin, antithrombin, and thrombin. Only, the 25 % to 50 % of LMWH species that are above this critical chain length are able to inactivate thrombin. In contrast, all LMWH chains that contain the high-affinity pentasaccharide, catalyze the inactivation of Factor Xa. Consequently, commercial LMWHs have ratios of anti–Factor Xa to anti–Factor IIa in the range of 4:1 to 2:1, depending on their molecular size distribution. In contrast to LMWH, virtually all UFH molecules contain at least 18 saccharide units. Therefore, UFH has an anti–Factor Xa to anti–Factor IIa ratio of 1:1 [73]. The anticoagulant effect of UFH and LMWH are also shown in Figure 16 and Figure 17, respectively [76].

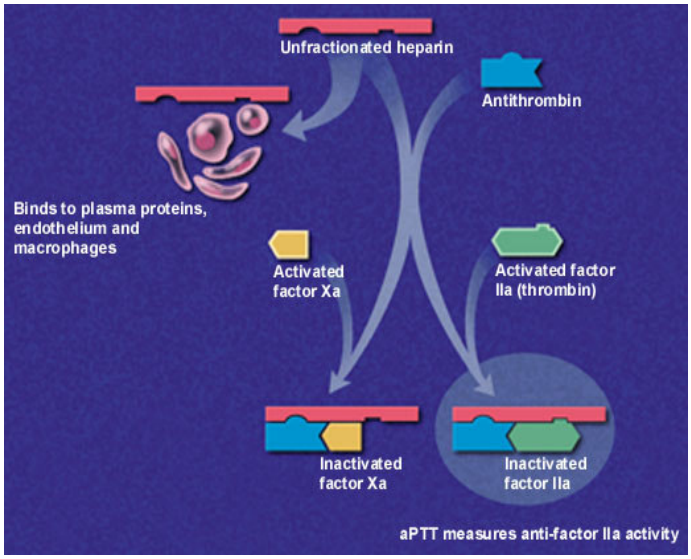

Figure 16 Anticoagulant effect of unfractioned heparin.

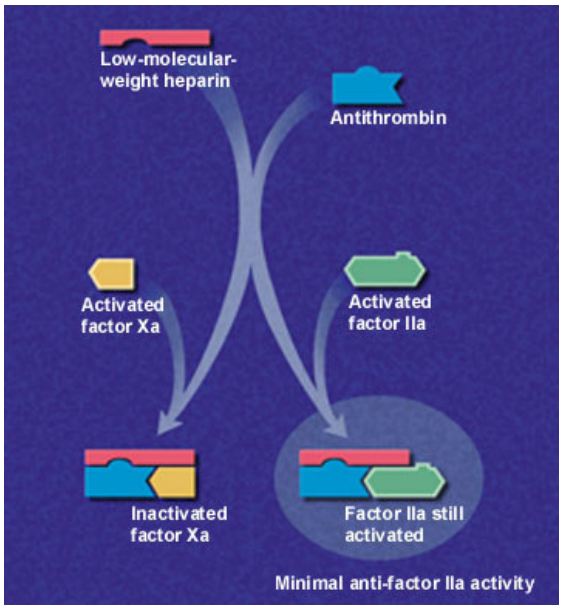

Figure 17 Anticoagulant effect of low molecular weight heparin.

Depolymerization of UFH into lower-molecular weight fragments results in five main changes in its properties; all are caused by reduced binding of LMWH to proteins or cells. These properties include [72, 74]:

1. Reduced ability to catalyze the inactivation of thrombin because the smaller heparin fragments cannot bind to thrombin (they retain their ability to inactivate factor Xa).
2. Reduced nonspecific binding to plasma proteins, with a corresponding improvement in the predictability of their dose-response characteristics.
3. Reduced binding to macrophages and endothelial cells, with an associated increase in plasma half-life.
4. Reduced binding to platelets.
5. Possibly reduced binding to osteoblasts, which results in less activation of osteoclasts and an associated reduction in bone loss.

Low molecular weight heparins (below approximately 8000 Da) inhibit AT-III but have a higher ratio of anti-factor Xa to anti-AT-III activity than unfractionated heparin. LMWH have lower effect on platelet aggregation compared to UFH. Table 5 gives the summary of biological consequences of LMWH, which are important in blood coagulation [73].

Table 5 Biological consequences of reduced binding of LMWH to proteins and cells.

Binding target	Biologic effects	Clinical consequences
Thrombin	Reduced anti-IIa to anti-Xa ratio	Unknown
Proteins	More predictable anticoagulant response	Monitoring of anticoagulant effect unnecessary
Macrophages	Cleared through renal mechanism	Longer plasma half-life.
Platelets	Reduced incidence of heparin-dependent antibody	Reduced incidence of heparin-induced thrombocytopenia
Osteoblasts	Reduced activation of osteoclasts	Lower incidence of osteopenia

1.5.5 Methods to Immobilize Heparin on Polyurethane

Heparin is a naturally occurring anticoagulant synthesized and secreted primarily by the mast cells in the body and inhibits thrombin or some other coagulating proteases preventing fibrin network formation [69]. Heparinizable polyurethanes were obtained by different methods as given in literature. Ito et al. synthesised an antithrombogenic polyetherurethaneurea containing quaternary ammonium groups in the side chains and then covalently bound heparin [77]. Other spacers such as diamine diisocyanate [78] and poly(amino-amine) [79] were introduced onto the urethane linkages and then heparinization was carried out of by dipping technique. Among these methods, using functional group grafting by oxygen plasma glow discharge followed by graft polymerization was an effective method that increase the immobilizing sites for heparin [80]. Heparin-immobilized polyurethanes were also prepared by coupling reactions of NH_2 and COOH functional groups with heparin and with acrylic acid, and acryloylbenzothiazole [81, 82]. The blood compatibility of heparinized polyurethanes of grafted functional groups showed lower activation of platelets and plasma proteins which lead to reduced thrombus formation as compared to nonheparinized polyurethanes.

However up to date none of these mentioned methods have been completely successful to prevent platelet activation and coagulation. Thrombi formation occurs on the interface when a polymer based medical device come in contact with blood in vivo. Therefore, there is still and will be more intense research in the synthesis and modifications of new materials with new techniques to be used in the production of blood contacting implantable devices.

1.6 The Aim of This Study

The aim of this study is to synthesize polyurethane (PU) films in medical purity from main components of diisocyanate (TDI) and polyol without using any other ingredients (solvent, catalyst, chain extender, etc) and to modify their surfaces by covalent immobilization of different types of heparin to enhance their blood compatibilities. Polyurethane films were prepared in various compositions with different TDI / polyol ratios and their chemical, thermal and mechanical properties were characterized by solid state NMR, FTIR, GPC, DMA, mechanical tests and TGA. The optimum PU film composition was selected and surface modification studies by covalent immobilization of heparin were carried out with that PU composition. Two types of heparin, unfractionated (UFH) and low molecular weight heparin (LMWH), were immobilized on PU to investigate their anticoagulant effect on the surface. It was the first time that, LMWH was immobilized on PU surface as an alternative anticoagulant to UFH. Also the anticoagulant activities of the surfaces containing UFH or LMWH were examined and compared for the first time. The surface properties of these modified PUs were examined with goniometer, ESCA, ATR-FTIR and AFM. The effects of different types of surface-immobilized heparins on blood protein adsorption and on platelet adhesion were examined after incubating the samples with platelet poor plasma (PPP) and platelet rich plasma (PRP). Protein adsorption kinetics were analyzed by electrophoresis and the platelets adhered on the surfaces were examined by SEM at different incubation times.

CHAPTER 2

EXPERIMENTAL

2.1 Polyurethane Synthesis

2.1.1 Materials for Polyurethane Synthesis

Toluene diisocyanate (TDI) (Molecular weight: 174; Boiling point of 2,4-TDI at 1 bar: 120°C; Boiling point of 2,6-TDI at 1 bar: 129-133°C; density at 25°C: 1.22 g/cm^3 ; degree of purity: 99.5%) was obtained from Dow Chemical Company (USA) as a mixture of 2,4 and 2,6 toluene diisocyanate in the ratio of 80:20. Polyol (polyoxypropylene/polyoxyethylene triol) was obtained from Dow Chemical Company (USA) (Trade name: voranol 3322 polyol; a triol containing 88% polypropylene oxide and 12% polyethylene oxide with terminal secondary OH- groups, molecular weight 3400-3500; hydroxyl value 46-48 mg KOH/g; viscosity at 25°C, 51 MPa.s; water content 0.1% (w/w); flash point: 234°C.)

2.1.2 Method for Polyurethane Synthesis

Polyurethane prepolymers were synthesized from the condensation reaction of toluene diisocyanate (TDI) and polypropylene ethylene glycol (polyol) in a closed vacuum system in medical purity without adding any other ingredients (solvent, catalyst or activator). In this process, 20 mL of polyol was put into the reaction chamber, heated at about 80°C and evacuated for at least 1 h in order to avoid volatile chemicals especially water. Afterwards, desired amount of TDI, which was kept under nitrogen atmosphere, was added drop wise and the total solution was stirred for 6 h at 90ºC under vacuum. The formed viscous prepolymer was poured into glass molds and placed into vacuum

oven where they were kept for ~10 days at 90ºC - 110 ºC for complete curing [83-86]. After the formation of solid polymer films, they are dipped in boiling water for few minutes, the films were separated from glass molds and rinsed with distilled water. Various polyurethanes were prepared by using different amounts of polyol and TDI to examine the effects of components on the physical and chemical properties of the product. The compositions of prepared PU films are given in Table 6.

Table 6 Compositions of polyurethane films.

Sample Code	Volume ratio: polyol/TDI	Mol ratio: polyol/TDI
5PU	4.00	0.170
6PU	3.33	0.142
7PU	2.86	0.122
8PU	2.50	0.106
9PU	2.22	0.094
10PU	2.00	0.085

2.2 Polymer Characterization Methods

2.2.1 Solid State Nuclear Magnetic Resonance Spectroscopy (NMR)

The solid state NMR spectroscopy is a powerful technique in characterizing the detailed structure and molecular motion of the samples in the phase in which they are actually used. In solid state NMR, all interactions in the solids (spin-spin, spin lattice, chemical shift anisotropy) are maintained with a resulting line broadening in the NMR spectra. This line broadening is mostly reduced by cross polarization magic angle

spinning (CPMAS) experiment technique and by adjusting sample rates. The CPMAS is a special solid state NMR technique which is used to enhance sensitivity for low natural abundance nuclei (^{13}C) with high abundance nuclei (^{1}H) by polarization transfer and spinning the sample at an angle of 54.7′ which is known as magic angle [87].

The chemical characterization of polyurethane films was done by High Power Solid State 300 MHz NMR Spectrometer (Bruker, Superconducting FT.NMR Spectrometer Avance™, with 300 MHz Wide Board Magnet, Germany) running ^{13}C CPMAS analysis at a spin rate of 8000 Hz with a scan number of 20,000. In order to examine the microphase segregation between hard and soft segments, the spin rate was lowered to 1000 Hz and NMR analysis was performed without changing other parameters. In all experiments amount of polyurethane samples were kept constant and the samples were placed in 50 μL reduced volume ZrO_2 rotors. Reduced volume rotors were preferred to avoid the spinning problems of non powder samples.

2.2.2 Fourier Transform Infrared Spectroscopy (FTIR)

The polymerization reactions of polyurethanes were followed by Perkin Elmer Spectrum BX-FTIR Spectrometer (Italy). The viscous prepolymer solution was smeared on KBr pellet and after certain periods. FTIR spectra were taken directly. The PU samples were analyzed over 600-4000 cm^{-1} range with the resolution of 4 cm^{-1}. All spectra were averaged over 32 scans. For different compositions of PU films, the NH and carbonyl regions of the FTIR spectra were characterized to examine the microphase segregation between the hard segment domains and soft segment domains.

2.2.3 Gel Permeation Chromatography (GPC)

The molecular weight determination of polyurethane prepolymer and its molecular weight change during the curing process was studied by Gel Permeation Chromatography (Polymer Laboratories (UK), PL-GPC 220 with THF column). The

analyses were carried out till samples were soluble in THF. The Universal Calibration method was used during the GPC analysis.

2.2.4 Dynamical Mechanical Analysis (DMA)

Dynamic mechanical analysis (DMA) measurements were carried out using a Perkin Elmer Pyris Diamond DMA (USA). The samples were measured over a temperature range from -110°C to 140°C at a heating rate of 5°C min^{-1} under nitrogen atmosphere. The oscillation frequencies of 1 Hz, 2 Hz, 4 Hz, 10 Hz and 20 Hz were used and the analyses were carried out with oscillatory tension mode. The storage modulus (E′), loss modulus (E″) and tan delta values were recorded against temperature at different frequencies. The Tg values were obtained from the peak maxima of tan delta curves.

2.2.5 Mechanical Tests

Mechanical properties of PU films were studied by Lloyd LRX 5K Mechanical Tester, controlled by a computer running program (WindapR). PU films (thickness 1.20 ± 0.05 mm, width: 10.0 ± 0.05 mm, length 40.0 ± 0.05 mm) were attached to the holders (gauge length: 10 mm) of the instrument. A constant extension rate of 10 mm/min was applied. The load deformation curve was printed for each specimen. The tensile strength was obtained from equation $\rho = F/A$, where ρ is the tensile strength (MPa), F is the maximum load applied (N) before rapture, and A is the initial area (m^2) of the specimen. The load deformation curve was converted to stress–strain curve, where stress is the load applied per unit area (F/A) and strain is the deformation per unit length. Slope of straight line (elastic region of the stress-strain curve) is accepted as the Young's modulus of the specimen [84]. For each type of sample, at least five experiments were achieved and the average values of Young's modulus, tensile strength, and percent elongation at break were calculated.

2.2.6 Thermogravimetric Analysis (TGA)

Thermal stability and thermal decomposition investigations of PU films were achieved by thermogravimetric analysis using a Perkin Elmer Pyris 1 TGA instrument (USA) under N_2 atmosphere.

2.3 Heparin Immobilization on Polyurethane

2.3.1 Materials for Heparin Immobilization on Polyurethane

Two types of heparin types, high molecular weight unfractionated heparin (UFH, Sigma-Aldrich, USA, H3393, Mw~17000-19000 Da) and low molecular weight heparin (LMWH, Sigma-Aldrich, USA, H3400, Mw~3000 Da) were covalently immobilized on PU surfaces. Acrylic acid and N'-3-(dimethylaminoproply)-N'-ethylcarbodiimidehydrochloride (EDC), N-hydroxysuccinimide (NHS) used in grafting process were products of Sigma-Aldrich, USA.

Citrate Buffer (0.2 M, sodium citrate-citric acid buffer) was prepared from two stock solutions. First, 0.2 M sodium citrate solution was prepared by dissolving 58.8 g $Na_3C_6H_50_7.H_20$ (MW = 294.12) in distilled water (total volume 1L). Second, 0.2 M citric acid solution was prepared by dissolving 42.02 g $C_6H_80_7.H_20$ (MW = 210.14) distilled water (total volume 1L). These two solutions were mixed and the pH 5 was adjusted with HCl.

2.3.2 Method for Heparin Immobilization on Polyurethane

PU films (8PU was chosen as optimum films and used for blood experiments defining as PU) were cut into circular discs (d=8 mm) and ultrasonically cleaned in isopropyl alcohol for 10 min. The cleaned and dried films were treated with low temperature oxygen plasma (Advanced Plasma Systems Inc., USA) with the application of 100W RF power supplied by; Seren R300 13.56 MHz power generator for 10 min. After the power turned off, the system was opened to atmospheric pressure and the PU films

were taken out. Immediately a drop of aqueous acrylic acid solution (30%) was added on the surface and the samples were immersed into aqueous acrylic acid solution (30%) for 10 min, then rinsed with distilled water and dried in air [88]. These acrylic acid-grafted PU films were immersed into 20 mL of pH 5 citrate buffer solution containing 10 g/L EDC and let to react for 2 h at 4°C. In order to increase the stability of EDC solution NHS (1% of EDC amount) was added. Afterwards, some films were immersed in to high molecular weight unfractionated heparin (UFH, Mw~18000 Da) solution and some were immersed in to low molecular weight heparin (LMWH, Mw~3000 Da) solution which were prepared in citrate buffer (pH 5, containing 1.25 g/L heparin concentration). The immobilization reactions of the two different molecular weight heparins were continued for 24 h at 4°C then films were taken out, washed with distilled water and left to dry at room temperature in a desiccator. Surface modifications with plasma generally created peroxide active groups which go further reactions with acrylic acid and then can linked to heparin with help of EDC as shown in Figure 18.

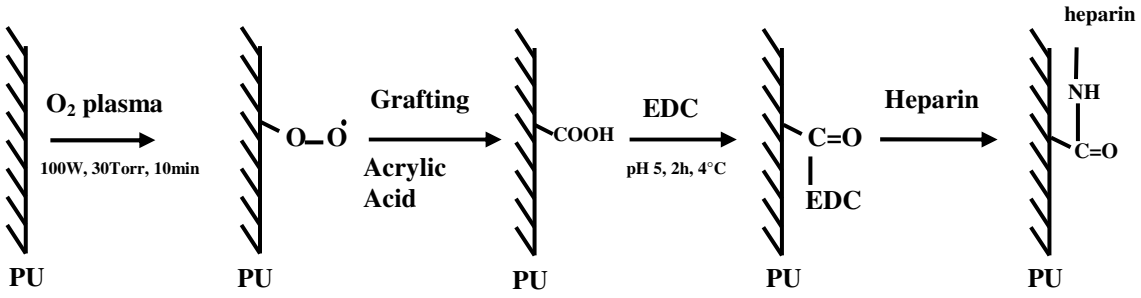

Figure 18 Heparin immobilization on PU films.

2.4 Surface Characterization Methods

2.4.1 Attenuated Total Reflectance-FTIR Spectroscopy (ATR-FTIR)

Chemical structures of the surfaces were examined with Attenuated Total Reflectance-FTIR (ATR-FTIR) using a Perkin Elmer Spectrum BX-FTIR spectrometer (Italy) equipped with a ZnSe crystal at 45°. The samples were analyzed over 500-4000 cm^{-1} range with the resolution of 4 cm^{-1}. All spectra were averaged over 32 scans.

2.4.2 Electron Spectroscopy for Chemical Analysis (ESCA)

Surface atomic compositions of PU films were analyzed by using Specs (Germany), Electron Spectroscopy for Chemical Analysis (ESCA) system equipped with MgKα at 1253 eV and 284 W power at the anode.

2.4.3 Surface Hydrophilicity

Contact angle of a liquid drop is the angle formed by the line of the surface and the tangent of the drop at the point it touches to the surface. Contact angle indicates the strength of noncovalent forces between the liquid and the first monolayer of the material. Small contact angles show high attractions between liquid and the surface. Surface hydrophilicities of the prepared films were studied with deionized triple distilled water by a contact angle goniometry equipped with high-performance image processing system (KSV-CAM200, USA). Water contact angles after each step of surface modification was measured. For each sample at least 10 contact angle measurements were carried out.

2.4.4 Surface Free Energy (SFE)

Surface free energy (SFE) is a property resulted from the chemical structure and the orientation of the molecules at the surface boundary of the materials. For solids, it can be calculated from the contact angles of liquid drops with known surface tension,

formed on the solid surface. For any material, the molecules in the bulk have no net force acting on them, while the ones at the surface encounter a net inward force. For solids, this force is called as ‘‘surface free energy’’ (SFE) and defined as the amount of energy required to change the surface area of a material by one meter square.

The surface free energies of the heparin immobilized PU films were evaluated by contact angle measurements with test liquids of: water, bromonapthalene, formamide and dimethyl sulfoxide. The test liquids formamide ($HCONH_2$) and bromonapthalene ($C_{10}H_7Br$), were product of Merck (Darmstadt, Germany). and dimethyl sulfoxide (C_2H_6OS) was product of Acros (NJ). In all the experiments deionized triple distilled water was used. All the liquids were of reagent grade. A drop (5 μL) of the liquids (water, formamide, bromo napthalene and dimethyl sulfoxide) was added by a motor driving syringe on the smooth disc (diameter = 8 mm) samples at room temperature. For each material at least ten contact angles were measured for each liquid by using a Goniometer (KSV-CAM200, USA). The final average values were presented as the resultant data.

The surface energy of heparin immobilized PU films and its components (polar and dispersive) were calculated by means of the Owens, Wendt, Rabel and Kaelble (OWRK) and Wu Harmonic Mean methods. Additionally, the Lewis acid and basic contributions to the surface energy were calculated using the acid–base method (AB method). The AB method requires at least three liquid system from which two should be polar and one non-polar. Water and formamide were used as polar liquids and bromonapthalene was employed as the non-polar one. The values of SFE were detected by the programme used in the instrument.

2.4.5 Atomic Force Microscopy (AFM)

The surface morphologies of control, UFH and LMWH immobilized PUs were investigated by Atomic Force Microscopy (AFM, Quesant, USA) in non-contact mode, using standard non-contact cantilever with silicone tips.

2.5 Blood Compatibility Tests

The blood compatibility tests include two main parts of experiments. The first experimental part was the investigation of blood cell adhesion on to the heparinized PU surfaces, and this part of the experiments was carried out at METU.

The second part of the experiments mainly focuses on the protein adsorption studies on heparinized PU surfaces. These experiments include; the determination of the proteins types adsorbed on the surfaces, the investigation of the absorption kinetics of these proteins, their binding strength to surface, and studies about platelet adhesion and aggregation. These parts of the experiments were carried out at Trento University, Italy.

2.5.1 Biological Materials for Red Blood Cell Adhesion Studies

For red blood cell adhesion studies, fresh human whole blood was obtained from METU Health Center. The whole human blood was collected into separate Venous Blood Collection Tubes (13x100 mm, 6.0 mL BD Vacutainer® glass whole blood tube. Additive: ACD Solution B of trisodium citrate, 13.2 g/L; citric acid, 4.8 g/L; and dextrose 14.7 g/L, 1.0 mL.) and used as fresh blood.

2.5.2 Methods for Red Blood Cell Adhesion Studies

The untreated PU (8PU) and different type of heparin immobilized samples (PU-UFH, PU-LMWH) were prepeared in 1x1cm^2 pieces and immersed venous blood collection tubes having 6 mL fresh human blood. The samples were kept in vibrating water bath

at 37°C for 15 min then rinsed with PBS buffer and the cells attached to the surfaces were fixed with a fixation solution of glutaraldehyde for 30 min. Then the samples were left to dry in a dessicator at room temperature before SEM (JEOL JSM-6400 Electron Microscope, Japan) investigation.

Fixation solution was prepared with the following composition [per liter]; glutaraldehyde (30.0 g), NaH_2PO_4 (0.2 g), Na_2HPO_4 (1.9 g), NaCl (7.8 g), KCl (0.4 g). All diluted to 1L with distilled water.

Phosphate buffer saline (PBS) solution of 0.1M was prepared by dissolving 80 g NaCl, 2 g KCl, 14.4 g Na_2HPO_4 and 2.4 g KH_2PO_4 in 800 mL distilled water. The pH 7.4 was adjusted with HCl and the solution was diluted to 1L with distilled water.

2.5.3 Biological Materials for Protein Adsorption Studies

For protein adsorption and platelet adhesion tests, platelet-poor plasma (PPP), and platelet-rich plasma (PRP) were used, respectively. PPP, obtained from healthy drug-free donors (S.Chiara Hospital Blood Bank, Trento Italy), was prepared by plasmapheresis through a continuous system with Hemonetic cell separators. Acid citrate dextrose (8% w/v) was added to the human plasma to avoid coagulation. Platelet concentrate was obtained from whole human blood by subsequent centrifugation steps (3 min at 2250 g, 5 min at 4750 g, and 8 min at 410 g) at 21°C. The obtained platelet concentrate was mixed with PPP to obtain PRP, and platelet concentration was adjusted to a physiological value (200,000/µL ca.). PPP and PRP were obtained and treated according to conventional processes that do not modify plasma properties and that don't influence platelets vitality and activity.

2.5.4 Protein Adsorption Studies

For protein adsorption tests, control PU and heparin immobilized PU (PU-UFH and PU-LMWH) films were prepared as disk samples (diameter = 8 mm and surface area = 50 mm^2) placed into 24-well tissue culture plate (TCP) wells. Empty TCP wells were analyzed as positive control. In order to have reproducibility and statistical relevance, 3 samples for each type were examined for each experiment.

2.5.5 Protein Adsorption from Platelet Poor Human Plasma (PPP)

Protein adsorption tests were performed by incubating the PU samples in fresh human plasma (Platelet Poor Plasma, PPP) obtained from healthy donors at S.Chiara Hospital Blood Bank, Trento, Italy. Fresh human plasma (75 µL) was put on the sample surfaces. The samples were incubated at 37°C under static conditions for predetermined experimental periods. Three exposure times were selected (5 min, 15 min and 25 min) in order to evaluate the adsorption kinetics of plasma proteins. After each incubation period, contacting PPP was removed from the surface and unbound proteins were gently washed with deionized water. The excess water on the surface of films was gently removed by capillarity action of a tissue paper by touching to edge of each sample. Therefore, it was maintained that only adsorbed protein layer remains adsorbed on the sample surface.

The contacting PPP removed from the surface was prepared for electrophoresis analysis as described in section 2.5.7.

The adhered protein layer was eluted from the surfaces by 1 h incubation with sodium dodecyl sulfate (SDS) solution (0.1% w/v in water, 200 µL). The eluted protein–SDS solutions were also prepared for the electrophoresis analysis as described in section 2.5.7.

2.5.6 Materials for Electrophoresis Analysis

The electrophoresis analyses were performed with Invitrogen Electrophoresis Kit, including the necessary chemicals and different types of electrophoresis gels and gels staining kits.

For the materials of electrophoresis analysis, the chemicals NuPAGE® LDS sample buffer and NuPAGE® reducing agent were directly used from the Invitrogen Electrophoresis Kit.

The gel running buffer (NuPAGE® SDS running buffer); were prepared by adding 50 mL of NuPAGE® MES running buffer to 950 mL of deionized water. This running buffer was filled in to buffer chamber of electrophoresis equipment with addition of 435 µL of NuPAGE® Antioxidant.

Electrophoresis gels: Two different electrophoresis gels were used. NuPAGE® Tris-Acetate 3-8% porosity gradient gels were used for high molecular weight protein determination and NuPAGE® Bis-Tris 4-12% porosity gradient gels were used for low molecular weight protein determination.

Molecular weight standards: Himark™ Unstained High Molecular Weight Protein Standart (LC5688, MW range 40-500 kDa, Invitrogen) was used and loaded on NuPAGE® Tris-Acetate 3-8% porosity gradient gels for the determination of high molecular weight proteins in plasma. Protein Marker, Broad Range (P7702S, MW range 2-212 kDa, Biolabs) was used as low molecular weight protein standart and loaded on NuPAGE® Bis-Tris 4-12% porosity gradient gels.

Gel stains: For gel staining, both Coomassie® Blue Staining (Invitrogen) and Silver Staining (SilverQuest™, Silver Staining Kit, Invitrogen) were used.

Other solutions used in gel staining: The fixative solution-I was prepared by mixing 50 mL methanol with 7 mL acetic acid and diluting to 100 mL with distilled water. The fixative solution-II was prepared by mixing 40 mL ethanol with 10 mL acetic acid and diluting to 100 mL with distilled water. The washing solution-I is the 30% v/v ethanol in water. Developer solution is prepared by mixing 10 mL of developer stock, 1 mL of developer enhancer (both obtained from SilverQuest™, Silver Staining Kit, Invitrogen) and diluting to 100 mL with distilled water. Also stopper solution is directly used from SilverQuest™, Silver Staining Kit, Invitrogen. Coomassie® Blue Staining (Invitrogen) was used without dilution but Silver Staining (SilverQuest™, Silver Staining Kit, Invitrogen) solution was diluted to 0.01 % v/v with water.

2.5.7 Preparation of Samples for Electrophoresis Analysis

Preparation of contacting plasma for electrophoresis analysis:

5 µL of contacting plasma was diluted with 175 µL NuPage® LDS buffer and 20 µL NuPAGE® reducing agent, and then heated at 70°C for 10 min. The prepared contacting plasma samples were loaded in to NuPAGE® Tris-Acetate 3-8% porosity gradient gels, with running conditions of 150V and 60 min. The gel was fixed and stained with commasine blue staining as described in section 2.5.8.

Preparation of the adsorbed protein layer for electrophoresis analysis:

The proteins adsorbed on PU surfaces were eluted from the surfaces by 1 h incubation with sodium dodecyl sulfate (SDS) solution (0.1% w/v in water, 200 µL). The 19.5 µL of the eluted protein-SDS solution were diluted with 7.5 µL NuPAGE® LDS sample buffer, and 3 µL NuPAGE® Reducing Agent and heated at 70°C for 10 min. The prepared samples and molecular weight standards were loaded on the gels. NuPAGE® SDS running buffer was filled in to buffer chamber of electrophoresis equipment with addition of 435 µL of NuPAGE® Antioxidant.

Two different gels were used for the detection of high molecular weight proteins (NuPAGE® Tris-Acetate 3-8% porosity gradient gels, running conditions: 150V, 60 min), and low molecular weight proteins (NuPAGE® Bis-Tris 4-12% porosity gradient gels, running conditions: 200V, 35 min).

The gels were fixed and stained with both Coomassie® Blue Staining (Invitrogen) and Silver Staining (SilverQuest™, Silver Staining Kit, Invitrogen). The images of running gels were digitalized by Gel Logic 200 Kodak 1D instrument (USA).

2.5.8 Gel Fixation and Staining Procedure after Electrophoresis Analysis

After each electrophoresis experiments each gel was removed from the cassette and placed in 100 mL of fixative solution-I for 15 min under single rotation on shaker. Then the fixative solution was decanted and the gel was washed three times with distilled water for 15 min and then incubated in Coomassie® Blue Staining for 2h. After the staining is complete, staining solution was decanted and the gel was washed in a container with distilled water over night on a shaker. Also a tissue paper was placed in to the container in order to absorb excess dye.

Silver Staining was performed after Coomassie® Blue Staining. The Coomassie® Blue Stained gel was rinsed with water for 10 min and then fixed by using fixative solution-II for 20 min. The gel was washed with washing solution-I for 10 min and with distilled water for 10 min. It was followed by incubation in silverquest™ staining solution (0.01%v/v) for 15 min. Other steps were the incubation in developer solution (for 8 min) and the incubation in non-diluted stopper solution (10 mL for 10 min). Finally, the silver stained gel was washed with distilled water (100 mL, 10 min).

2.5.9 Concentration of Adsorbed Proteins

After each incubation time (5 min, 15 min or 25 min), adsorbed protein layers on the surfaces were eluted by SDS solution as described above and the concentrations of the adsorbed proteins were measured by NanoDrop 3.0.1 protein reader instrument (USA). The measurements were repeated 5 times. The results of the measured protein concentrations (mg/mL SDS solution) were converted 'adsorbed protein amount per surface area'.

2.5.10 Protein Binding Strength

After the incubation of untreated control PU, PU-UFH, PU-LMWH and TCP with fresh PPP for 25min, the excess of plasma was removed from the samples. The samples were washed with deionized water and dried by capillarity action of a tissues paper as described above. Then the samples were incubated in deionized water three times consecutively using 500 μL each time. Then all samples were washed sequentially with isopropanol/water solutions with increasing concentrations (10, 30, 50 and 70% v/v). In each washing step, samples were dipped in 500 μL of elution solutions for 20 min under static conditions at room temperature. The solutions were freeze-dried overnight and were prepared for electrophoresis analysis as in section 2.5.7.

2.5.11 Stability of Immobilized Heparin

Heparin immobilized PU samples were thoroughly washed with sodium dodecyl sulfate (SDS) solution (0.1% w/v in water, 200 μL) for 30 min. Heparin concentrations in the washing solutions were measured by NanoDrop 3.0.1 instrument. Heparin stability tests were carried out for 5 replicates for each sample. The results were calculated and given as amount of heparin released per surface area.

2.5.12 Morphologies of Adhered Platelets

The samples (PU, PU-UFH, PU-LMWH and TCP were incubated in Platelet Rich Plasma (PRP, at physiological concentration about 200.000 platelets/μL) for various times (5, 15 and 25 min) under static conditions. The morphology of adhered platelets was characterized by SEM. For the SEM investigations, the PRP incubated samples were fixated with glutaraldehyde (2.5% GA in 0.1M sodium cacodylate buffer pH 7.2) for 30 min, and rinsed 3 times with sodium cacodylate buffer (0.1M, pH 7.2). Then, they were dehydrated with graded ethanol series (500 μL of 30%, 50%, 70%, 90%, and 2 times with pure ethanol) for 10 min each and then dried in air. The samples were mounted onto stubs, using carbon adhesive, and sputtered with gold (20 nm ca). The SEM analyses were carried out with ESEM-FEG XL30 (Fei Company, Holland) at 5 kV, spot 4, magnification 250-10000x.

CHAPTER 3

RESULTS AND DISCUSSION

3.1 Polyurethane Synthesis

Polyurethane films were synthesized by condensation reaction of polypropylene ethylene glycol (polyol) and toluen diisocyanate components without adding any other ingredient in to the reaction medium.

Presence of excess TDI ensures the complete reaction of polyol creating isocyanate ended chains. The excess isocyanate present in these systems, causes additional crosslinking reactions resulting in the formation of allophanate and biuret groups. This provides the desired elastomeric and mechanical properties. Polyurethane formation and cross-linking reactions of urethanes and ureas with isocyanate are shown schematically in Figure 19. During the reactions great care was given to remove excess moisture from the medium so that two-component polyurethane formulations would take place without undesirable reactions.

Polyurethane becomes cross-linked because of allophanate linkage that occurs in the presence of excess diisocyanate. These reactions lead a kind of accumulation of aromatic groups and creates hard segment of polyurethanes (Figure 20) while polyol chains creates soft segments of polyurethanes.

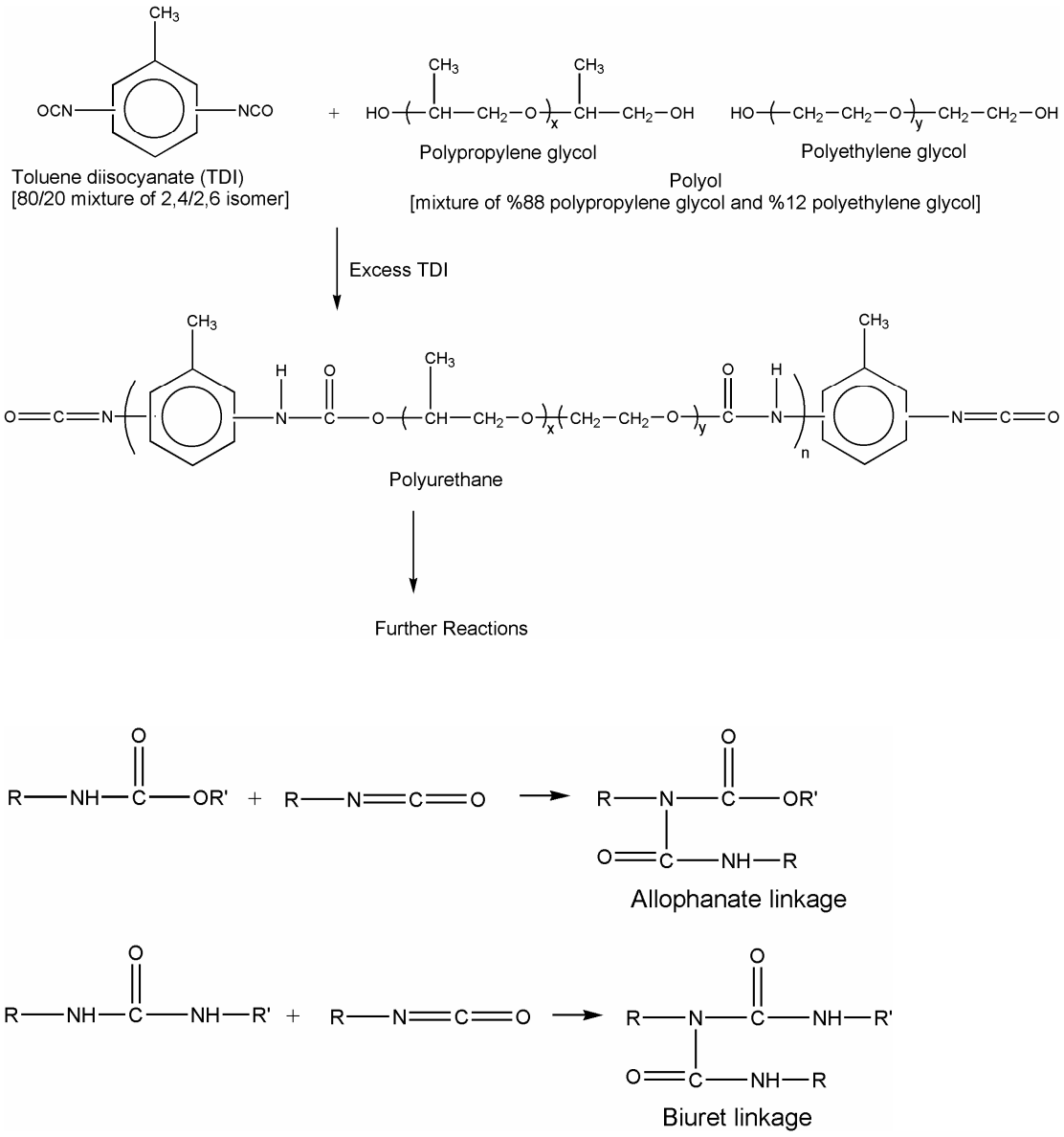

Figure 19 Polyurethane synthesis and formation of allophanate and biuret reactions.

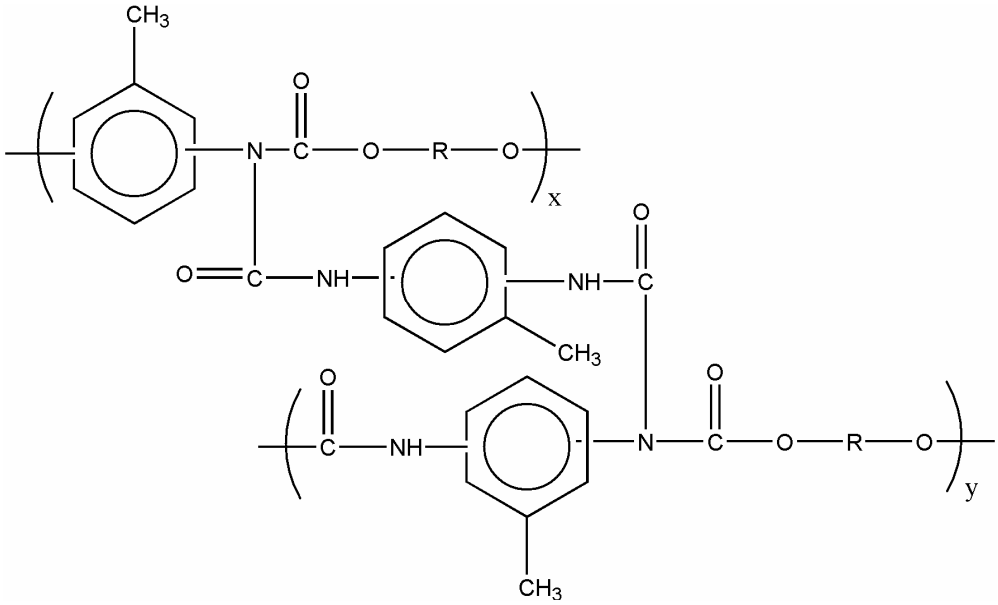

Figure 20 Allophanate linkages forming crosslinks in polyurethane.

The properties and performance of segmented polyurethanes are strongly dependent on their phase separated micro phase morphologies, which consists of domains of hard segments distributed in a continuous soft segment matrix. It is generally believed that one of the most important factors or driving forces for the micro phase separation in polyurethanes is the strong hydrogen bonding between the urethane hard segments [89]. The thermal and mechanical properties of these polymers prepared in medical purity without addition of chain extenders, showed very strong dependence on the amount of the diisocyanate.

The characterization techniques, thermal and mechanical properties of the prepared polyurethanes, emphasize the influence of the amounts of hard and soft segments and presence of hydrogen bondings on the structure-property relations.

3.2 Polyurethane Characterization Results

3.2.1 Solid State NMR Analysis Results

The ^{13}C CPMAS analysis was performed for chemical characterization of PU films and for examining micro phase separation of hard and soft segments in PU structure. The repeating unit of PU is shown in Figure 21 and the carbons having different chemical environments are labeled. Since polyol is a mixture of polyoxypropylene / polyoxyethylene, x and y labels indicate the presence of these repeating units.

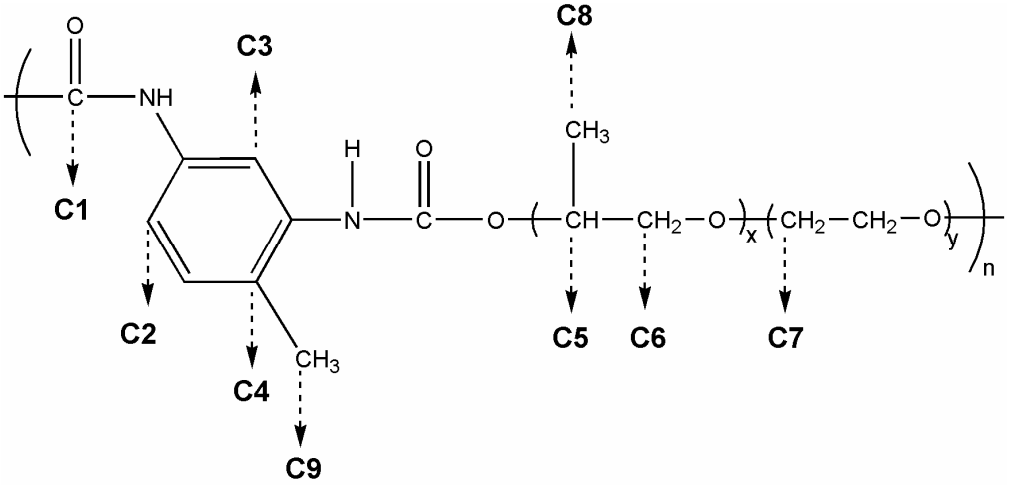

Figure 21 Carbon atoms labeled according to their chemical environment.

In the repeating unit of PU, the carbons belong to hard segments are C1, C2, C3 and C4; while the carbons belonging to soft segment are C5, C6, C7 C8 and flexible C9. Figure 22 shows the ^{13}C CPMAS spectrum of 5PU membrane at 8000Hz spin rate. In the ^{13}C CPMAS NMR spectrum the region between 10-20 ppm corresponds aliphatic carbons of the soft segment C8 and flexible C9 carbon in PU repeat unit. The region between 60-80 ppm can be characterized as C5, C6 and C7 carbons. These are the flexible and the soft segments of the PU structure. C4 peak is observed between 110 -

120 ppm. C3 aromatic carbon is observed as two components C3D at 124 ppm and C3U at 128 ppm indicating the downfield and the upfield resonance lines, as respectively. C2 carbon is characterized between 140-130 ppm and the C1 carbonyl is observed around 150 ppm [90 - 92].

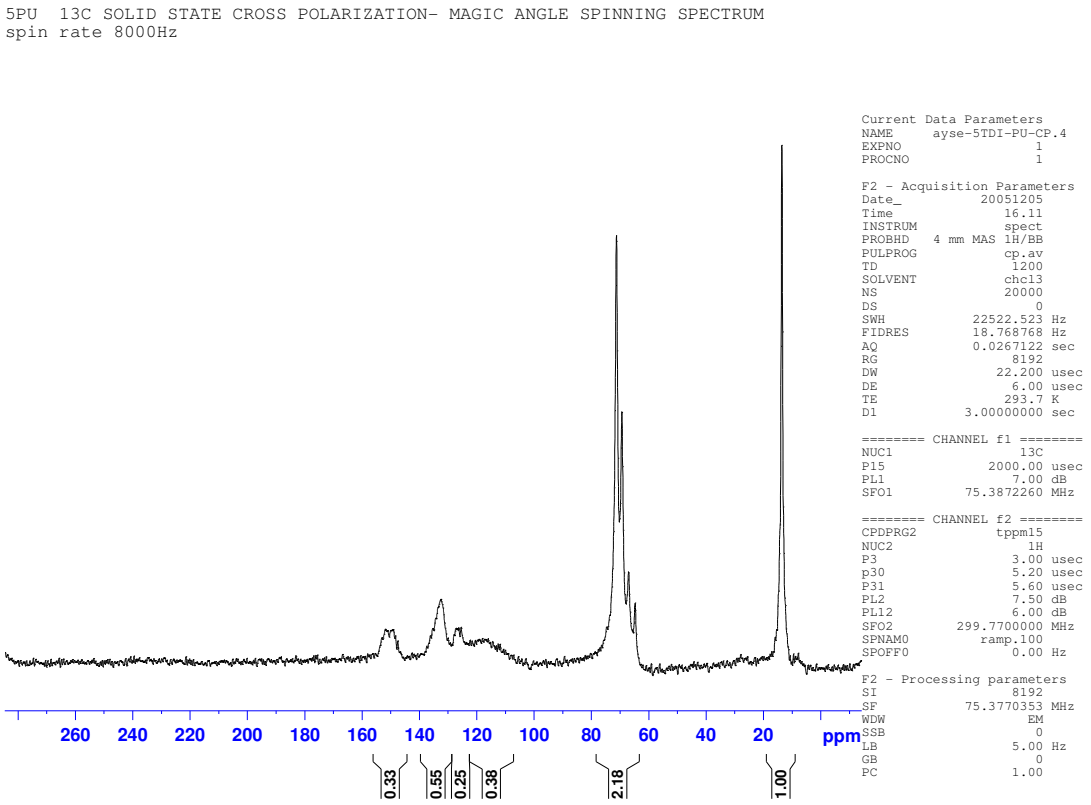

Figure 22 ^{13}C CPMAS spectrum of 5PU sample.

For the other composition of PU film (8PU), same amount of sample was used to obtain ^{13}C CPMAS NMR spectrum which is shown in Figure 23. For 8PU the characterization the peaks correlates 5PU, indicating the presence of similar chemical structure. For 8PU, the volume ratio of TDI / polyol was higher than that of 5PU. This

caused an increase in the intensities of the C1, C2, C3 and C4, which belong to hard segments. The carbon peak areas of 5PU and 8PU samples were tabulated at Table 7.

Table 7 Carbon peak areas of 5PU and 8PU samples.

	Hard Segment				Soft Segment	
	C1	C2	C3	C4	C5, C6,C7	C8, C9
5PU	0.33	0.55	0.25	0.38	2.18	1.00
8PU	0.52	0.78	0.42	0.35	1.75	1.00

TDI / polyol mol ratio for 5PU and 8PU was 5.88 and 9.43, respectively. The increase in TDI mol number about 1.6 times caused an increase in the peak area of C1, C2 and C3 about 1.6, 1.4 and 1.7 times increase, respectively. Results show that C1, C2 and C3 almost directly reflect hard segment content of the polymers.

Solid state NMR spectroscopy was used to identify the microphase separation between rigid and flexible segments of PU structure by using different sample spin rates. Spin rate was adjusted to 1000 Hz (low spin rate) and 8000 Hz (high spin rate). For this purpose, 8PU sample is rotated at low spin (1000 Hz) and at high spin (8000 Hz). ^{13}C CPMAS spectrum of 8PU membrane at 8000 Hz spin rate and at 1000Hz spin rate is shown in Figure 23 and Figure 24, respectively. These two experiments were carried out for the same duration with the same scan number.

8PU 13C SOLID STATE CROSS POLARIZATION- MAGIC ANGLE SPINNING SPECTRUM
spin rate 8000Hz

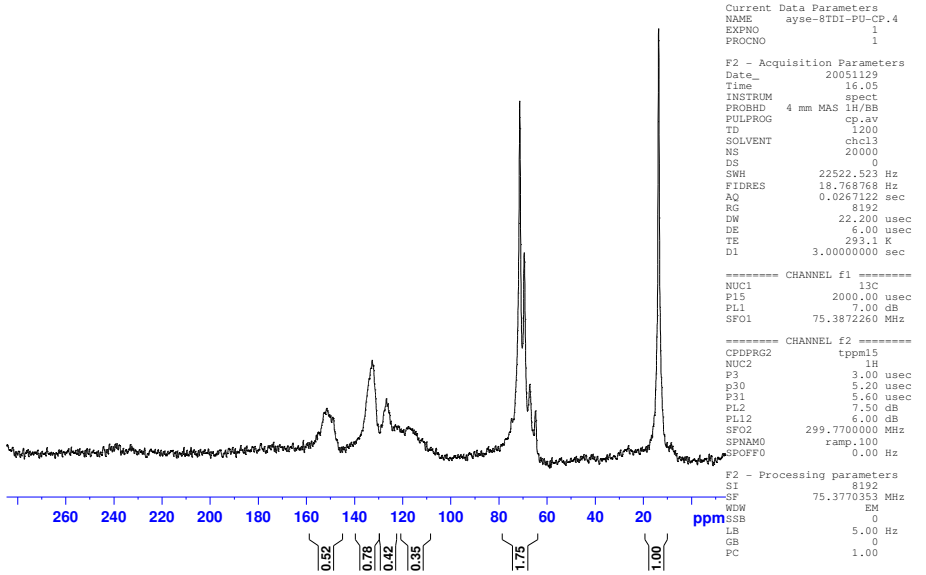


```
Current Data Parameters
NAME      ayse-8TDI-PU-CP.4
EXPNO                    1
PROCNO                   1

F2 - Acquisition Parameters
Date_           20051129
Time               16.05
INSTRUM             spect
PROBHD   4 mm MAS 1H/BB
PULPROG             cp.av
TD                  1200
SOLVENT            chcl3
NS                 20000
DS                     0
SWH            22522.523 Hz
FIDRES         18.768768 Hz
AQ             0.0267122 sec
RG                  8192
DW                22.200 usec
DE                 6.00 usec
TE                293.1 K
D1            3.00000000 sec

======== CHANNEL f1 ========
NUC1                 13C
P15              2000.00 usec
PL1                 7.00 dB
SFO1          75.3872260 MHz

======== CHANNEL f2 ========
CPDPRG2           tppm15
NUC2                 1H
P3                3.00 usec
p30               5.20 usec
P31               5.60 usec
PL2               7.50 dB
PL12              6.00 dB
SFO2         299.7700000 MHz
SPNAM0          ramp.100
SPOFF0             0.00 Hz

F2 - Processing parameters
SI                  8192
SF           75.3770353 MHz
WDW                   EM
SSB                    0
LB                5.00 Hz
GB                     0
PC                  1.00
```

Figure 23 ^{13}C CPMAS spectrum of 8PU sample at high spin rate.

8PU 13C SOLID STATE CROSS POLARIZATION- MAGIC ANGLE SPINNING SPECTRUM
Spin rate 1000Hz

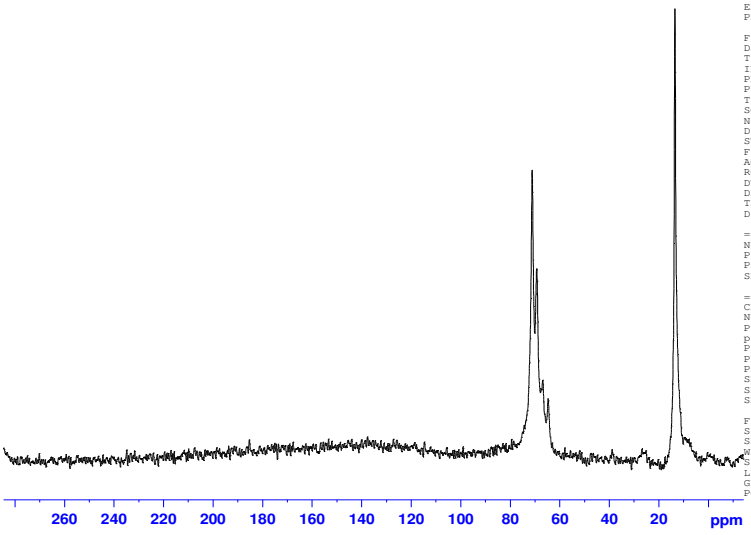


```
Current Data Parameters
NAME      ayse-8PU-SLWSPN-CP.4
EXPNO                    1
PROCNO                   1

F2 - Acquisition Parameters
Date_           20051219
Time               16.05
INSTRUM             spect
PROBHD   4 mm MAS 1H/BB
PULPROG             cp.av
TD                  1200
SOLVENT            chcl3
NS                 20000
DS                     0
SWH            22522.523 Hz
FIDRES         18.768768 Hz
AQ             0.0267122 sec
RG                  8192
DW                22.200 usec
DE                 6.00 usec
TE                291.0 K
D1            3.00000000 sec

======== CHANNEL f1 ========
NUC1                 13C
P15              2000.00 usec
PL1                 7.00 dB
SFO1          75.3872260 MHz

======== CHANNEL f2 ========
CPDPRG2           tppm15
NUC2                 1H
P3                3.00 usec
p30               5.20 usec
P31               5.60 usec
PL2               7.50 dB
PL12              6.00 dB
SFO2         299.7700000 MHz
SPNAM0          ramp.100
SPOFF0             0.00 Hz

F2 - Processing parameters
SI                  8192
SF           75.3770353 MHz
WDW                   EM
SSB                    0
LB                5.00 Hz
GB                     0
PC                  1.00
```

Figure 24 ^{13}C CPMAS spectrum of 8PU sample at low spin rate.

When we compare the spectra of 8PU at different spin rates (Figure 23 and Figure 24); at low spin rate the hard segment carbons (C1, C2, C3, C4) between 110-140 ppm region couldn't be observed. They are belong to the rigid segment of the PU structure, which is stericly restricted part for the segmental motion, so at low spin rate enough anisotropy to give a chemical shift of NMR signal could not be obtained. Region between 10-20 ppm corresponds to soft and flexible segment carbons (C5, C6, C7, C8, C9) therefore no steric hindrance is exists, and the corresponding peaks were observed at low spin rates (Figure 24). By applying high spin rate (8000 Hz) for the same sample (8PU), segmental motions of the hard segment carbons (C1, C2, C3, C4) could be obtained and the corresponding peaks between 110-140 ppm region were observed (Figure 23).

3.2.2 Fourier Transform Infrared Spectroscopy Results

The progress and completion of polymerization reactions were monitored by FTIR spectroscopy. For this purpose, viscous prepolymer solution was smeared on KBr pallet and FTIR spectra were taken at certain time intervals. The FTIR spectra of the polyurethane prepolymer and the cured PU (8PU) samples are shown in Figure 25. The bands at 3300 cm^{-1} and 1726-1705 cm^{-1} are the two typical stretching vibrations observed for polyurethanes [93]. The polyurethanes prepared from toluene diisocyanate and polypropylene ethylene glycol exhibited these characteristic peaks. The band at 3297cm^{-1} corresponds to NH stretching vibration in the presence of hydrogen bonding. Two stretching band 2968 cm^{-1} and 2866 cm^{-1} corresponds to C-H asymmetrical and symmetrical stretching in -CH_3, respectively. Strong C=O stretching bands is observed at 1716 cm^{-1} in the FTIR spectrum of the cured polyurethane [94]. Additional peaks at 1600 cm^{-1} and 1537 cm^{-1} and 1535 cm^{-1} are attributed to stretching vibrations of C=C bond in aromatic ring and bending mode of NH bond, C-N stretching respectively. Very sharp peaks at 1075 cm^{-1} and 1230 cm^{-1}, represent urethane or C-O stretching and C-O-C vibration.

As the reactions proceed and the samples solidify with formation of crosslinking, a decrease in the adsorption peaks of isocyanate groups at 2270 cm^{-1} occurs. Almost no free isocyanate is left on the 20^{th} day. Presence of very reactive isocyanate groups in higher amounts, leads to the secondary reactions even reacting with already formed urethane groups, as well as forming new urethane bonds. These further reactions cause an increase in crosslinking leading to an increase in the rate of solidification. Also for cured PU no free isocyanate groups at 2270 cm^{-1} was observed since the reaction between these groups and water is very fast and forms urea bonds.

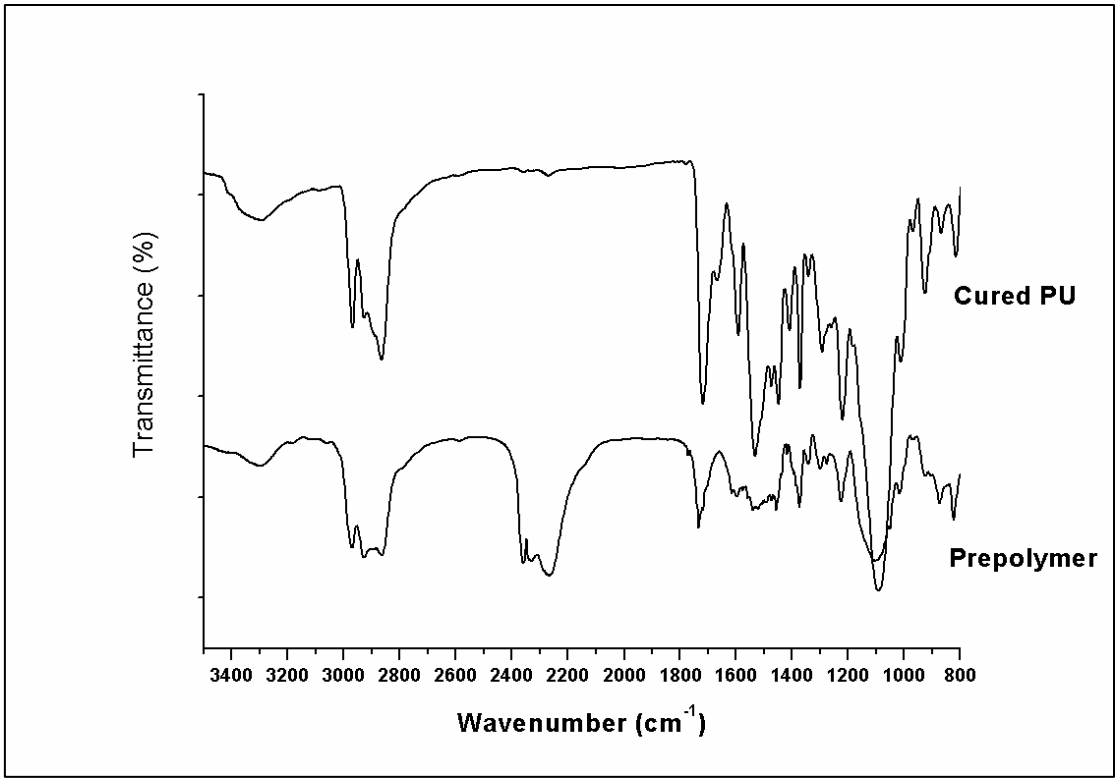

Figure 25 FTIR spectra of prepolymer and 8PU film.

PU contains proton donor group (N-H) and proton accepter group (C=O). Therefore, hydrogen bonding between hard segments can exist. Hydrogen bonding has significant

effect on the physical properties of PU. Hydrogen bonded NH peak in infrared spectra displays frequency shift, changes in intensity and bandwidth [95].

Table 8 provides a list of peak positions for (C=O) and (N-H) groups on urethane and urea linkages based on the nature of their hydrogen bonding. While non hydrogen bonded (free) urethane carbonyl gives a sharp peak in the 1730–1740 cm^{-1} range, strongly hydrogen bonded and ordered carbonyl peak (C=O...H-N) is in the 1680–1695 cm^{-1} range. Depending on the hydrogen bonding environment, other urethane C=O peaks are also observed between 1740 and 1680 cm^{-1} [95].

Table 8 Characteristic IR absorption frequencies for C=O and N-H groups in segmented polyurethanes and polyureas.

Group	Mode	Frequency (cm^{-1})
N-H	Free	3445–3450
N-H	N-H ... N-H	3300–3340
N-H	N-H ... O (ether)	3260–3290
C=O (urethane)	Free	1730–1740
C=O (urethane)	C=O ... H-N	1703–1710
C=O (urethane)	C=O ... H-N	1680–1695 (ordered)
C=O (urea)	Free	1690–1700
C=O (urea)	C=O ... H-N	1660–1670 (disordered)
C=O (urea)	C=O ... H-N	1630–1645 (ordered)
NH-C=O	Amide II	1540–1560

There are two regions of FTIR spectra which get particular interest in the investigation of phase separation of segmented polyurethanes. The first area of interest is the N-H stretching region, which is located between 3100 - 3500 cm^{-1}. This region is shown in

Figure 26 for PU films prepared with different hard segment ratios. In the present spectra, the N-H stretching without occurrence of hydrogen bonding is located at 3445 cm^{-1}. The peak at 3415 cm^{-1} corresponds to vibrations of N-H group connected by ∏ electrons in the aromatic ring. The disordered, hydrogen-bonded N-H groups are characterized by absorbance near 3300 cm^{-1}. The intensity around 3300 cm^{-1} increases with hard segment content from 5PU to 10PU with exhibiting broadening in this region.

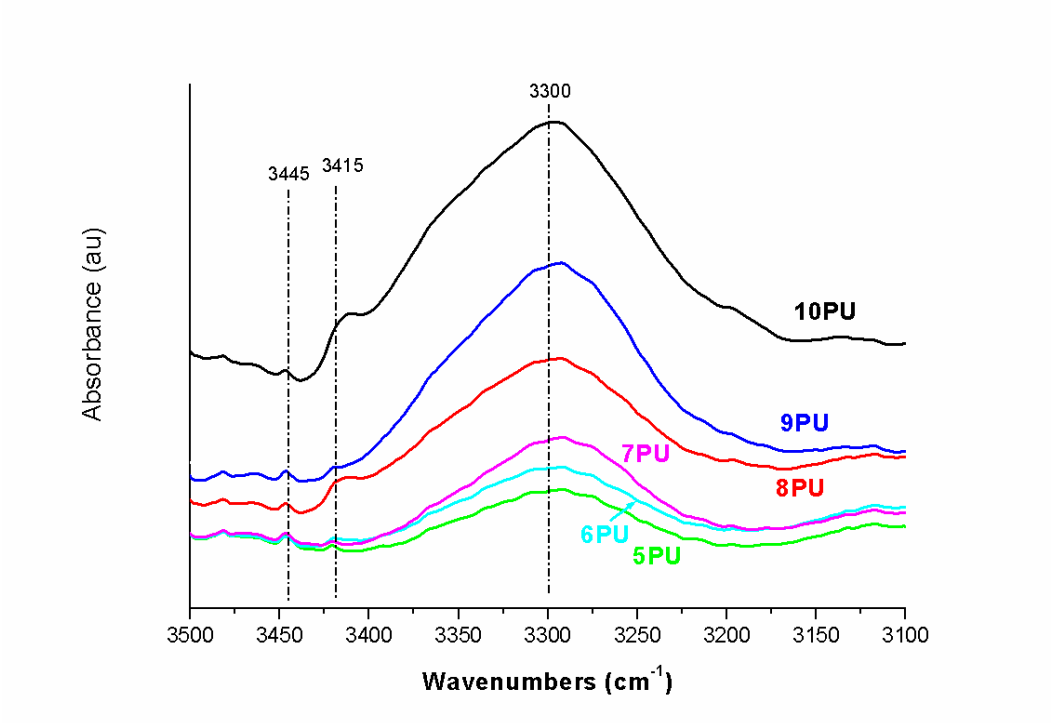

Figure 26 FTIR spectra of PU films in the N-H stretching region.

The second region is the carbonyl stretching region, which is located between 1640 - 1780 cm^{-1} (Figure 27). The hydrogen-bonded and non-bonded urethane C=O are found at 1716 cm^{-1} and 1732 cm^{-1}, respectively. Ordered hydrogen bonded C=O peak in urethane C=O stretching is observed at 1684 cm^{-1}. Due to the excess of TDI in

composition, urea groups are also presented in the PU structure and free urea C=O peak is observed at 1698 cm^{-1} while disordered urea C=O is observed at 1670 cm^{-1}. Non-bonded carbonyls may not be completely 'free', as the corresponding N–H in the urethane linkage may be bonded to another carbonyl, or to ether oxygen of the soft segment. In Figure 27 it is seen that the intensity of urethane C=O region around 1716 cm^{-1} increases with increasing hard segment content up to 10PU, indicating an increase in hard–soft segment microphase separation with increasing hard segment content [96].

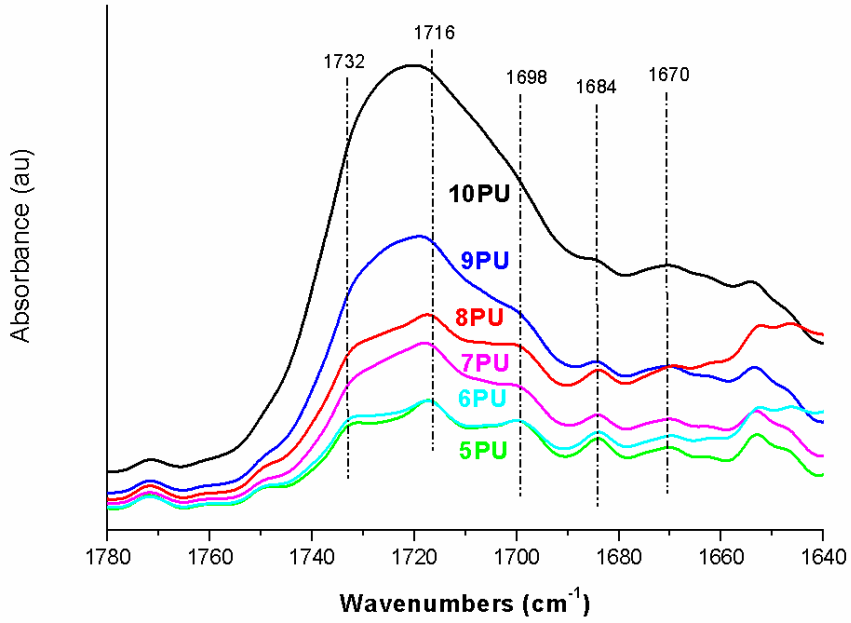

Figure 27 FTIR spectra of PU films in the carbonyl stretching region.

3.2.3 Gel Permeation Chromatography Results

The average molecular weight of 8PU prepolymer and its molecular weight during curing process were determined by gel permeation chromatography (GPC) and the results are tabulated in Table 9. GPC traces showed that the molecular weight of

prepolymers increased during the curing step. GPC analysis were carried out as long as the prepolymers are soluble in THF. During the curing process, solubility of 8PU prepolymer in THF was decreased, also branching of polyurethane was observed as an increase in heterogenity index (HI). After 18h of curing, prepolymer becomes insoluble in THF. The molecular weight distribution plots were also given in Appendix A.

Table 9 Average molecular weights and HI values of 8PU prepolymer.

Sample	Mn (g/mol)	Mw (g/mol)	HI
PU prepolymer (0h cured)	8647	9238	1.0684
PU prepolymer (6h cured)	14756	18567	1.25827
PU prepolymer (12h cured)	26271	70393	2.67947
PU prepolymer (18h cured)	30131	83138	2.75917

3.2.4 Dynamical Mechanical Analysis Results

Polyurethane elastomers are block polymers whose chains are composed of alternating low glass-transition temperature (Tg) 'soft segments' and rigid urethane 'hard segments'. The hard and soft segments are joined end-to-end through covalent urethane bonds and, therefore, polyurethanes are classified as multiblock copolymers. The differences in polarity between the hard and soft segments render these regions incompatible and the result is that they do not mix on a molecular level, producing a microphase segregation. The hard segment rich domain is generally characterized as semi-crystalline and provides stiffness and reinforcement to the polymer. The soft segment domains are responsible for elastic behavior and are usually amorphous with a Tg below room temperature [97].

Dynamic mechanical behaviors of the samples were studied to determine the relationship between dynamic properties (tan delta, storage modulus E' and loss modulus E") and structural properties of PU films. The moduli of polymers are temperature dependent and the mechanical properties change significantly around Tg. In dynamic mechanical studies, the storage modulus decreases rapidly and loss modulus, tan delta exhibit maxima at glass transition temperature. Storage modulus (E') is an index of elastic behavior, it was found to decrease with increasing temperature [83]. Figure 28 compares the elastic behaviors (storage modulus, E') of the PU films as a function of temperature at 1Hz.

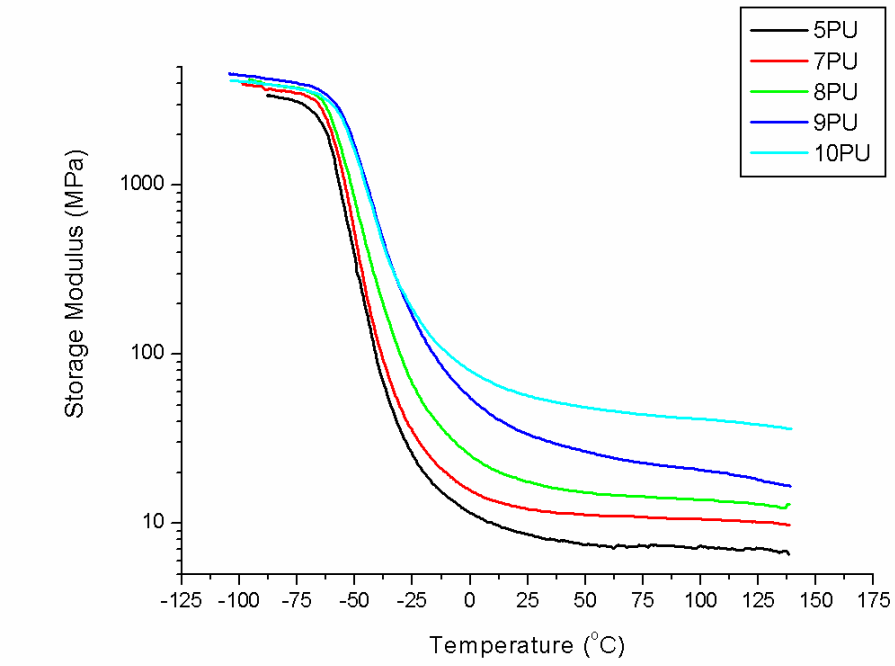

Figure 28 Storage modulus versus temperature curves of PU films at 1Hz.

At temperatures below Tg, like all glassy materials, all compositions of PU films have almost the same value of modulus. At that glassy plateau region E' was found to be

around 4170 MPa for all PU samples. With an increase in temperature, modulus rapidly drops in the region of Tg and reaches to a secondary plateau region called rubbery plateau. Also storage modulus E' is a measure of material stiffness and can be used to provide information regarding polymer molecular weight, degree of cure and crosslink density [98]. The difference between the storage modulus ΔE' in the plateau regions before and after the glass transition is related to the degree of crosslink density. A smaller ΔE' is associated with greater crosslink density. With the incorporation of higher amounts of TDI from 5PU to 10PU, the hard segment amount in the composition increases, crosslinking increases and this leads to a smoother decrease in the slope of E' through the rubbery plateau region. Measurements of ΔE' for PU films indicated that 10PU demonstrated highest crosslink density (smallest ΔE') compared to others. This also shows that with an increase in the TDI amount, the crosslink density increases. Polyurethanes are commonly used in the production of medical devices ranging from catheters to total artificial hearts. This utilizes the importance of dynamical mechanical properties at room temperature and body temperature. Therefore, the storage modulus values of the prepared PU films were calculated at both 25°C and 37°C, and are given in Table 10.

Table 10 Storage modulus of PU films at 25°C and 37°C

Sample	E' (MPa) at 25°C	E' (MPa) at 37°C
5PU	8.55	8.07
7PU	12.27	11.80
8PU	17.61	16.33
9PU	33.70	30.06
10PU	57.40	54.21

According to E' values at 25°C and 37°C, the PU films gains stiffness, rigidity and resistant to elongation and mechanical deformation with an increase in hard segment content. On the other hand, there is a small decrease in E' values (about 0.5 – 3.2 MPa) as the temperature increase from 25°C to 37°C.

The loss factors (loss modulus and tan delta) are very sensitive to the molecular motions. Loss modulus and tan delta exhibits a maxima at glass transition temperature (Tg) with the initiation of the micro-brownian motion of the polymer chains in the amorphous regions (soft segment) of the polyurethane elastomer [99]. The loss modulus (E") behavior of PU films with temperature (at 1Hz) is given in Figure 29 and the change in tan delta is given in Figure 30.

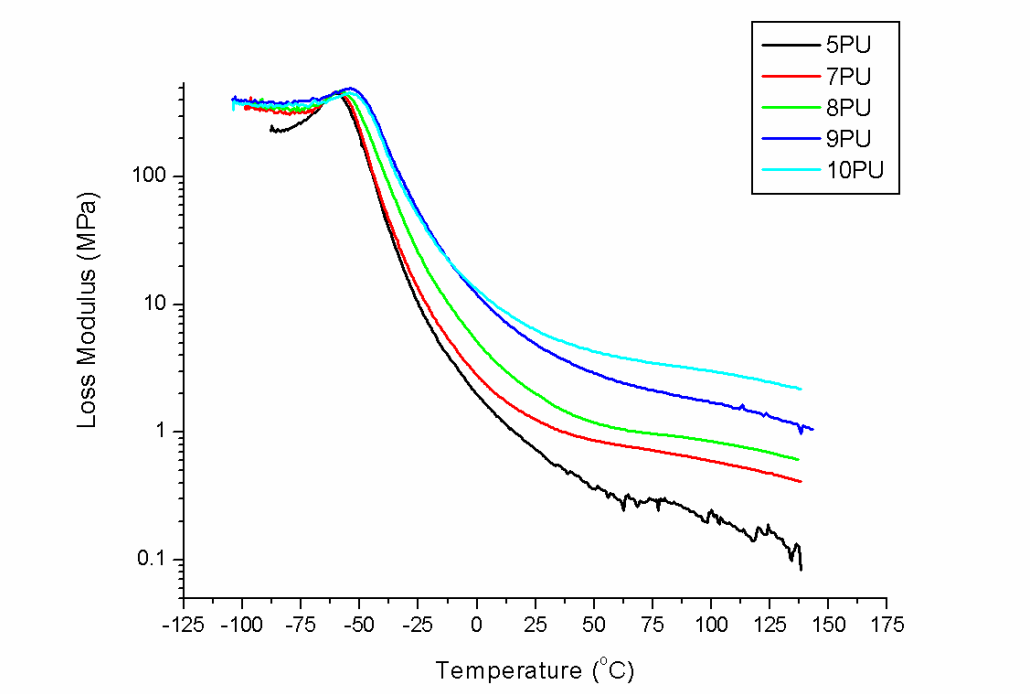

Figure 29 Loss modulus versus temperature curves of PU films at 1Hz.

The relative heights of the tan delta, ratios of loss modulus (E") to storage modulus (E'), are known to be an in indicator of capability of energy dissipation within the microstructures of the PU films [100]. Tan delta peak maxima give the corresponding Tg of the samples. The data show that, the tan delta peak magnitude and Tg are sensitive to the composition of the PU films.

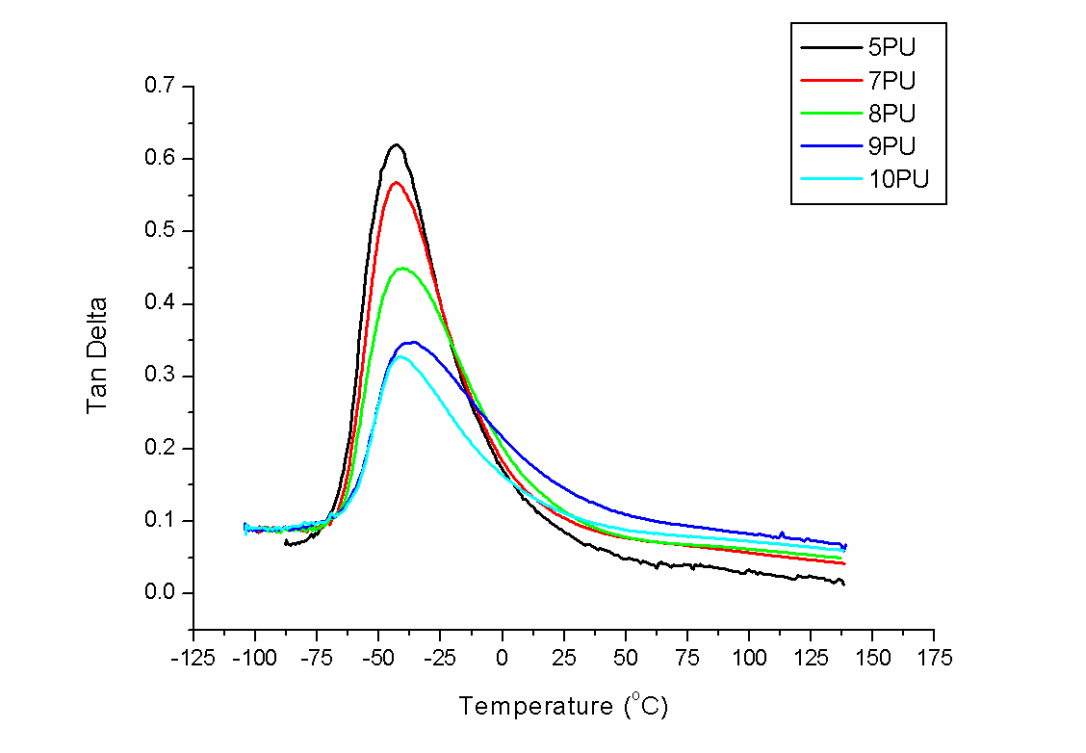

Figure 30 Tan delta versus temperature curve.

As seen in Figure 30, as the hard segment content of the polyurethane is increased from 5PU to 9PU, the tan delta peak magnitude decreased and the capability of energy dissipation as heat within microstructures upon mechanical deformation decreased, also the glass-transition temperature was shifted to slightly higher temperatures. The increasing hard segment content results in larger hard microcrystalline domains that

restrict the molecular motion of the soft segment thereby increasing the glass-transition temperature. For 10PU sample due to excess amount of TDI high amount of microphase separation between hard and soft segments was occurred and Tg value was found to be quite lower compared to 8PU and 9PU samples. The height of the tan delta peak is related to the amount of the soft segment present. Also sharper tan delta transition suggests more uniform crosslink density, where broader tan delta suggests greater degree of heterogeneity in crosslinking [97]. As shown in Figure 30, only one major α relaxation (single Tg) is observed for all films indicating a single homogeneous phase in all compositions. The Tg and the tan delta values of the PU samples are summarized in Table 11.

Table 11 Tan delta peak magnitude and Tg of PU samples at 1Hz.

Name	Tg °C	Tan delta
5PU	- 43.08	0.62
7PU	- 42.63	0.57
8PU	- 40.94	0.45
9PU	- 38.14	0.35
10PU	- 41.63	0.32

The dynamic mechanical analyses of all samples were carried on at oscillatory tension mode with different frequencies. It is known that the mechanical behaviors of polymers are depending on frequency. The effect of frequency on storage modulus and tan delta for sample 5PU are shown in Figure 31 (a) and (b), respectively. As can be observed from Figure 31 (a) with an increase in frequency, the storage modulus of the sample was increased, this is known as strain hardening of the polymer.

Above Tg there is an increase in free volume and allows space for molecular motions to occur easily. Significant damping occurs when the applied test frequency is equal to the natural frequency of the main chain motion. At higher frequencies there will be unsufficient time for chain uncoiling to occur and the material will be relatively stiff.

Figure 31 (b) shows the tan delta curves obtained at different strain rates. Since the Tg values were obtained from maximum tan delta peaks, it was observed that the glass transition temperature shifts to higher values, with increasing frequency. For 1Hz the Tg was obtained as -43°C. As frequency increase to 2 Hz, 4 Hz, 10 Hz and 20 Hz Tg was obtained as -42°C, -40°C, -38°C, -36°C, respectively. The glass transition region and maxima of tan delta linearly shifted to higher temperatures with an increase in frequency.

For all the prepared samples, storage modulus, loss modulus and tan delta curves at all frequencies were plotted, Tg values were tabulated and shown in Appendix B.

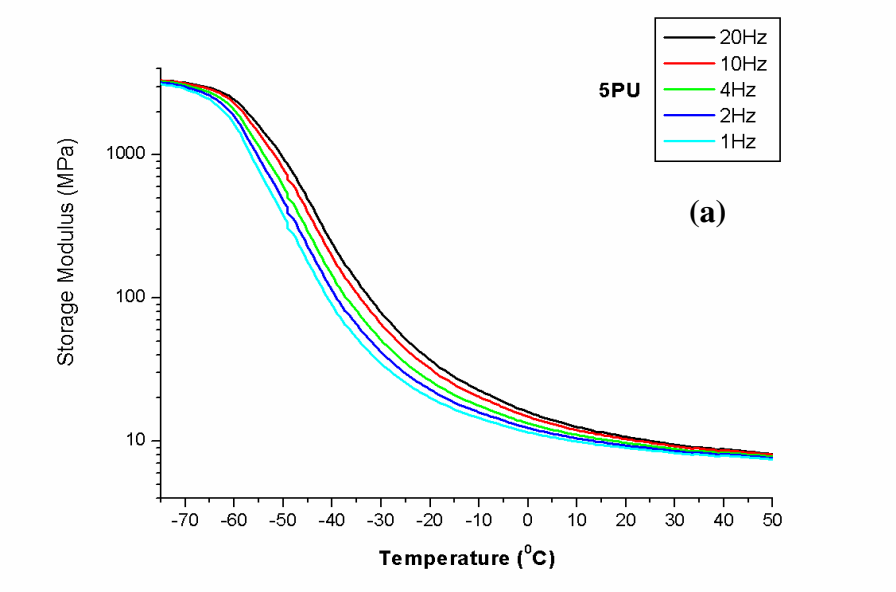

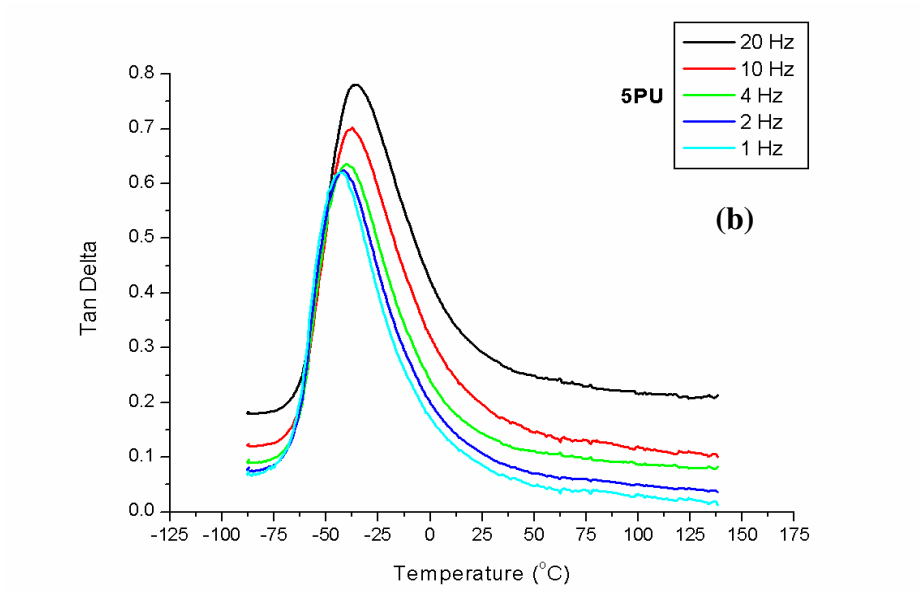

Figure 31 DMA curves of 5PU sample at different frequencies (a) Storage modulus versus temperature, (b) Tan delta versus temperature.

Figure 32 shows the glass transition temperature shift with frequency. For all samples it was observed that glass transition temperature shift is almost linear with frequency. This is a shift in 'apparent glass transition temperature', meaning the glass transition temperature that the material mechanically recognizes at certain frequency. The Tg values of all samples obtained from tan delta peak maxima at all frequencies were given in Appendix B.

There is a linear relationship to high strain rate regime. The extrapolation of these linear lines to the higher frequency regime can make it possible to estimate the temperature dependence of the modulus at high frequencies.

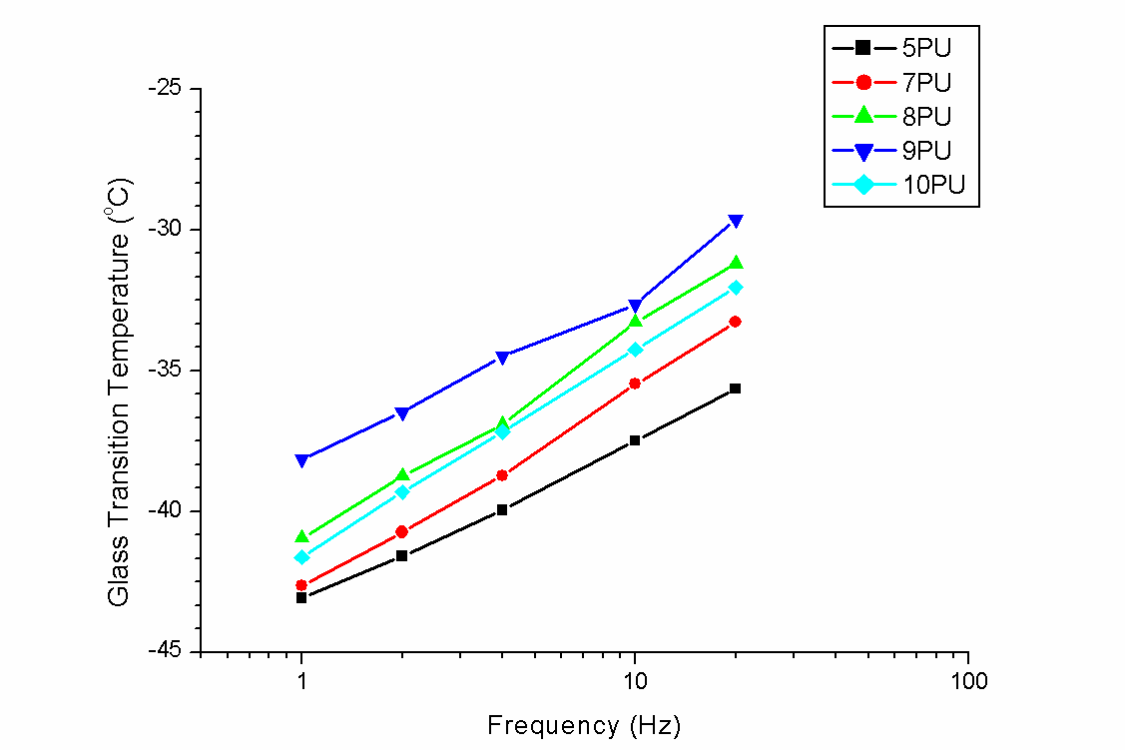

Figure 32 The Tg shifts at different frequencies.

3.2.5 Mechanical Test Results

In mechanical tests, samples are subjected to a progressively increasing tensile force until it fractures. The strain is directly proportional to the stress and the specimen returns to its original length upon the removal of stress. In this region load is not enough to cause permanent shifting between the molecules. Beyond this elastic limit the applied stress produces plastic deformation, so the permanent extension remains by the removal of applied load. The tensile strength of a polymer is defined as the force required to break a sample by tensile force. In the linear elastic regions, the ratio of applied stress to the amount of elongation gives modulus of elasticity. The maximum force which cause break of the sample is reported as tensile strength, and the elongation is compared to the original sample is reported as percent elongation [101].

Molecular weight, crosslinking, and other chemical structure affect tensile properties of polymers. Tensile strength of the prepared PU samples are related to the inter- and intramolecular forces that hold the polymer together under stretching stress. The backbone of PU, consists of different covalent bonds and the urethane bond is the common one besides ethers, esters, amides and aromatic linkages. Each bond has a cohesive energy that defines how much energy is required to tear it apart physically. This characteristic clearly has an effect on the strength of the polymer. Table 12 compares the cohesive energies of most of the important chemical bonds in PU [101].

Table 12 Molar cohesive energy of organic groups in polyurethanes.

Group	Cohesive Energy (kcal/mol)	Cohesive Energy (kJ/mol)
–CH– (Methylene)	0.68	2.84
–O– (Ether)	1.00	4.18
–COO– (Ester)	2.90	12.14
$–C_6H_4–$ (Aromatic)	3.90	16.33
–CONH– (Amide)	8.50	35.59
–OCONH– (Urethane)	8.74	36.59

Molecular weight typically influences tensile strength up to some limiting value. Intermolecular forces, hydrogen bonding, van der Waals forces, and dipole moment tend to hold molecules together under stress in a way similar to the covalent bonding of a polymer backbone. The increase in hard segment content increases the brittleness, and decreases the elongation. Crosslinking in PU elastomers controls tensile strength and elasticity. The weight percent of hard segments controls stiffness. In polyurethanes, isocyanates and crosslinked domains are considered hard segments [3]. In this study, different amounts of hard segment containing PU films were prepared. Amounts of hard segment domains influenced the mechanical properties. It is known that increase in the proportion of hard segment in polyurethane elastomers gives the material higher modulus [84]. In tensile test experiments modulus of elasticity, ultimate tensile strength and elongation at break values were calculated and given in Figure 33-35. Also the summary of all mechanical results of the films are given in Table 13.

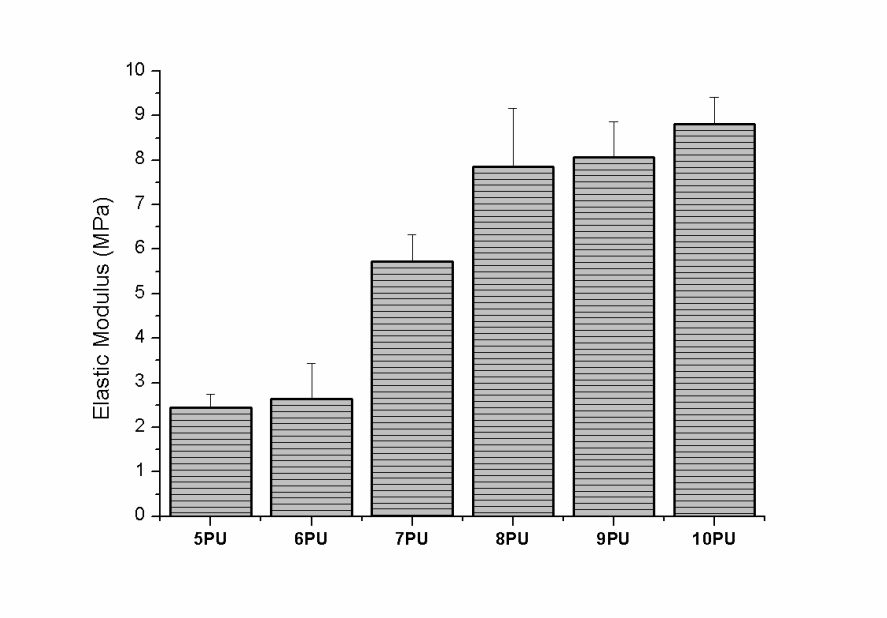

Figure 33 Elastic modulus of PU films.

The elastic modulus values were found as 2.44 MPa, 2.64 MPa, 5.72 MPa, 7.86 MPa, 8.07 MPa and 8.82 MPa for 5PU, 6PU, 7PU, 8PU, 9PU and 10PU, respectively (Figure 33). It was observed that elastic modulus was increased with an increase in hard segment content as expected since the polymer structure becomes stronger. There are similar results reported in literature [84-86].

Ultimate tensile strength (UTS) values are given in Figure 34. Increase in hard segment content, increased the UTS values leading to harder polymeric structures. For 5PU sample; UTS is found to 2.40 MPa. As the hard segment increased to 6PU, 7PU, 8PU, 9PU and 10PU, UTS values changed from 2.54 MPa, 4.99 MPa, 4.29 MPa, 4.11 MPa and 6.40 MPa, respectively. The increase in the UTS is due to the increase in the number of cross-links between the chains providing more resistance to the applied force. Also it is mentioned in the literature that, the increase in NCO/OH ratio increases the intermolecular attractions of the hard segments and decreases elongation [84, 85].

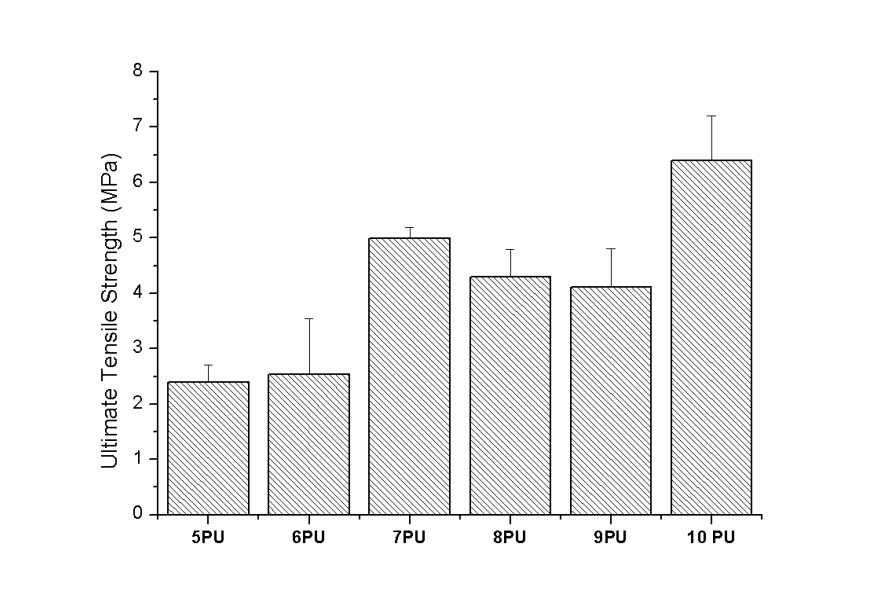

Figure 34 Ultimate tensile strength of PU films.

The elongation at break (EAB) values of PU films are shown in Figure 35. The 5PU sample showed the highest EAB value with about 303 %. Increase in hard segment content cause a decrease in elongation at break values to about 192 % for 10PU. The values of E, UTS and EAB for all the examined samples are given in Table 13.

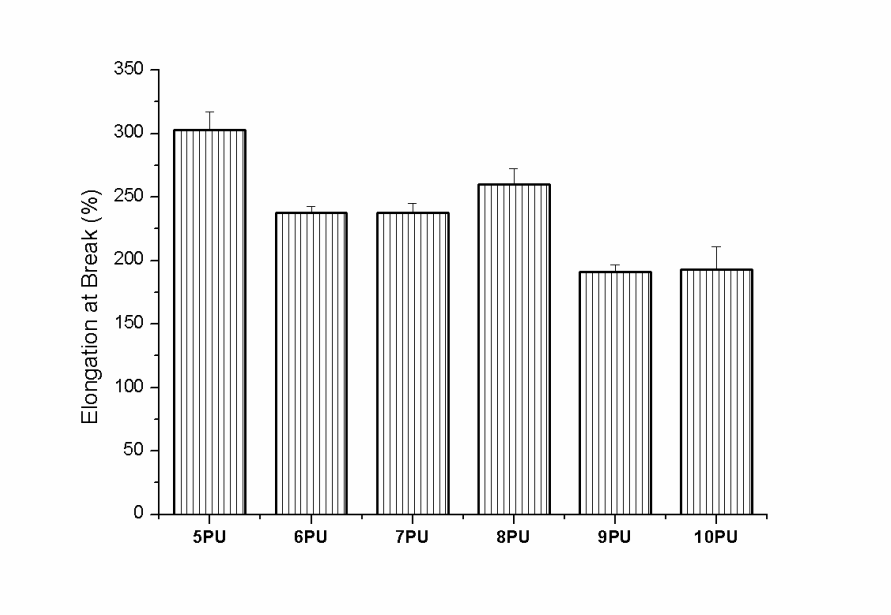

Figure 35 Percent elongation at break of PU films.

Table 13 Mechanical test results of all PU samples.

Sample	UTS (MPa)	E (MPa)	EAB (%)
5PU	2.40 ±0.3	2.44 ±0.3	302.75 ± 14.3
6PU	2.54 ± 1.0	2.64 ± 0.8	237.71 ± 4.76
7PU	4.99 ±0.2	5.72 ± 0.6	237.49 ± 7.68
8PU	4.29 ±0.5	7.86 ± 1.3	259.73 ± 12.8
9PU	4.11 ± 0.7	8.07 ± .0.8	191.00 ± 5.4
10PU	6.40 ±0.8	8.82 ± 0.6	192.91 ± 18.2

3.2.6 Thermogravimetric Analysis Results

Polyurethanes synthesized in this study are aimed to be used in the production of blood contacting biomedical devices. Therefore their thermal and mechanical stabilities at room and body temperatures are important. TGA analyses were performed for 5PU, 8PU and 10PU films to get a general idea about their degradation temperatures. Because of their complex segmented structures and complicated structures formed by degradation, it is difficult to relate the basic degradation mechanism. Figure 36 shows the TGA curves of 5PU, 8PU and 10PU films. All PU films decompose at temperatures over 200°C. 10PU sample started to decompose at 225°C. 5PU and 8PU started to decompose around 250°C. This may be due higher amount of microphase segregation between the hard and soft segment domains in 10PU sample. At 300°C, 15% of 10PU degrades while less than 10% of 8PU degrades. The TGA curves and first derivatives of the samples were also given in Appendix C.

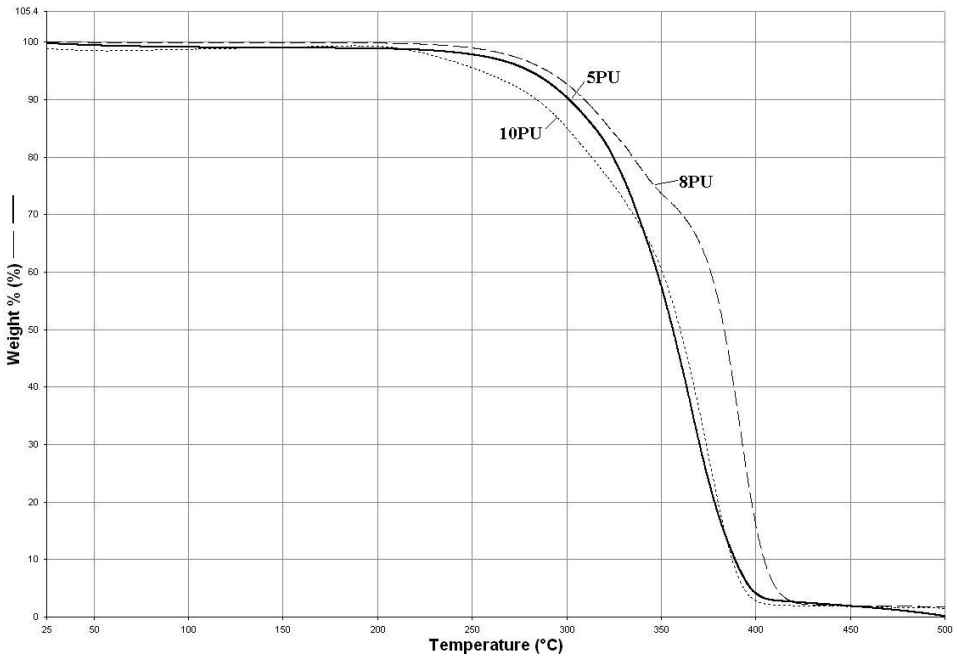

Figure 36 TGA curves of 5PU, 8PU, 10PU samples.

3.3 Surface Characterization Results

3.3.1 Surface Hydrophilicity Results

For the improvement of blood compatibility of PU films, surface modification steps were carried out by oxygen plasma treatment, acrylic acid grafting and finally two different types of heparin (UFH and LMWH) immobilization on to the PU surfaces. Surface hydrophilicities of the prepared PU films were studied with contact angle goniometry after each step of modification. The water contact angles on 8PU surfaces decreased from 77 to ~62 after oxygen plasma treatment and acrylic acid grafting (Table 14). It is expected that formation of the hydroperoxide or carboxyl groups generated by the oxidation of the PU surface increased surface polarity and caused a decrease in water contact angle. After immobilization of heparin, surface hydrophilicity increased more and contact angle values decreased down to 32° for PU-LMWH and to 39° for PU-UFH samples. PU-LMWH samples exhibited the lowest contact angle among all. Similar low contact angles were reported for unfractioned heparin [80].

Table 14 Water contact angle of PU and surface modified PU samples.

Sample	Water contact angle
8PU	76.45 ± 2.41
PU-plasma	62.16 ± 1.83
PU-AA	62.92 ± 1.17
PU-LMWH	31.80 ± 1.74
PU-UFH	38.48 ± 4.82

The increase of surface hydrophilicity by heparin immobilization has an importance in the surface-protein interaction since it creates biocompatible surfaces.

Another set of contact angle measurement was carried out with other three liquids (bromonapthalene, formamide and dimethyl sulfoxide) in addition to water in order to obtain the surface free energy values of PU films. Table 15 shows the equilibrium contact angle values of the liquids used for both untreated PU (8PU) and heparinized (PU-LMWH and PU-UFH) samples.

Table 15 The equilibrium contact angle values of different liquids.

Sample	Water	Formamide	Dimethyl sulfoxide	Bromonapthalene
8PU	76.45 ± 2.41	40.91 ± 3.27	34.38 ± 1.99	22.92 ± 2.06
PU-LMWH	31.80 ± 1.74	47.39 ± 7.35	44.78 ± 2.23	18.89 ± 5.55
PU-UFH	38.48 ± 4.82	40.35 ± 3.54	42.38 ± 4.26	19.317 ± 3.28

3.3.2 Surface Free Energy Results

The values of acidic basic components, polar dispersive components of the test liquids used in the experiments were obtained from the literature and are given in Appendix D [114, 115]. The surface free energy values of untreated PU (8PU), heparin immobilized PU samples (PU-LMWH and PU-UFH) obtained from the Owens-Wendt-Rabel-Kaelble (OWRK) method, Wu Harmonic Mean method and Acid-base (AB) method are tabulated in Table 16-18. The formulas used by the instrument for the calculation of SFE were given in Appendix D.

The OWRK method has been widely used for the calculation of the total surface energy and its corresponding polar and dispersive components. Generally, the polar component value is used as an estimation of the concentration of the polar groups on the polymer surface [103]. The total OWRK surface free energy values of the samples were found to be 39.08 mN/m for untreated PU, 56.04 mN/m for PU-LMWH and 54.45 mN/m for PU-UFH (Table 16). An increase in total OWRK surface free energy were observed after heparin immobilization. This is due to the increase of polar component values by introduction of additional polar groups (SO_3 and COO^-) of heparin molecules with the surface modification processes. Heparin immobilization resulted in a higher value of the polar component (31.30 mN/m for PU-LMWH and 27.17 mN/m for PU-UFH) compared to that calculated for untreated PU (4.79 mN/m).

Table 16 Surface free energy and its components calculated by OWRK method.

	OWRK Total SFE	OWRK Dispersive component SFE	OWRK Polar component SFE
Sample	γ_s (mN/m)	γ_s^d (mN/m)	γ_s^p (mN/m)
8PU	39.08	34.29	4.79
PU-LMWH	56.04	24.74	31.30
PU-UFH	54.45	27.28	27.17

Wu harmonic mean approach divides the surface energy into two components, dispersive and polar, and uses a harmonic mean equation to sum the dispersive and polar contributions. The total surface energy values obtained by the Wu harmonic mean method are given in Table 17 and the results correlate very well with the values achieved by OWRK method. According to Wu harmonic mean approach, the total

surface free energy values of the samples were found to be 41.10 mN/m for untreated PU, 59.90 mN/m for PU-LMWH and 58.34 mN/m for PU-UFH. The PU-LMWH had the highest total SFE and polar component value among all samples. The values obtained by OWRK and Wu harmonic mean approaches for SFE, dispersive and polar components were quite close to each demostrating similar trends for heparin modified samples.

Table 17 Surface free energy and its components calculated by Wu Harmonic Mean method

	WU Harmonic Total SFE	WU Harmonic Dispersive component SFE	WU Harmonic Polar component SFE
Sample	γ_s (mN/m)	γ_s^d (mN/m)	γ_s^p (mN/m)
8PU	41.10	32.98	8.12
PU-LMWH	59.90	26.78	33.12
PU-UFH	58.34	28.66	29.68

The term ‘‘polar’’ is used to designate three classes of compounds, namely: i) dipolar compounds; ii) hydrogen bonding compounds and iii) compounds that interact as Lewis acids and bases. The Van Oss–Chaudhury–Good theory distinguishes the acid–base (AB) interactions as a component of the surface free energy:

$$\gamma_s = \gamma_s^{LW} + \gamma_s^{AB} \quad \text{.....(3.1)}$$

where γ_s^{LW} is the surface energy corresponding to Lifshitz–Van der Waals forces and γ_s^{AB} describes the contribution of the AB interaction to the surface tension:

$$\gamma_s^{AB} = 2(\gamma_s^- \gamma_s^+)^{1/2} \quad \text{.....(3.2)}$$

where γ_s^- and γ_s^+ represent the ion pair donor (Lewis base) and the ion pair acceptor (Lewis acid) contributions, respectively [103].

Surface free energy and its components calculated by AB method are given in Table 18. PU-LMWH sample exhibited the highest total surface free energy value of 52.41 mN/m among all samples by acid–base (AB) method. Moreover, for all samples the acid component was found to be very small about 0.5-0.7 mN/m. An increase in acid-base interaction from 5.04 to 10.18 mN/m was observed by heparin immobilization. The basic component of acid–base interaction had an increase after heparin immobilization. The untreated PU films presented lowest basic component SFE values (3.65 mN/m) while PU-LMWH and PU-UFH samples present the higher values of the basic component (7.98 mN/m and 7.52 mN/m).

Table 18 Surface free energy and its components calculated by AB method.

	Acid Base Total SFE	Acid Base Lifshitz–Van der Waals component SFE	Acid Base Acid-Base intreaction	Acid Base Square root of acidic component SFE	Acid Base Square root of basic component SFE
Sample	γ_s (mN/m)	γ_s^{LW} (mN/m)	γ_s^{AB} (mN/m)	γ_s^+ (mN/m)	γ_s^- (mN/m)
8PU	46.19	41.15	5.04	0.69	3.65
PU-LMWH	52.41	42.23	10.18	0.64	7.98
PU-UFH	50.13	41.86	8.27	0.55	7.52

The type of adsorbed proteins and their orientation are related to the surface properties, especially the surface free energy. Moreover, it has been reported that the dispersive and polar components of the surface free energy are of key importance for the

interfacial interactions. It has been also reported that Lewis basicity is a key factor in surface biocompatibility [104].

3.3.3 Attenuated Total Reflectance-FTIR Spectroscopy Results

The ATR-FTIR spectra of PU films after each surface modification step are shown in Figure 37. No significant difference is observed in the spectra of control polyurethane (PU) and oxygen plasma treated polyurethane (PU-plasma) samples. This similarity in the spectra before and after plasma treatment may be the result of high penetration of infrared light so that it can not detect the plasma treated upper layers. The effect of plasma on the surface is only at a depth of few nanometers.

The ATR-FTIR spectra of PU-AA is also similar to that of PU; this may be due to the carbonyl adsorption of carboxylic acid groups of PU-AA overlapping with that of the urethane bond of PU. In the ATR spectra of heparin immobilized polyurethanes the intensity of the C=O peak at 1713 cm^{-1} decreased and the small peak at 1690 cm^{-1} corresponding to the strong H-bonding disappeared. 1600–1577 cm^{-1} aromatic region (C=C) of PU changed and the peak was shifted to 1583 cm^{-1} with the presence of carboxylate group of heparin. The C-H stretching of polyurethane CH_3 at 1373 cm^{-1} disappeared and heparin SO_2 asymmetrical stretching was observed at 1402 cm^{-1}. FTIR-ATR of both PU-LMWH and PU-UFH showed sharp shoulders around 1000-1100 cm^{-1}, compared with other samples, which were due to the symmetric stretching of S=O and C-O-C in the saccharide group of heparin. Also, the intensity of the CN stretching peak (1200 cm^{-1}) decreased and the absorbance at 1220 cm^{-1}, corresponding to sulfonic acid groups of heparin, significantly broadened. For these two peaks similar results were also reported in literature [77]. Since the characteristic absorption peaks of SO_3^- and C-O-C exists in heparin overlaps with the host PU peaks at 1000-1220 cm^{-1} range, further studies of heparin immobilized PU surfaces were carried out by using ESCA.

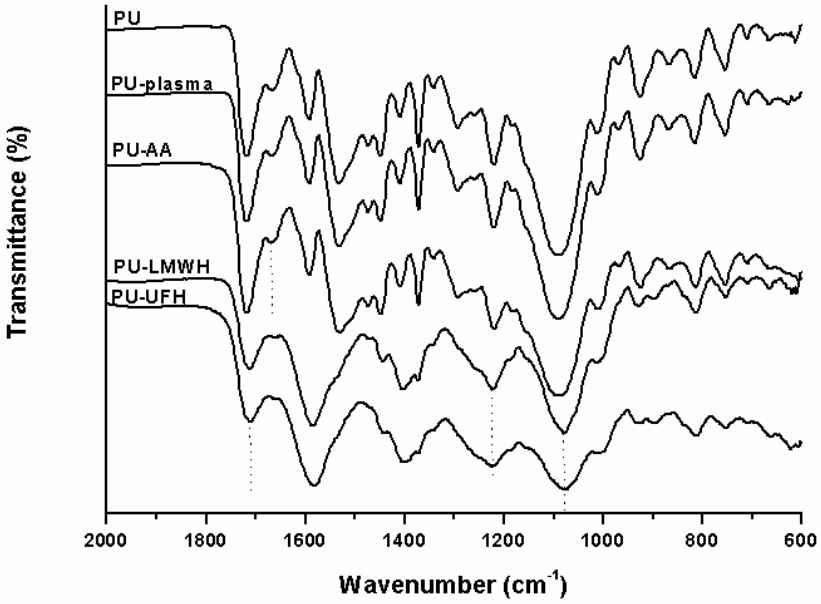

Figure 37 ATR-FTIR spectra of modified PU samples.

3.3.4 Electron Spectroscopy for Chemical Analysis Results

ESCA is a highly sensitive surface characterization technique, in which the chemical structure near the outmost of the surface (0.5-8 nm) can be analyzed with the quantification of surface atomic composition. Surface atomic compositions of untreated PU films and heparin immobilized PU films (PU-LMWH and PU-UFH) were analyzed by ESCA. In order to compare the pristine and heparin immobilized PUs, the core level spectra of different atoms of PU, PU-LMWH and PU-UFH were combined and the peaks corresponding to oxygen-1s core level (binding energy, 540-525 eV), nitrogen-1s core level (binding energy, 408-396 eV), carbon-1s core level (binding energy, 294-278 eV) and sulfur-2p core level (binding energy 174-162 eV) are presented in Figures 38 – 41, respectively.

The oxygen-1s spectra (Figure 38) and nitrogen-1s spectra (Figure 39) of both PU-LMWH and PU-UFH are slightly broadened due to increase of oxygen and nitrogen content of heparinized surfaces.

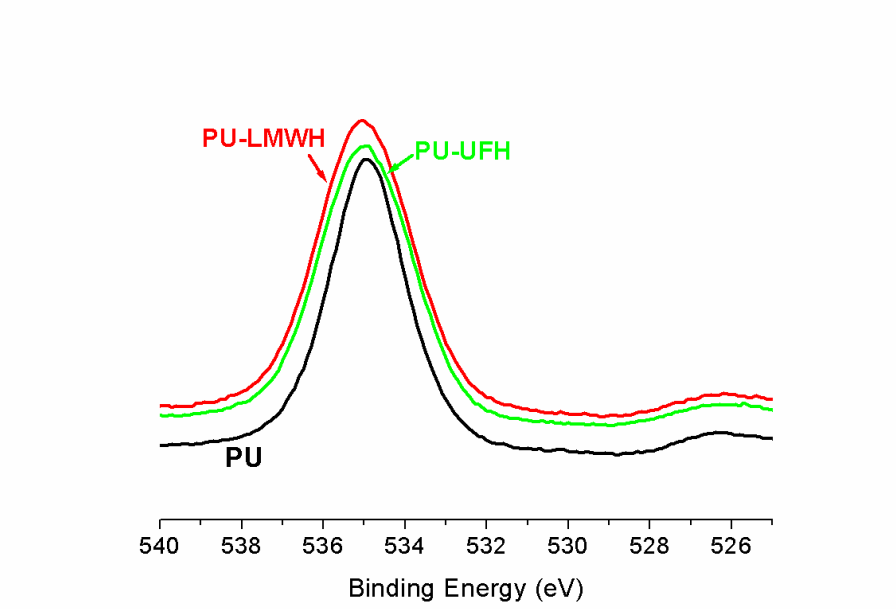

Figure 38 ESCA Oxygen-1s core level spectra of PU, PU-LMWH, PU-UFH.

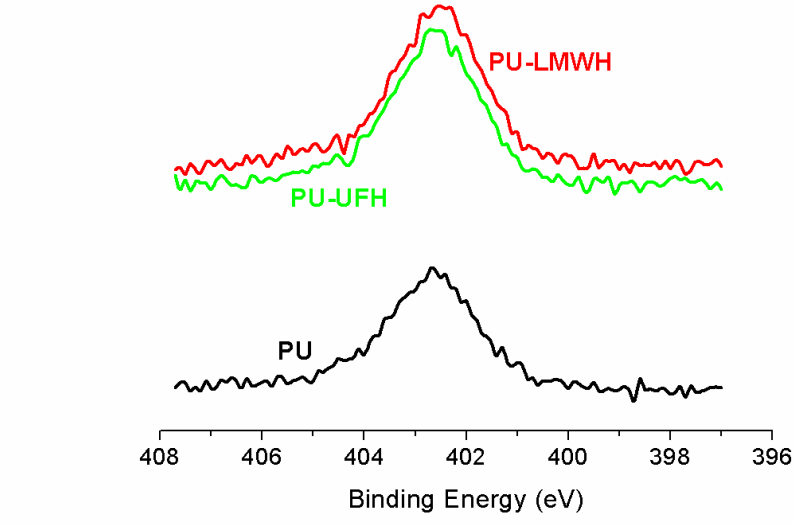

Figure 39 ESCA Nitrogen-1s core level spectra of PU, PU-LMWH, PU-UFH.

The carbon-1s core level spectra of all films had a peak maximum at 285 eV resulting from hydrocarbon C-C backbone. After heparin immobilization, the C-1s spectra of PU-LMWH and PU-UFH became broadened as a result of overlapping of signals for many carbon sources (Figure 40). The shouldering at 286.6 eV corresponds to C-O from both PU and heparin immobilized PU surfaces, finally peak broadening at around 289 eV belongs to carboxyl groups of heparin [22].

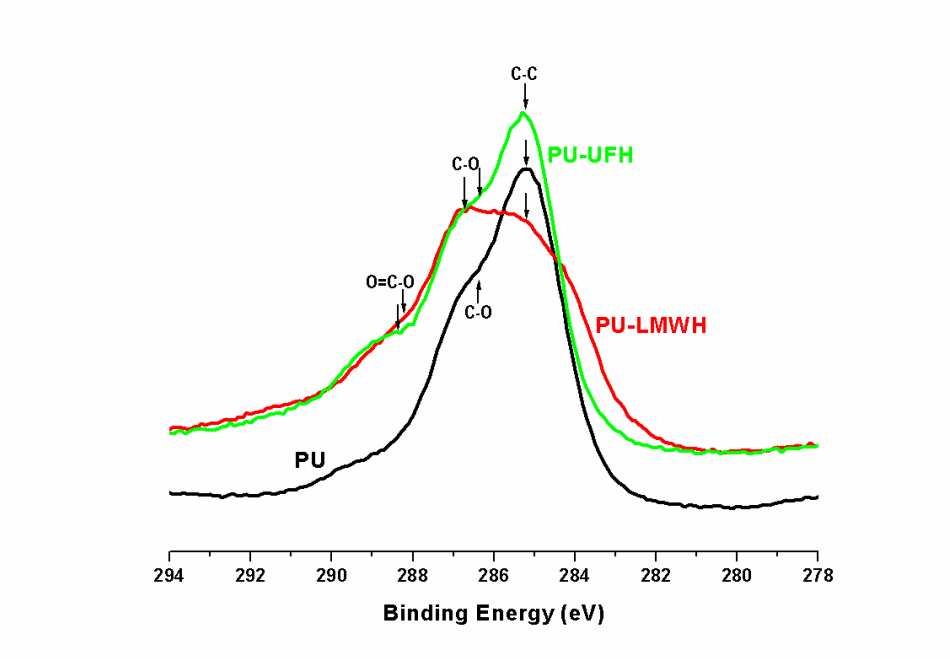

Figure 40 ESCA Carbon-1s core level spectra of PU, PU-LMWH, PU-UFH.

Figure 41 shows sulfur-2p core level spectra and the samples of PU-LMWH and PU-UFH exhibited a peak at 168 eV which is based on the sulfonate group ($-SO_3Na$) resulting from immobilized heparin [105]. The chemical structure of heparin molecule is also shown in Figure 41. These results indicate that both types of heparin were covalently bonded onto the surfaces of the PU-LMWH and PU-UFH samples.

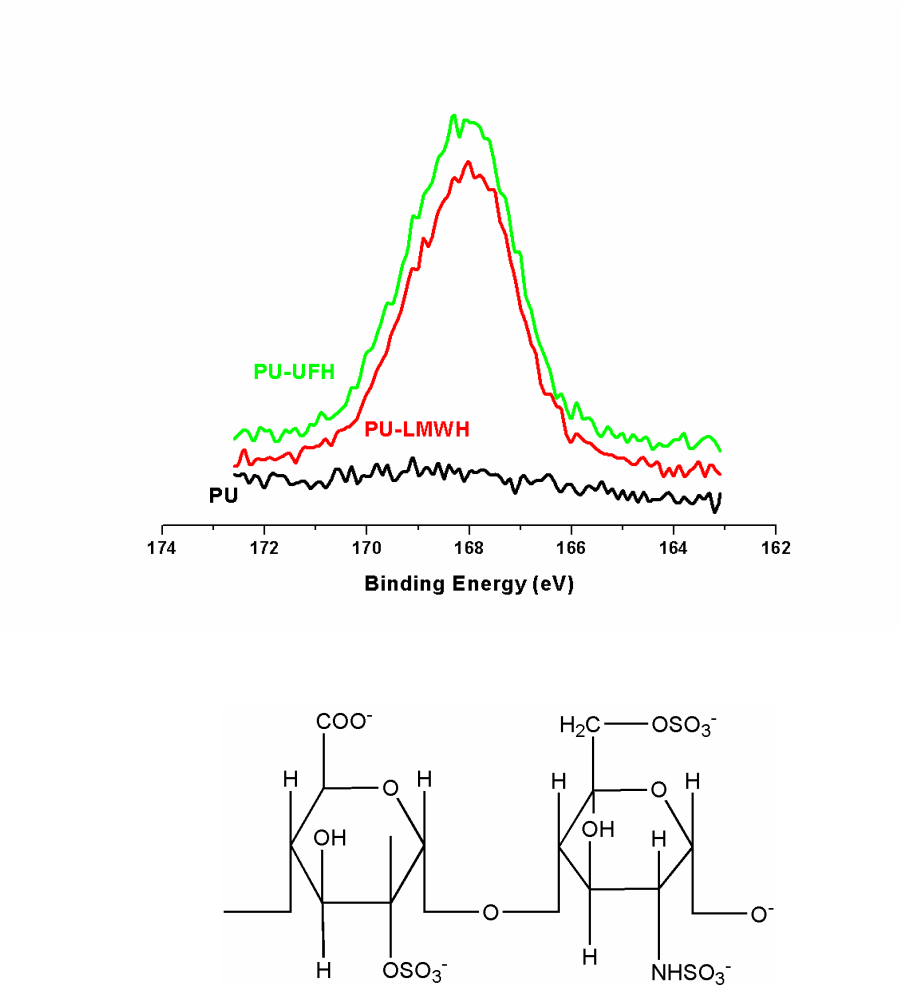

Figure 41 ESCA Sulfur-2p core level spectra of PU, PU-LMWH, PU-UFH and chemical structure of heparin.

The surface atomic compositions obtained from ESCA survey scan spectra are given in Table 19. It can be seen that after the surface modification by acrylic acid grafting and heparin immobilization, the oxygen atomic content has slightly increased from 33% (PU) to 33.7% for PU-UFH and 35.4 % for PU-LMWH. Nitrogen content has also increased from 2.5% (PU) to 2.8 % for PU-UFH and 3.1% for PU-LMWH. Sulfur, which is an indicative atom for heparin immobilization, was found on both heparin modified surfaces to be at the level of ~1.7%.

Table 19 Surface atomic compositions of samples calculated from ESCA survey scan spectra.

	Atomic %			
Sample	C 1s	O 1s	N 1s	S 2p
PU	64.5	33.0	2.5	-
PU-LMWH	59.8	35.4	3.1	1.7
PU-UFH	61.8	33.7	2.8	1.8

3.3.5 Atomic Force Microscopy Results

Application of the surface modification techniques completely changes the surface properties and the surface topographies of the samples. The best method for investigating the surface topography of the sample with high resolution, is to perform atomic force microscopy (AFM).

Heparin layer morphology; uniformity of coating, the part of the heparin molecule attached on the material surface and heparin molecule conformation plays an important role in hemocompatibility of the material. The formation of a uniform heparin immobilization on the biomaterial surface is very important for its performance, because the presence of incomplete heparin coating or crevices permit platelet adherence and aggregation on the surface [106].

Surface topography of untreated PU, heparin immobilized PU surfaces (PU-UFH and PU-LMWH) were observed by AFM (Figure 42). The untreated PU surface was very smooth compared with heparin immobilized samples. UFH immobilized PU surface shows a dendrite-like morphology of high molecular weight heparin chains with uniform distribution of heparin layer. Similar surface topographies were reported by AFM for unfractioned heparin on silicon surfaces [107]. LMWH immobilized PU

showed less uniform heparin immobilization compared with PU-UFH and this may be an important factor affecting the blood cell adhesion evaluations.

These heparin immobilized samples were hard zoomed at smaller area (12.5 μm x 12.5 μm) in order to observe the detail of morphology of heparin layer (Figure 43). Untreated PU and oxygen plasma treated PU samples had smooth surfaces (Figure 43 a and b) while LMWH and UFH modified surfaces presented different topographies. In the hard zoomed patterns, it is more clear to observe PU-LMWH chains showed a brush like morphology of short heparin chains (Figure 43 c) where PU-UFH showed an ordered structure with a preferential orientation of long heparin chains (Figure 43 d). PU-UFH surface demonstrated helical conformation of the high molecular weight heparin chains. In both cases heparin molecules demonstrated self assembled organization. This difference in the morphology may influence the level of platelet adhesion and thrombus formation. Some extra AFM images are given in Appendix E.

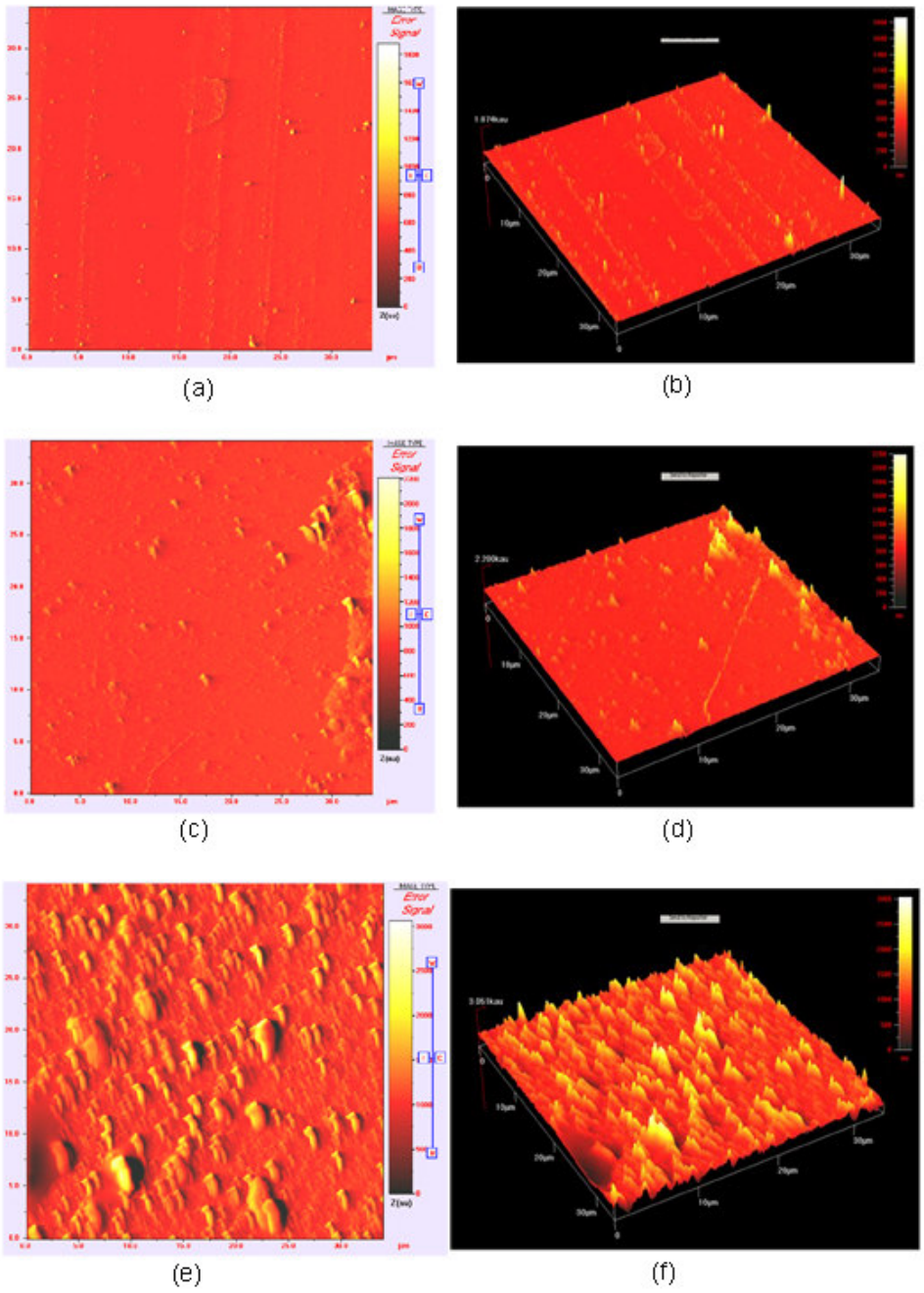

Figure 42 AFM images in non-contact mode for surfaces of (a-b) PU, (c-d) PU-LMWH, (e-f) PU-UFH. The scan size is 30 μm x 30 μm.

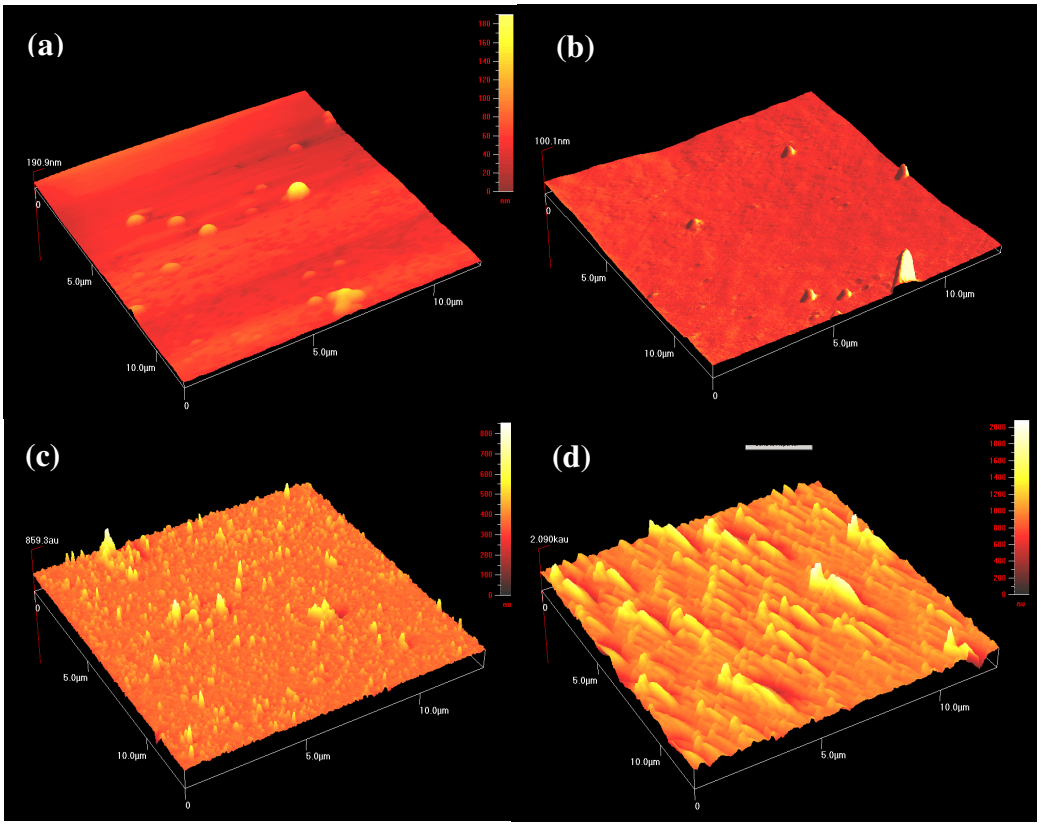

Figure 43 Hard zoomed AFM images (a) PU, (b) PU-oxygen plasma treated, (c) PU-LMWH, (d) PU-UFH. The scan size is 12.5 µm x 12.5 µm.

3.4 Blood Cell Adhesion Studies

In blood cell adhesion studies on untreated PU and two different type heparin immobilized polyurethane surfaces (PU-LMWH and PU-UFH) were brought into contact with fresh human blood at 37°C for 15 min then fixed with glutaraldehyde solution as given in the Section 2.5.2. It is known that heparin prevents blood coagulation and platelet adherence. Blood cell adhesion studies demonstrated that cell adhesion was reduced and blood compatibility of the material was improved after heparin immobilization (Figure 44). Also it is important to know that no thrombi formation was observed during these tests since the samples were treated with blood collected in anticoagulant additive tubes (Section 2.5.1).

Pristine samples demonstrated very high adherence of red blood cells having more than 50,000 cell/mm^2 (Figure 44-a and b) while the cell adherence decreased to ~14,000 cell/mm^2 for PU-LMWH (Figure 44-c and d), and only a little adhesion ~3,000 cell/mm^2 has occurred for PU-UFH (Figure 44-e and f). From these results, it may be concluded that heparin immobilization improved the anti-adhesion effect of blood cells on the surfaces compared to untreated PU. It is mentioned in the literature that, there is no main factor, but several factors affect cell-material interaction on the surface. These are the surface characteristics like; topography, wettability, surface energy, surface chemistry etc [58]. The water contact angles on PU surfaces were found to be 76° and after surface modification, surface hydrophilicity increased more and contact angle decreased down to 39° for PU-UFH samples, and 32° for PU-LMWH. This may also play an important role on the adhesion of proteins and preventing adhesion of blood cells on the surfaces of the modified samples.

In this study, UFH immobilized surface exhibited a more anti-adhesion effect on blood cells than LMWH immobilized surface. This may be due to; the more uniform heparin layer of the UFH immobilized surface compared with LMWH immobilized surface or it may be due to the result of the different biological activities of LMWH and UFH. For heparins in order to produce an anticoagulant effect; formation of ternary complex of heparin, anti-thrombin, and thrombin is necessary. Also it is known that minimum chain length of 18 saccharides in heparin structure is required for the formation of heparin, anti-thrombin, and thrombin ternary complex. Only 25% to 50% of LMWH species are above this critical chain length and able to form this ternary complex. In contrast to LMWH, all UFH molecules contain at least 18 saccharide units and have longer chain and able to form this tertiary complex [73]. This may be the biological activity point of the obtained results. In order to have more detailed information about the blood compatibilities of heparinized surfaces, more detailed tests were performed starting from the protein adsorption tests which are the first steps taking place in blood coagulation cascade during the blood-material interaction.

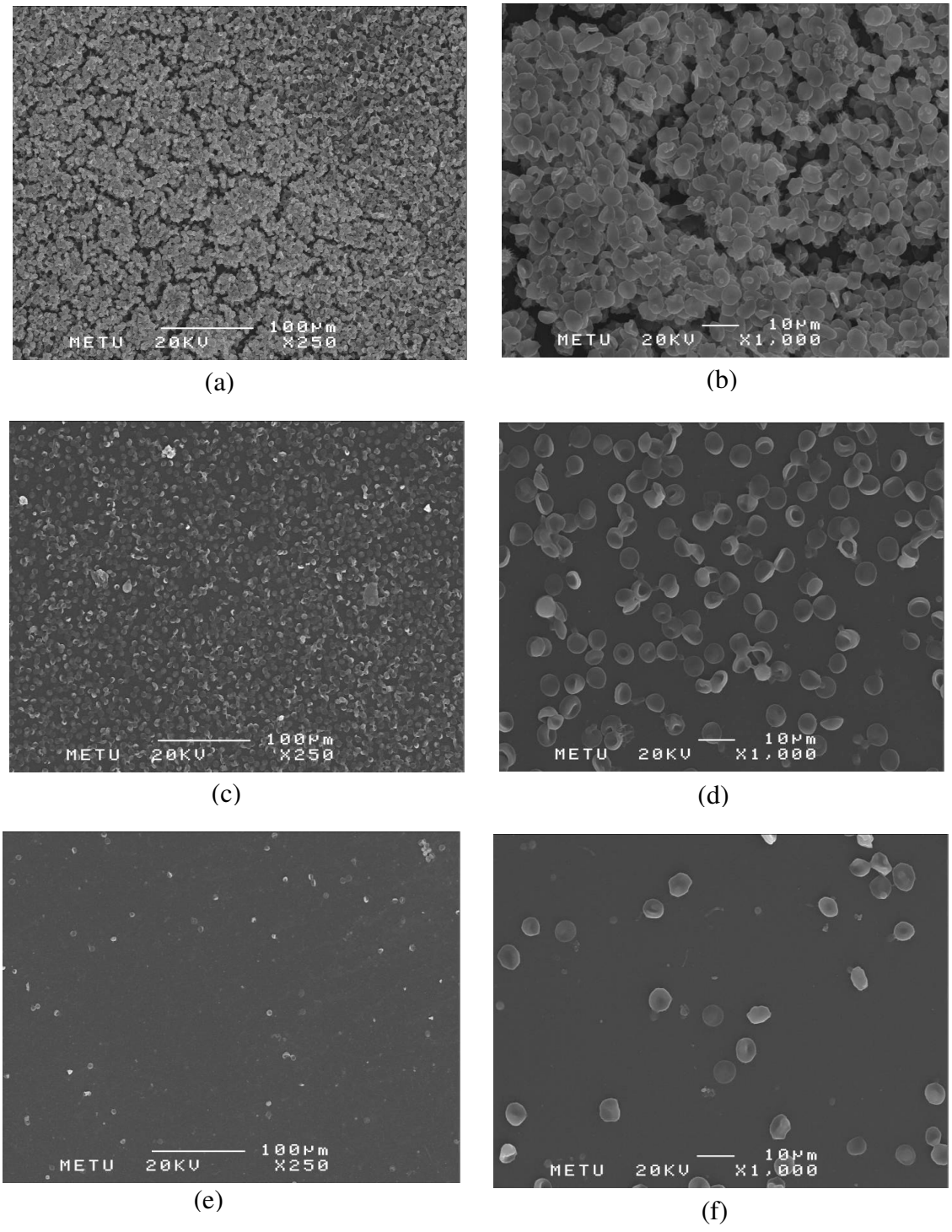

(a) (b)

(c) (d)

(e) (f)

Figure 44 SEM images after blood contact (a) PU (250x), (b) PU (1000x), (c) PU-LMWH (250x), (d) PU-LMWH (1000x), (e) PU-UFH (250x), (f) PU-UFH (1000x)

3.5 Protein Adsorption Studies

3.5.1 Amount of Adsorbed Plasma Proteins on Surfaces

Human platelet poor blood plasma (PPP) was incubated on the surfaces of PU-LMWH, PU-UFH, control PU samples and on TCP for 5 min, 15 min, 25 min periods. The amounts of plasma proteins adsorbed on each surface during these incubations were measured by NanoDrop spectrophotometer and the values of the protein amounts adsorbed per unit area on each sample after incubation with human PPP the results are shown in Figure 45.

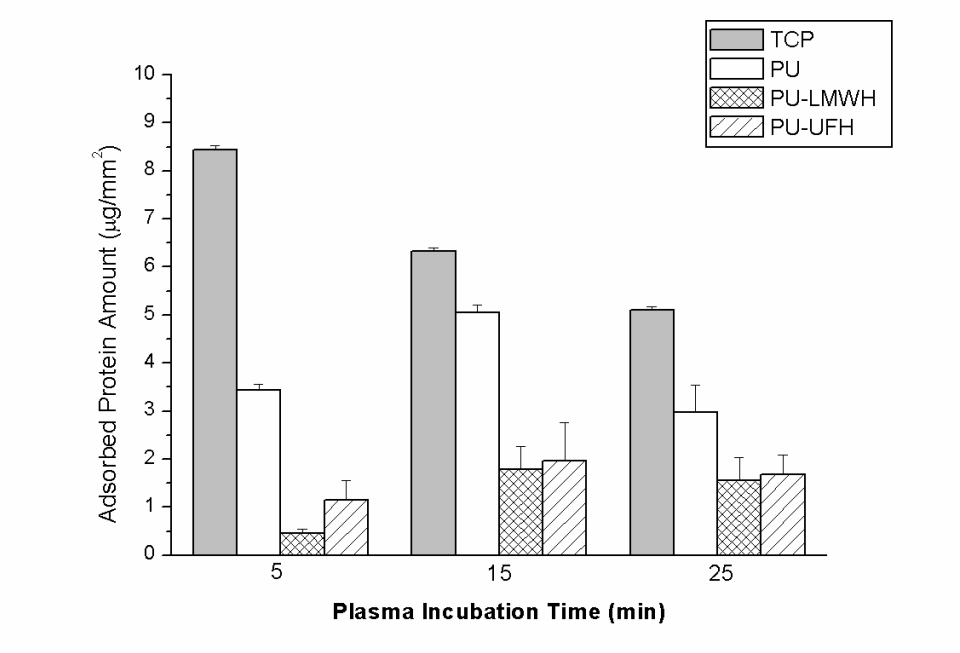

Figure 45 Adsorbed protein concentrations on the samples.

Different protein adsorption kinetics was highlighted for the various materials tested. TCP demonstrated the highest initial adsorption (8.44 μg/mm^2) decreasing over time (down to 6.32 μg/mm^2 and 5.10 μg/mm^2 for 15 and 25 min, respectively). PU showed

an increase in total protein adsorption with a peak at 15 min (5.04 μg/mm^2), while the modified materials adsorbed initially quite low (0.46 μg/mm^2 for PU-LMWH and 1.15 μg/mm^2 for PU-UFH) protein amounts, increasing by time up to 1.79 μg/mm^2 for PU-LMWH and 1.96 μg/mm^2 for PU-UFH after 15 min, and than reaching a plateau to 1.55 μg/mm^2 for PU-LMWH and 1.68 μg/mm^2 PU-UFH at 25 min.

As expected, control PU demonstrated lower plasma protein adsorption than with TCP at all incubation times and, after 5 min, the amount of adsorbed protein was more than two times higher for TCP (8.44 μg/mm^2) than for control PU (3.44 μg/mm^2) samples. Polyurethanes are in fact considered as good materials for blood-contacting applications. But still depending on the composition of PU, preparation methods and modification techniques, variation on protein adsorption can be observed. The effect of surface modification by heparin immobilization on protein adsorption was examined for all incubation times, since a lower amount of plasma proteins was adsorbed on heparinized surfaces (about 7 times less for PU-LMWH and 3 times less for HMWH) with respect to the unmodified PU surfaces.

PU-LMWH demonstrated lower protein adsorption when compared with PU-UFH in the early stage of surface-plasma interaction (Figure 45). The amount of protein adsorbed from plasma after 5 min incubation was found to be 0.46 μg/mm^2 and 1.15 μg/mm^2 for PU-LMWH and PU-UFH surfaces, respectively. This difference might be due to the different biological activities of low molecular weight and unfractionated forms of heparin, in fact, LMWH is reported to have lower binding to plasma proteins in comparison with UFH in intravenous applications [73-75]. After 15 min and 25 min incubation, the difference between the amount of adsorbed proteins on PU-LMWH and PU-UFH samples was no more significant. Nevertheless, from the results of the adsorbed protein concentrations, it is measured that slightly lower amount of plasma protein adsorption occurred on the PU-LMWH surface for the examined incubation times. But we must also take in to account that; the standard deviation of the measured

protein concentration from the PU-UFH surface is high and we believe that this high standard deviation value represents uncertainty of UFH behavior and it may be due to the 'variable anticoagulant activity' of UFH as mentioned in literature [108, 109].

3.5.2 Protein Adsorption Kinetics from Human Blood Plasma

After total protein fraction quantification, adsorbed proteins were analyzed in terms of their molecular weight by means of 1D electrophoresis. The adsorption kinetics of the low molecular weight plasma proteins and the high molecular weight plasma proteins were studied for 5 min, 15 min, 25 min incubation times. Two kinds of gradient porosity gels were used to detect low (1.5-212 kDa) and high (30-500 kDa) molecular weight plasma proteins.

The electrophoresis profiles of adsorbed proteins are shown in Figure 46 and Figure 47, respectively. These two gels were stained with both Comassie blue and silver staining in order to observe the protein bands more clearly. Contacting plasma (PPP) electrophoresis profiles are given in Appendix F.

In general, higher adsorption was confirmed on untreated PU and TCP with respect to heparinized surfaces. Specially, PU-LMWH samples demonstrated the lowest protein adsorption at 5 min incubation time among all samples.

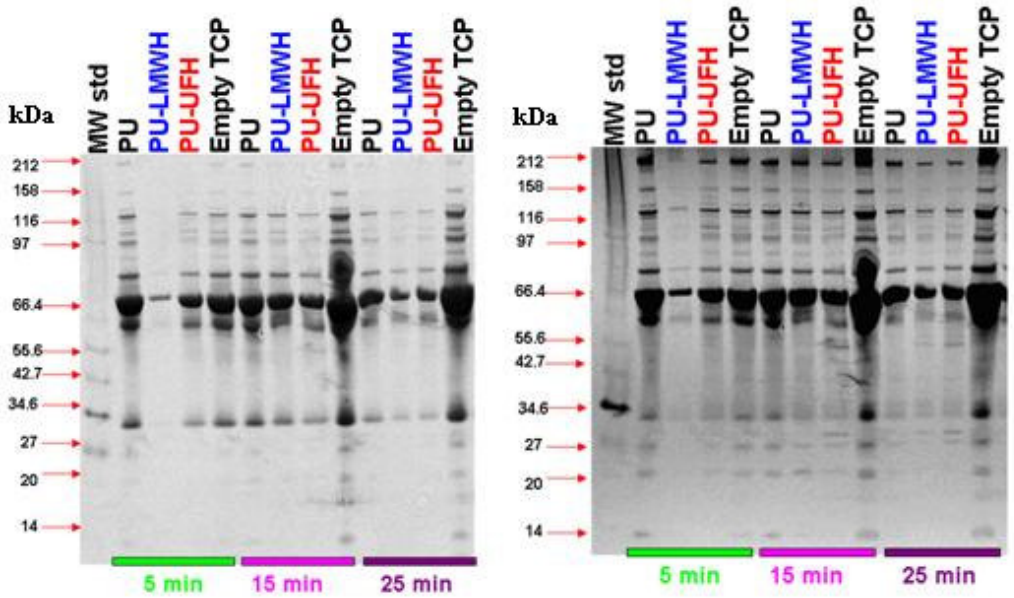

(a) (b)

Figure 46 Electrophoresis profiles of low MW plasma proteins (a) Comassie blue staining, (b) Silver staining.

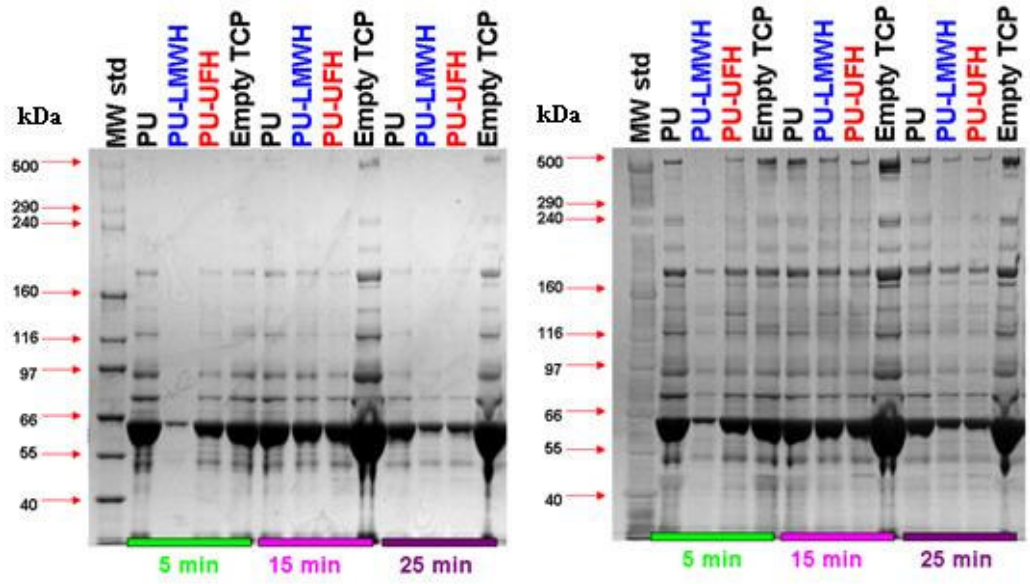

(a) (b)

Figure 47 Electrophoresis profiles of high MW plasma proteins (a) Comassie blue staining, (b) Silver staining.

The adsorption of contact phase proteins plays an important role in intrinsic coagulation system. Also, the protein absorption onto biomaterial surface is a dynamic multi-step process and divided into different phases, as schematized in Figure 12. The shape, conformation and amount of adsorbed protein layer changes with time. Generally fibrinogen and fibronectin are classified as adhesive plasma proteins and they play important roles in blood coagulation**.** Fibrinogen is known to be a protein with high surface activity. It plays an important role in the clotting system in both the plasma phase (intrinsic) and the cellular phase (platelet aggregation) in normal hemostasis and has also been implicated in thrombosis on foreign surfaces. Fibrinogen adsorption is a well-known contributor to surface-induced thrombosis. Platelets contain a receptor site specific for fibrinogen, which is active only when platelets are activated (Figure 13). On the other hand, albumin is a major protein having an anti-thrombogenic potential. So it is important to determine, if the first adsorbed protein on biomaterial surface is albumin. If so**;** the thrombus formation decreases. With this notion, the discussion of the electrophoresis profiles will be done in term of these plasma proteins; albumin, fibrinogen and fibronectin.

The presence of albumin, is recognized by a band at 66 kDa as shown in Figure 48 [110]. Albumin is most abundant plasma protein and due to its high concentration and its relatively small size, it is the dominating protein at the initial stage of adsorption. Albumin is not involved in blood coagulation or platelet adhesion processes, once adsorbed it is often referred as a passivating agent, able to reduce thrombogenic potential of the surface.

Figure 48 SDS-PAGE gels demonstrating adsorption of human albumin.

On our electrophoresis profiles albumin was observed by its peculiar drop-like band at 66.5 kDa ca, and were strongly existed in all the tested samples (Figure 46 and Figure 47). Albumin showed the strongest band among all other plasma proteins at electrophoresis profiles and this is important since it forms a reduced thrombogenic potential of the surface. For both PU-LMWH and PU-UFH, the amount of adsorbed albumin showed an increase from 5 to 15 min, and then a decrease from 15 to 25 min.

PU-LMWH presented a high selectivity with few protein bands at 5 minutes, while PU-UFH showed a random adsorption. Some protein bands correspond to fibronectin and apolipoproteins, are discussed below.

Fibronectin is a plasma protein known to mediate platelet adhesion to the surfaces and assume to play a prominent role leading blood-material interaction and it is recognized at 220 kDa as shown in Figure 49 [64].

Figure 49 SDS-PAGE gels demonstrating adsorption of human fibronectin.

In our samples, some bands at 220 kDa ca. could be associated to fibronectin units (Figure 47). This fibronectin band is observed more clearly at silver stained gel Figure 47 (b) and also in Figure 50 which is the enlarged figure of the same gel. At 5 min PPP incubation, PU-LMWH demonstrated almost no fibronectin adsorption while PU-UFH had fibronectin absorption band. At 15 min incubation, fibronectin band is slightly observed on both heparinized samples. At 25 min incubation time, due to the change in

protein adsorption process, the fibrinogen selectivity of the surfaces were changed and adsorbed fibronectin amount was decreased on heparinized samples.

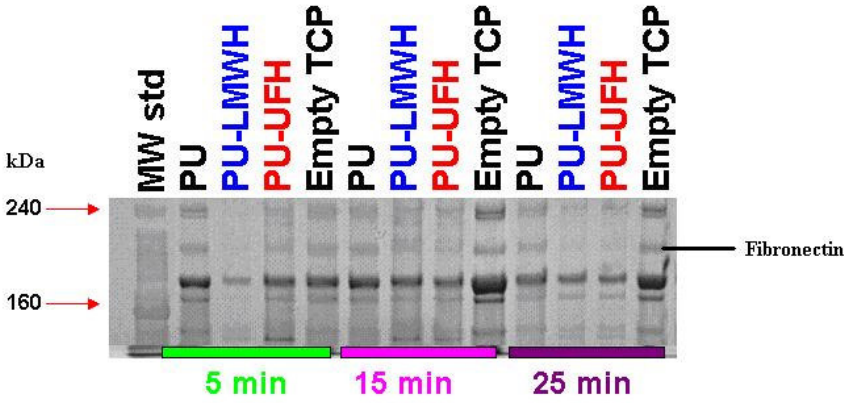

Figure 50 The enlarged view of electrophoresis gel between 240 kDa – 160 kDa.

In literature; fibrinogen could be recognized from the bands between 60-50 kDa as shown in Figure 51 [110].

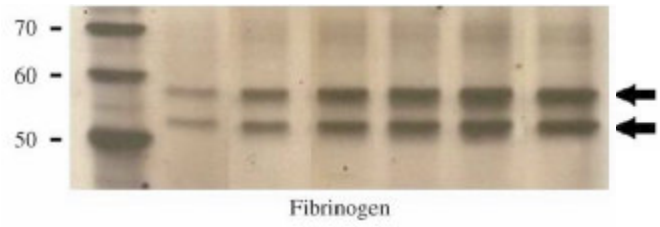

Figure 51 SDS-PAGE gels demonstrating adsorption of human fibrinogen.

The fibrinogen bands of our samples could be more clearly observed from Figure 52. Fibrinogen exhibited two subunit bands on the electrophoresis profiles; they are the β-

fibrinogen observed at 58 kDa and γ-fibrinogen observed at 53 kDa. When the β-fibrinogen bands are compared at 5 min incubation time; PU-LMWH sample showed lower β-fibrinogen adsorption compared to control PU and PU-UFH samples. At 15 min incubation time, β-fibrinogen adsorption increased on PU-LMWH. At 25 min incubation time, β-fibrinogen adsorption on heparinized samples (PU-LMWH and PU-UFH) seems to be lowered than that of 15 min incubation. The other subunit of fibrinogen; γ-fibrinogen (53 kDa ca) is observed on PU-UFH at 15 min and 25 min incubation times, while PU-LMWH had no γ-fibrinogen adsorption at 15 min, but at 25 min this surface had a slight tendency to absorb γ-fibrinogen.

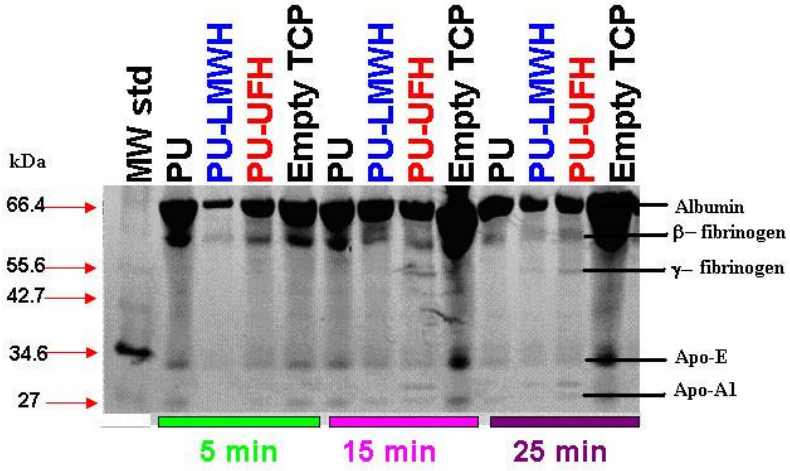

Figure 52 The enlarged view of electrophoresis gel between 66 kDa – 27 kDa.

Also the other low MW protein bands observed approximately at 35 kDa and 25 kDa on electrophoresis profile (Figure 52), are possibly apolipoproteins [110]. The protein bands at 35 kDa was defined as apolipoprotein E (Apo-E) and the protein band at 25 kDa was defined as apolipoprotein A1 (Apo-A1). Apolipoprotein A1 is known to be

the major component of high density lipoprotein. These proteins were clearly more abundant on control PU and TCP than on heparinized surfaces (Figure 46 a-b and Figure 52). Also the adsorption of apolipoprotein on the different surfaces was discussed in the literature in terms of surface hdyrophilicity. These selective adsorption of these apolipoproteins on control PU surface rather than heparinized PU surfaces may be due to the higher hydrophobic character of control PU.

3.5.3 Protein Binding Strength on Surfaces

For the samples which were incubated with plasma for 25 min, an alternative method was used for the elution of adsorbed plasma proteins. Sequential washes with water and isopropanol solutions of increasing alcohol concentrations were used for selective removal of the adsorbed proteins on the basis of their binding strength due to their hydrophobic binding sites [111]. The electrophoresis of eluates is shown Figure 53 for low molecular weight proteins and Figure 54 for high molecular weight proteins.

The electrophoresis profiles of eluates (Figure 53 and Figure 54) showed that protein binding on PU surfaces were not strong, since most of the proteins were removed from the surfaces within the first two water washes. As it could be observed from Figure 53 that, albumin (66 kDa) was removed from PU-LMWH surface with the first and second water wash. The most of the adsorbed albumin on PU-UFH surface was removed with the first water wash leaving almost negligible amount for the second wash. Untreated PU presented higher amount of albumin binding and albumin protein band (66 kDa) also observed in the solution eluted by 10% v/v isopropanol. The first washing with water caused detachment of most of them, but still there were some remaining which were strongly bonded to the surface and removed from the surface by the washing of 10% v/v isopropanol.

Also the similar removal trend was observed for the fibrinogen. As it could be observed from in Figure 54, fibrinogen (58 kDa) was removed from PU surfaces with the first

and second water washes, but it exhibited a band in the elution solution of 10% v/v isopropanol for untreated PU. It can be concluded that, these two proteins, fibrinogen and albumin which play a key role in blood coagulation cascade;, are more strongly bonded on pristine PU surface rather than heparinized PU surfaces. This may be due to the effect of hydrophobic binding sides of PU surfaces, which may strongly bind blood plasma proteins. Weak protein binding to the heparinized surfaces can be related to increased hydrophilicity of heparinized surfaces with respect to untreated PU, and may affect materials hemocompatibility.

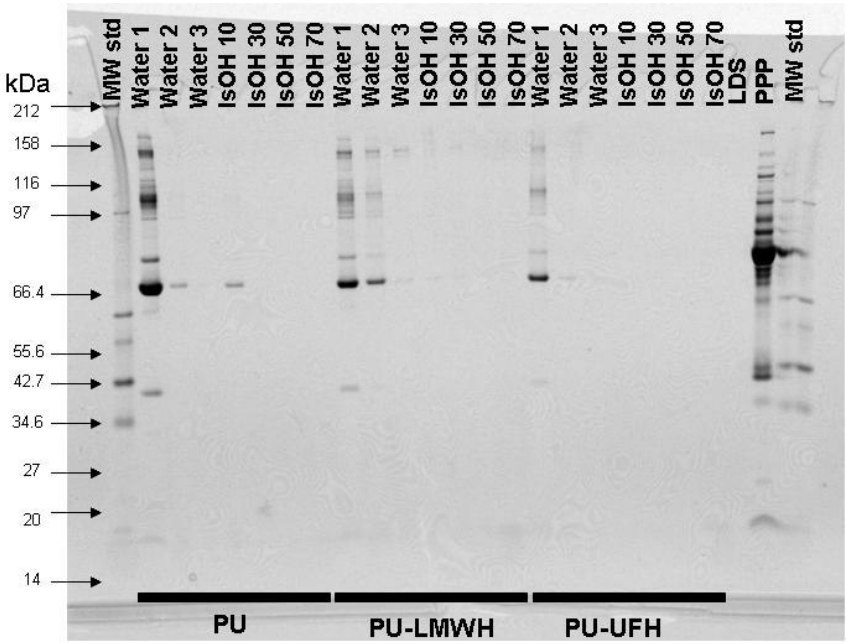

Figure 53 Electrophoresis profiles of binding strength of low MW plasma proteins.

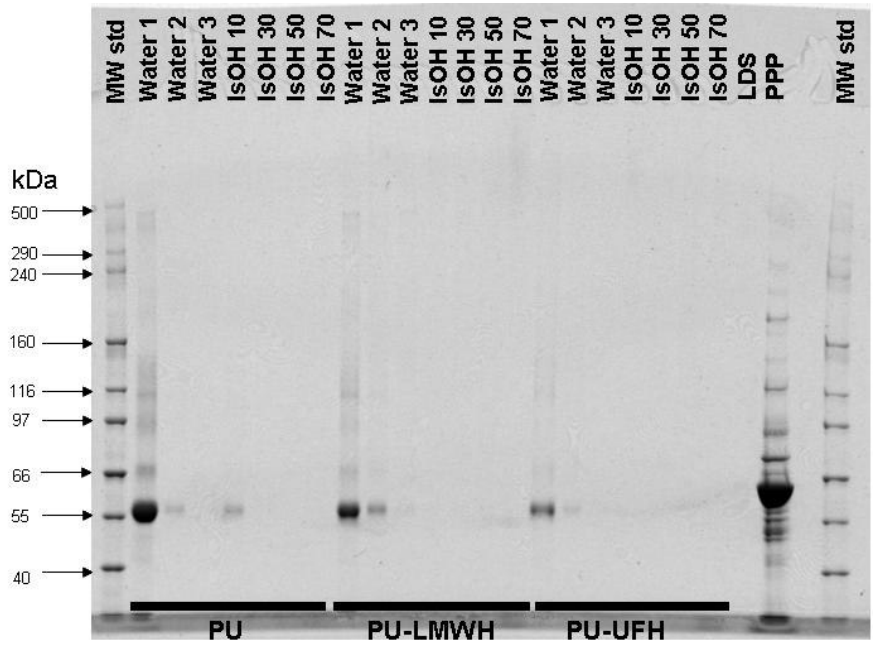

Figure 54 Electrophoresis profiles of binding strength of high MW plasma proteins.

3.5.4 Heparin Stability Results

To test stability of heparin immobilization on PU surfaces, heparinized surfaces were washed with sodium dodecyl sulfate (SDS) solution (0.1% w/v in water, 200 µL) for 30 min. SDS ($C_{12}H_{25}SO_4Na$) is used for disrupting non-covalent bonds on the surface. The amount of heparin released into the SDS wash solutions (removed or degraded fragments) was measured and the obtained results are tabulated in Table 20.

The highest heparin amount was obtained for PU-UFH samples as 0.412 µg/mm^2. This result can be explained as the release of heparin fragments. Heparin chains are bonded covalently at one terminus to the surface, the long and free polysaccharide chain may partially degrade in the exposing medium [108, 109]. The released amount of LMWH from the PU surface was found to be almost 3 times less compared with PU-UFH surfaces and found as 0.112 µg/mm^2.

Table 20 The amount of heparin released from the surfaces by SDS washing.

Sample	Amount of Heparin ($\mu g / mm^2$)
PU-LMWH	0.112 ± 0.002
PU-UFH	0.412 ± 0.004

3.5.5 Platelet Adhesion and Activation

The activation of intrinsic coagulation, the adhesion and aggregation of platelets, and the activation of the complement system may take place, depending on the composition and the conformation of the protein layer adsorbed on the surface. When the platelets are adhered to the surface, the extent of morphology change may be a more appropriate indicator than the number of adhered platelets adhesion in judging blood-material compatibility Platelet activation is marked by morphological changes from rest discoid shape to varying degrees of spreading [112]. The extent of platelet spreading could be categorized by platelet shapes into five morphological forms describing increasing activation. These are discoid or round (R), dendritic (D) or early pseudopodial, spread dendritic (SD) or intermediate pseudopodial, spreading (S), and fully spread (FS). The spreading stages are shown in Figure 55 and defined in the legend.

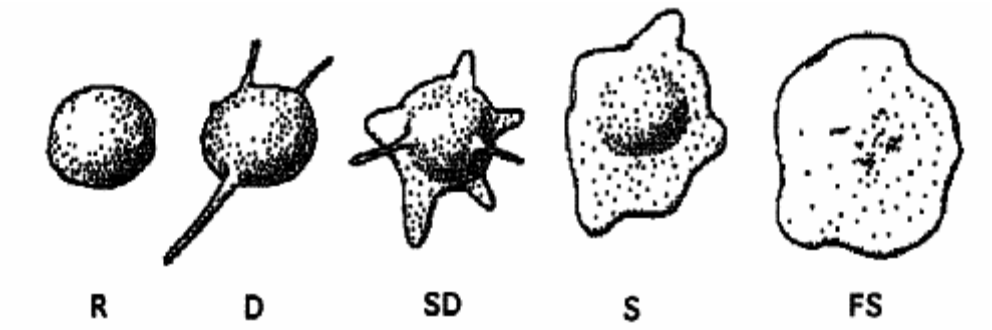

Figure 55 Stages of platelet spreading. Round (R) or discoid: no pseudopodia present; dendritic (D) or early pseudopodial: one or more pseudopodia with no evident flattening; spread dendritic (SD) or intermediate pseudopodial: one or more pseudopodia flattened, hyaloplasm not spread between pseudopodia; spreading (S): hyaloplasm spread between pseudopodia; and fully spread (FS): hyaloplasm extensively spread, no distinct pseudopodia.

With this notion, the platelet morphology and platelet activation on LMWH and UFH immobilized PU surfaces after PRP incubation (5min, 15min, 25 min), were studied by SEM and results are given in Figure 56. The low magnification SEM images were used to get information about the overview of platelet adhesion on the sample surfaces (Figure 57 and Figure 58). In order to determine the type of platelet morphologies on samples, higher magnification SEM images were also used (Figure 59-61). Also the SEM images of all surfaces without PRP incubation are given in Appendix G.

In general, the platelet numbers on the heparin immobilized PU films (PU-LMWH and PU-UFH) were lower with respect to the control materials and this could be clearly seen in Figure 56 for all incubation times. These differences can also be clearly observed from Figure 57 and Figure 58 which are the overall surface views of platelet distributions on samples with 250x magnification after 25 min incubation time. TCP demonstrated the highest amount and homogenous spreading of platelets (Figure 57 a), PU also showed high amount of platelets but with different platelet morphology (Figure 57 b). It could be observed from the comparison of Figure 57 and Figure 58 that; the

amount of platelets adhered on the heparinized surfaces (PU-LMWH and PU-UFH) are much less, and the effect of heparin is clearly observed at 25 min incubated samples.

Since the platelet morphology plays an important role in blood compatibility, we have to determine the platelet morphology differences on the surfaces with higher magnification SEM images. The platelets on TCP started to form spread (S) morphology at early stages of PRP incubation (Figure 59 a), and with an increasing incubation time (15 min, 25 min) platelet spreading was increased with pseudo extension, and fully spread (FS) platelet morphologies were observed (Figure 59 b). Many of the platelets adhered on control PU surface get dendritic and spread shapes after 15 and 25 minutes (Figure 56 e, f), with the start of platelet-platelet aggregation (clot). On the surface of the control PU, different platelet morphologies were observed (Figure 60) than TCP. They kept their dendritic forms even after accumulation. At 25 min incubation time, the platelets on control PU were not spreaded with pseudo extension as on TCP (Figure 59 b), they are in dendritic (D) form (Figure 60 a, b). The control PU and TCP presented higher degree of platelet adhesion and formation of thrombus-like aggregates compared with heparinized samples. Heparin affect was clearly observed especially for 25 min incubated samples.

If heparinized PU surfaces were compared, there were lower platelet adhesion on the PU-LMWH for all the experimental times, where platelets were round with minimal clustering at all testing time (Figure 56 g, h, i). This observation is in agreement to literature, where LWMH is characterized by reduced binding to platelets in intravenous applications [72-74]. The round (R) platelet morphology on PU-LMWH could be more clearly observed in Figure 61 a. In addition, PU-UFH showed a different kinetics, forming linearly aligned clusters with some pseudopodia extension at 15 min (Figure 56 k) followed by a decrease in adhered platelets at 25 min incubation time (Figure 56 l and Figure 61 b).

For PU-UFH samples, platelet adhesion kinetic was consistent with the trends observed for protein adsorption. The increased degree of platelet adhesion/activation and aggregation reported at 15 min can be in fact related to the high amount of pro-adhesive proteins adsorbed to the surface at the same experimented time, as reported by electrophoresis analysis (Figure 46). Type and conformation of the adsorbed plasma proteins on the heparinized surfaces influence the adhesion and activation of platelets on the same sample surfaces.

As a result, high degree of decrease in the number of platelets aggregated on the surfaces was observed for the samples modified with heparin immobilization. Even some platelets were observed in the early stages of incubation, they were not permanent and therefore only few were observed on the PU-LMWH and PU-UFH samples incubated for 25 min for PRP.

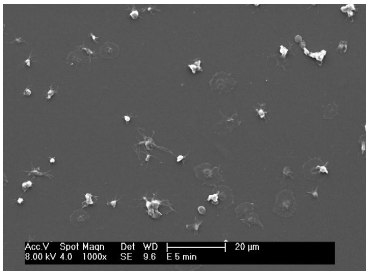

(a) TCP-5min.

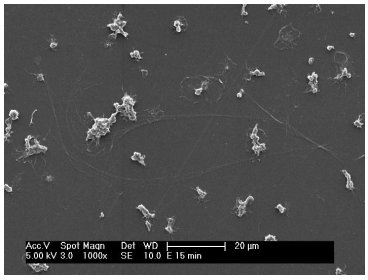

(b) TCP-15min.

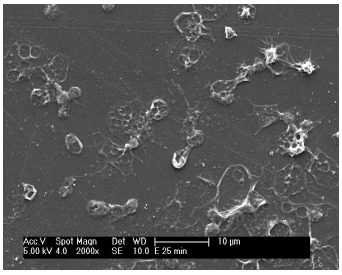

(c) TCP-25min.

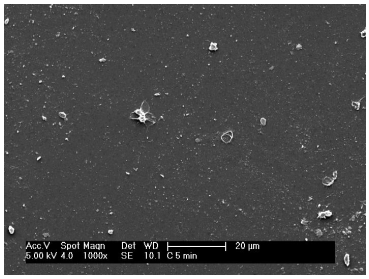

(d) PU-5 min.

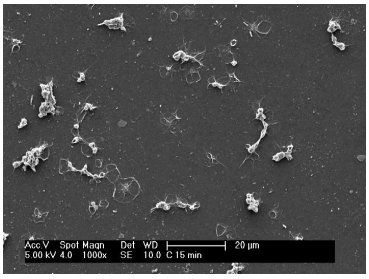

(e) PU-15 min.

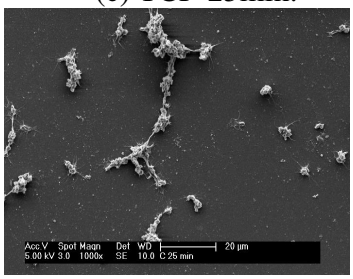

(f) PU-25 min.

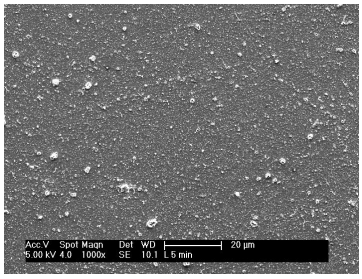

(g) PU-LMWH-5 min

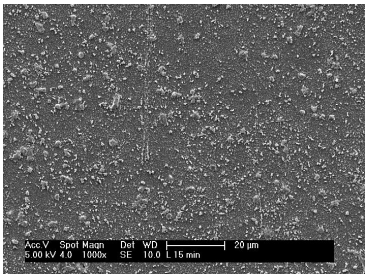

(h) PU-LMWH-15 min.

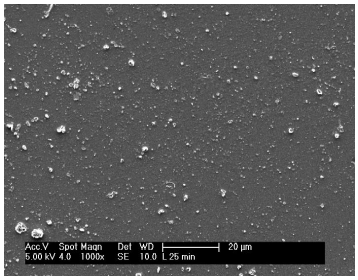

(i) PU-LMWH-25 min.

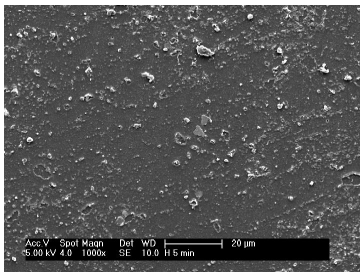

(j) PU-UFH-5 min.

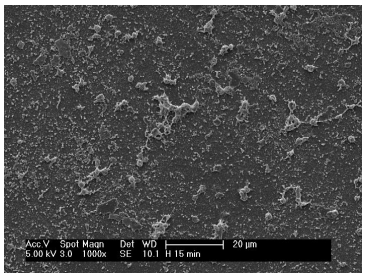

(k) PU-UFH-15 min.

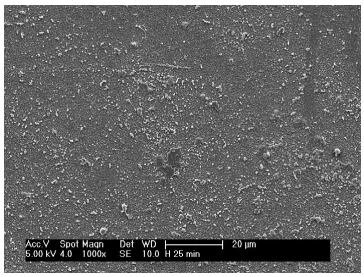

(l)PU-UFH-25 min.

Figure 56 SEM images of samples at different incubation times.

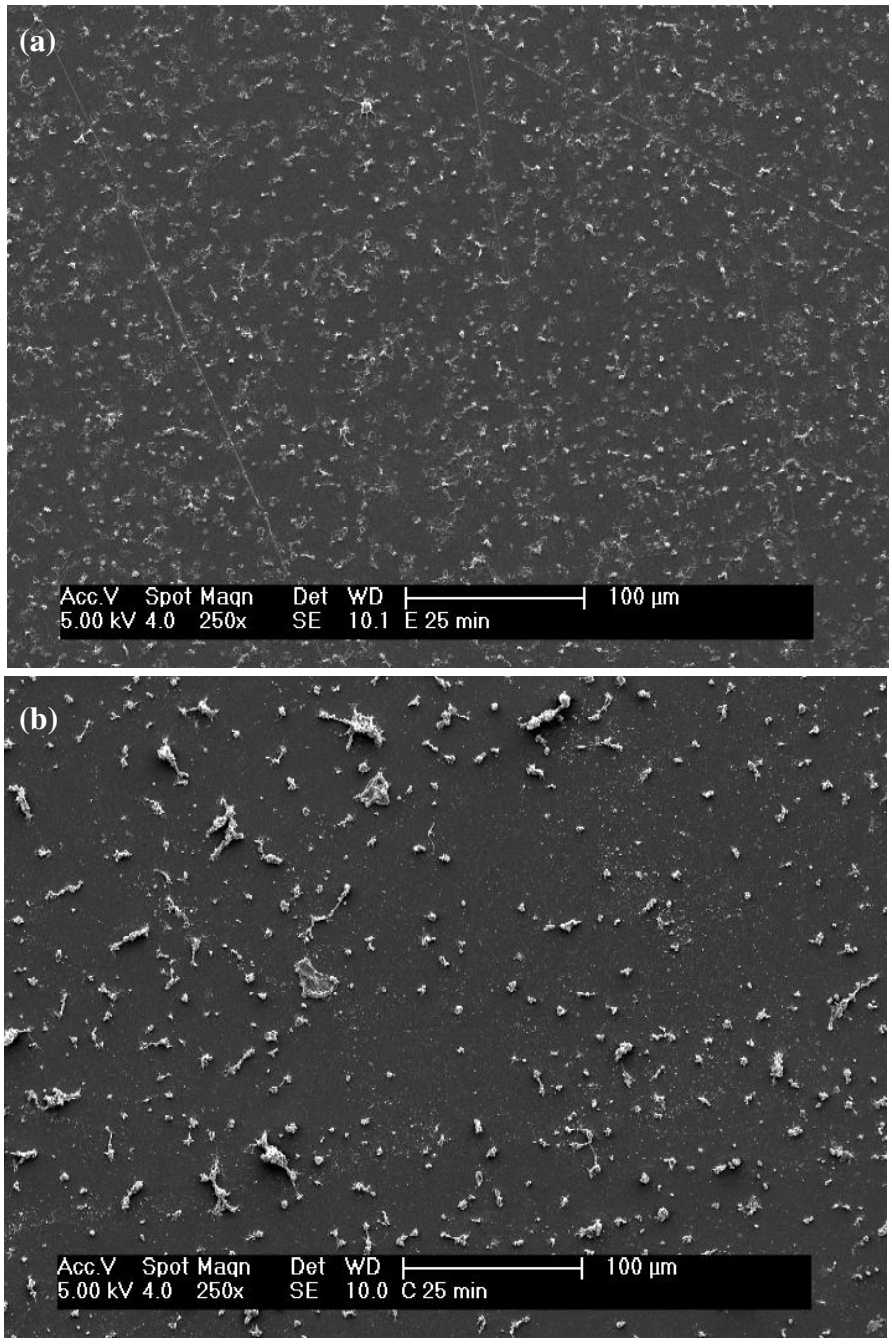

Figure 57 SEM images (250x) at 25 min incubation time (a) TCP, (b) Control PU.

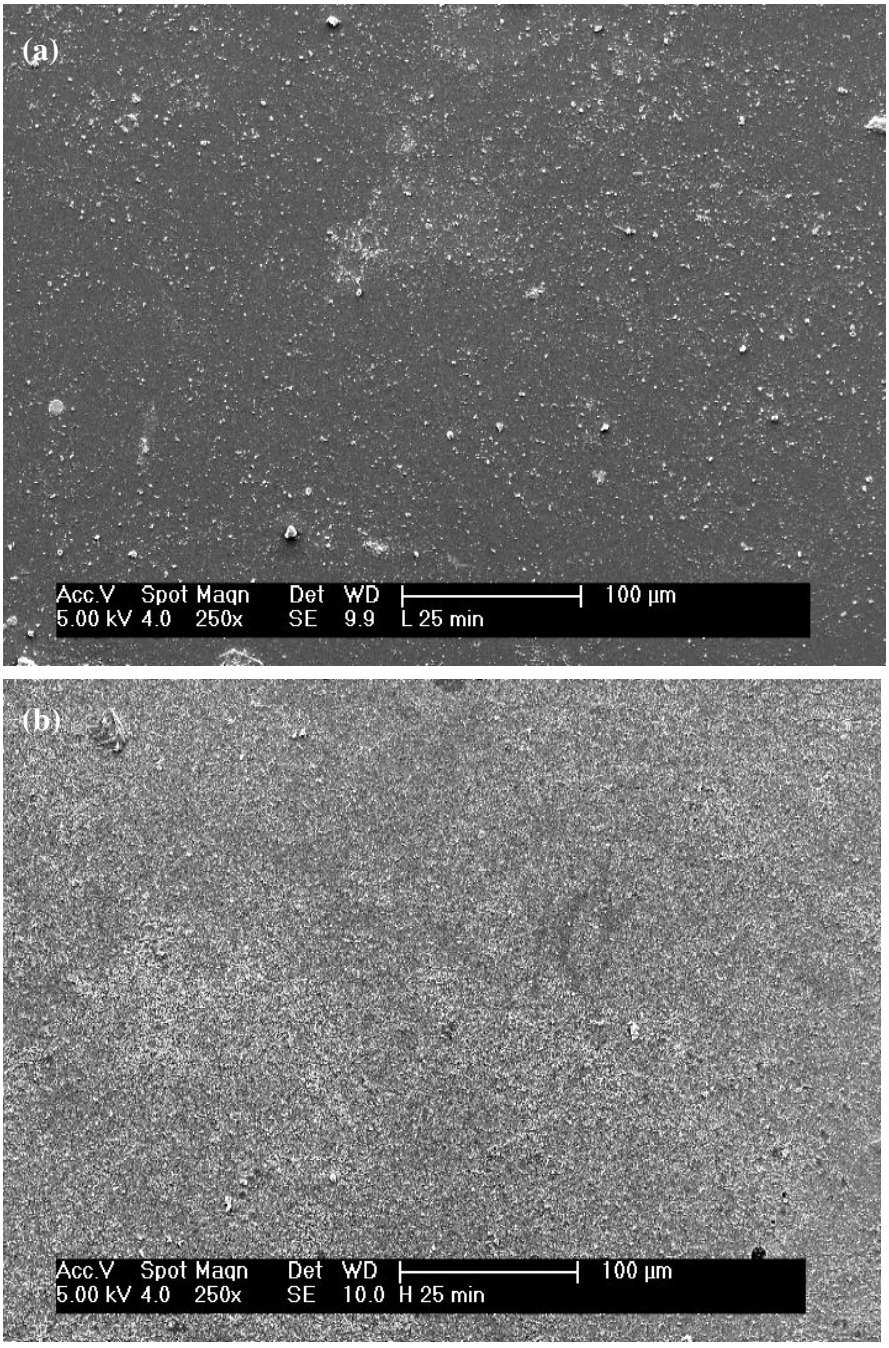

Figure 58 SEM images (250x) at 25 min incubation time (a) PU-LMWH, (b) PU-UFH.

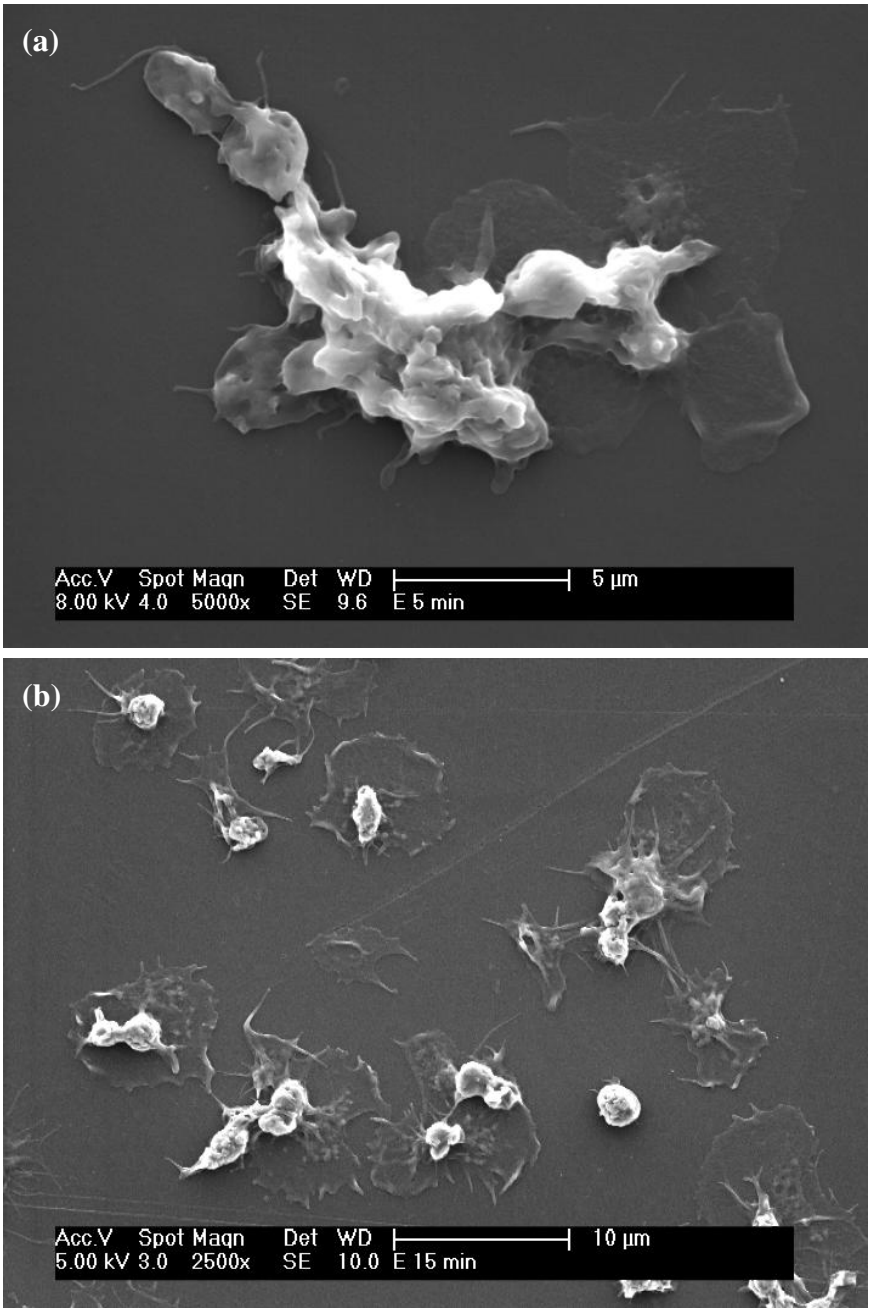

Figure 59 SEM images of TCP (a) 5 min incubation time (5000x), (b) 15 min incubation time (2500x).

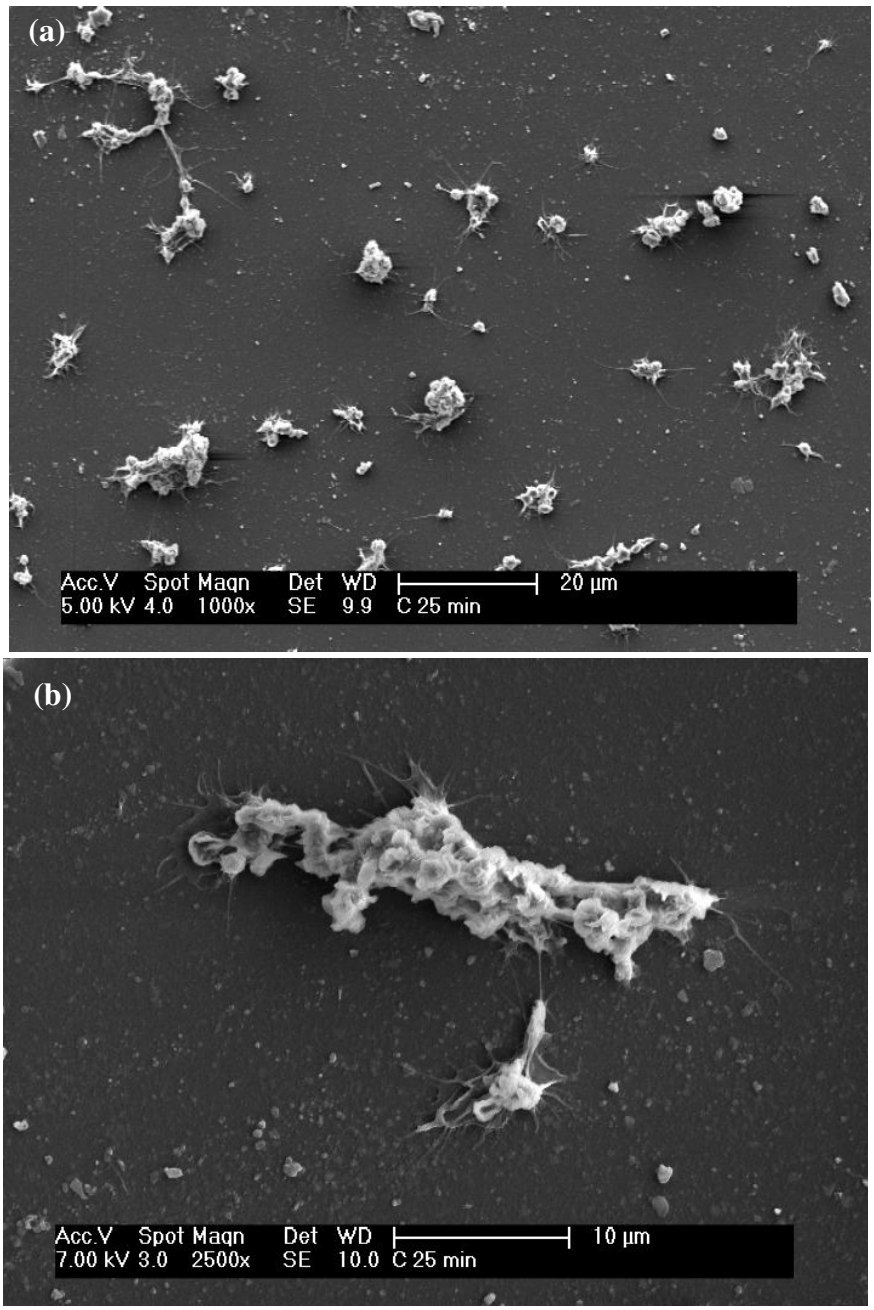

Figure 60 SEM images of control PU at 25 min incubation time (a) 1000x, (b) 2500x.

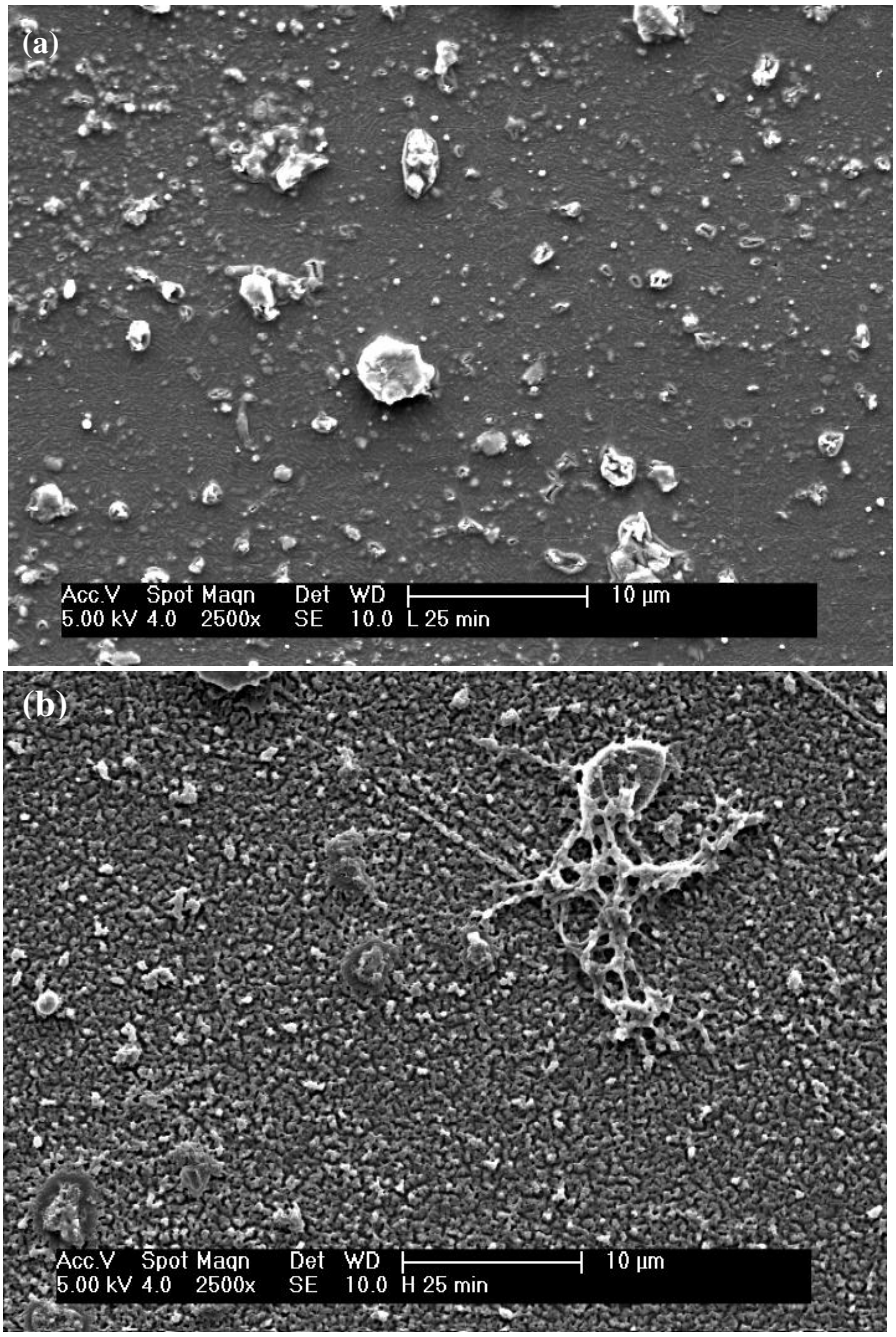

Figure 61 SEM images (2500x) of heparinized samples at 25 min incubation time (a) PU-LMWH, (b) PU-UFH.

CHAPTER 4

CONCLUSIONS

Polyurethanes are the most widely used polymers in the design and production of blood contacting devices due to their segmental structure and inherent blood compatibilities. This study focused on synthesis of polyurethanes in medical purity and modification of polyurethane surface with different types of heparins to improve their blood compatibilities. The results obtained in the current study are summarized as follows:

- The polyurethanes were synthesized in medical purity, from TDI and polypropylene ethylene glycol by changing the ratio of these components and with no addition of chain extender and catalyst.
- The PU films prepared with different TDI ratios, exhibited an increase in microphase segregation with increase in hard segment content in their structure. The solid state NMR spectroscopy allowed the solid state characterization of the hard segment carbons and the soft segment carbons by simply adjusting different spin rates. The FTIR spectra of PU films demonstrated a hydrogen bonding of NH and C=O groups.
- The DMA demonstrated that; with an increase in hard segment content, the PU structure gained stiffness and exhibited an increase in Tg. According to E' values at 25°C and 37°C, the PU films gain stiffness, rigidity and resistant to elongation and mechanical deformation with an increase in hard segment content. Also the mechanical tension test results showed that with an increase in hard segment content, modulus and strain at break values were increased while elongation at break values were decreased. Very high amounts of hard segment content lead to increase in the microphase segregation in structure which caused

a decrease in degradation temperature of the structure as observed in TGA.

- For best of our knowledge, it was the first time that LMWH was immobilized on PU surface as an alternative anticoagulant to UFH. Also it is the first time that anticoagulant activities of LMWH and UFH immobilized PU surfaces were examined and compared. The water contact angles on PU surfaces were found to be 76°. Surface hydrophilicity increased and contact angle values decreased to 39° for PU-UFH samples, and 32° for PU-LMWH. After surface modification polar and basic components of the surface free energy increased. This plays an important role in protein adsorption and platelet aggregation on the surfaces.
- The sulfur-2p core level spectra of the samples of PU-LMWH and PU-UFH exhibited a peak at 168 eV which shows the presence of sulfonate groups ($-SO_3Na$) resulting from heparin. Also carbon structure of the surface was changed with heparin immobilization. ESCA results indicate that both types of heparin were covalently bonded onto the surfaces of the modified PU samples.
- PU-UFH showed more uniform heparin immobilization compared with PU-LMWH and this is an important factor affecting the blood cell adhesion evaluations. LMWH chains showed a brush like morphology where the high molecular weight heparin demonstrated helical conformation of the long heparin chains.
- Pristine control samples demonstrated very high adherence of red blood cells while the cell adherence decreased for PU-LMWH and only a little adhesion has occurred for PU-UFH, most probably due to the uniform heparin coating.
- In the early stages of blood plasma-material interaction, the differences between the two types of heparin modified surfaces were clearly observed. After 5 min incubation, LMWH modified surfaces demonstrated about three times less blood protein adsorption than that of UFH modified surfaces. Total amount of adhered protein became similar as the incubation time was extended.

- Albumin showed the strongest band among all other plasma proteins at electrophoresis profiles and this is important since it reduced thrombogenicity of the surface. For both PU-LMWH and PU-UFH, the amount of adsorbed albumin showed an increase from 5 to 15 min, and a subsequent decrease from 15 to 25 min incubation time.
- Fibrinogen and fibronectin are plasma proteins known to mediate platelets adhesion to the surfaces and play a prominent role leading blood-material interaction. Fibrinogen exhibited two subunit bands β-fibrinogen and γ-fibrinogen. At 5 min incubation time; PU-LMWH showed lowest β-fibrinogen adsorption compared to control PU and PU-UFH. The γ-fibrinogen is observed on PU-UFH at 15 min and 25 min incubation times, while PU-LMWH had no γ-fibrinogen (53 kDa ca) adsorption at 15 min, but at 25 min this surface had a slight tendency to absorb the γ-fibrinogen. At 5 min PPP incubation PU-LMWH didn't adsorbed fibronectin while PU-UFH had shown a fibronectin absorption band. At 15 min incubation time fibronectin band is slightly observed on both heparinized samples. At 25 min incubation time due to the change in protein adsorption process, the fibrinogen selectivity of the surfaces was changed and adsorbed fibronectin amount was decreased.
- Since fibrinogen and fibronectin are platelet adhesive proteins, their adsorption on heparinized surfaces affected the platelet adhesion. At 15 min incubation time PU-UFH demonstrated higher fibrinogen adsorption compared to PU-LMWH which caused an increase in platelet adhesion on PU-UFH surface. At 25 min incubation time, due to the low fibronectin adsorption on PU-LMWH, platelet adhesion was decreased.
- The non-thrombogenic effect of polyurethane surface modification by heparin immobilization is clearly observed. The untreated PU and TCP presented a higher degree of platelet adhesion compared with heparin immobilized samples and the formation of thrombus-like aggregates. When the morphologies of platelets were examined, UFH modified surfaces had strung clusters with some

pseudopodia extension while LMWH modified surfaces showed round shapes with little clustering.

As a result, it can be concluded that, LMWH and UFH immobilized PU surfaces demonstrated promising results for the improvement of blood contacting devices (such as catheters, stents, artificial heart) but in order to have a definite answer about non-thrombogenicity of these surfaces, more detailed immuno-enzymatic experiments are needed to investigate the presence and quantification of platelet pro-adhesive proteins.

REFERENCES

1. Bayer, O., Siefken, W., Rinke, H., Orthner L., Schild H. 'A process for the production of polyurethanes and polyureas', German Patent DRP 728981, 1937.

2. Bhatnager, M.S. 'Polyurethane' in Polymeric Materials Encyclopedia, Salamone JC, CRC Press, Florida, 9: 6979-6985, 1996.

3. Hasirci, N. 'Polyurethanes' in High Performance Biomaterials: Comprehensive Guide to Medical and Pharmaceutical Application, Szycher, M. ed., Technomic Pub.Co., Lancaster, 71-93, 1991.

4. Elvers, B., Hawkins, S., Ravenscroft, M., 'Isocyanates' in Ullmann's Encyclopedia of Industrial Chemistry, Schulz, G. ed., VCH., Vol.A14, New York, 1989.

5. Backus, J.K., Blue, C.D., Boyd, P.U. 'Polyurethane' in Concise Encyclopedia of Polymer Science and Engineering, John Wiley, New York, 890-897, 1990.

6. Grand, M.H. 'Isocyanates' in Encyclopedia of Chemical Technologies, John Wiley, New York, 14: 903-993, 1991.

7. Mark, S.M. 'Isocyanates', in Polymer Science Dictionary, Elsevier, New York, 384-401, 1990.

8. Burke, A., Hasirci, N. 'Polyurethanes in Biomedical Applications', in Biomaterials: From Molecules to Engineered Tissues, Hasirci, N. and Hasirci, V. eds., Kluwer Academic/Plenum, New York, 83-94, 2004.

9. Hepburn, C. ‘Polyurethane Elastomers’, Galliard, New York, 67-80, 1982.

10. Crawford, D.M., Baas, R.G., Haas T.W. ‘Strain effects on thermal transitions and mechanical properties of thermoplastic polyurethane elastomers’, Thermochim. Acta, 323: 53-63, 1998.

11. Yilgor, I., Yilgor, E. ‘Structure-morphology-property behavior of segmented thermoplastic polyurethanes and polyureas prepared without chain extenders', Polym. Rev., 47: 4, 487–510, 2007.

12. Ulubayram, K., Hasirci, N. ‘Preparation of Polyurethane Elastomer For Biomedical Applications’, Hasirci, V. ed., Proceedings of the Second National Symposium on Biomedical Science and Technology, 1995.

13. Adrade, J.D. ‘Needs, problems, and opportunities in biomaterials and biocompatibility’, Clinical Materials, 11: 19-23, 1992.

14. Eden, M., Boretos J. W,. Contemporary Biomaterials, Park, R. ed., New Jersey, Noyes Publications, 193, 1984.

15. Back, J. ‘Systemic effects of biomaterials’, Biomaterials, 5: 12, 1984.

16. Boretos, J.W., Pierce, W.S. ‘A polyether polymer’, J. Biomed. Mat. Res., 2: 121, 1968.

17. Nylias, E. ‘Development of Blood Compatible Elastomers Theory, Practice and In-Vivo Performance’, 23rd Conference on Engineering in Medicine and Biology, 12: 147, 1970.

18. Lelah, M.D., Lambrecht, L.K., Young, B.R., Cooper, S.L. ‘Physicochemical characterization and in vivo blood tolerability of cast and extruded biomer’, J. Biomed. Mater. Res., 17: 1-22, 1983.

19. Hanson, S.R., Harker, L.A., Ratner, B.D., Hoffman, A.S. 'In vivo evaluation of artificial surfaces with a nonhuman primate model of arterial thrombosis', J. Lab. Clin. Med., 95(2): 289-296, 1980.

20. Abe, Y., Chinzei, T., Isoyama, T., Ono, T., Mochizuki, S., Saito, I., Guba, P., Karita, T., Pin San, Y., Kouno, A., Suzuki, T., Baba, K., Mabuchi, K., Imachi, K., 'Present Status of Artificial Heart in Tokyo University', Artif. Organs, 23(2): 221-228, 1999.

21. Klement, P., Jun Du, Y., Berry, L., Tressel, P., Chan, A. 'Chronic performance of polyurethane catheters covalently coated with ATH complex: A rabbit jugular vein model', Biomaterials, 27: 5107-5117, 2006.

22. Yuan, Y., A. Fei, Zang, X., Zhuang, W., Shen, J., Lin, S. 'Polyurethane vascular catheter surface grafted with zwitterionic sulfobetaine monomer activated by ozone', Colloid. Surface B, 35: 1–5, 2004.

23. Kondyurin, A., Romanova, V., Begishev, V., Kondyurina, I., Guenzel, R., Maitz, M.F. 'Crosslinked polyurethane coating on vascular stents for enhanced X-ray contrast', J. Bioact. Compat. Pol., 20 (1): 77-93, 2005.

24. Tepe, G., Schmehl, J. 'Reduced thrombogenicity of nitinol stents - In vitro evaluation of different surface modifications and coatings', Biomaterial, 27 (4): 643-650, 2006.

25. Verschuur, E.M.L., Homs, M.Y.V., Steyerberg, E.W., Haringsma, J., Wahab P.J., Kuipers E.J., Siersema P.D. 'A new esophageal stent design (Niti-S stent) for the prevention of migration: a prospective study in 42 patients', Gastrointest. Endosc., 63: 134-140, 2006.

26. Attmann, T., Steinseifer, U., Jochen C., Lutter, G. 'A novel low-profile PU valved stent', Eur. J. Cardio-Thorac., 30: 379, 2006.

27. Gorna, K., Gogolewski, S. ‘Molecular stability, mechanical properties, surface characteristics and sterility of biodegradable polyurethanes treated with low-temperature plasma’, Polym. Degrad. Stabil., 79: 475–485, 2003.

28. Mahkam, M., Sharifi-Sanjani, N. ‘Preparation of new biodegradable polyurethanes as a therapeutic agent’, Polym. Degrad. Stabil., 80: 199–202, 2003.

29. Khil, M.S., Cha, D., Kim, H.K., Kim, I.S., Bhattarai, N. ‘Electrospun nanofibrous polyurethane membrane as wound dressing’, J. Biomed. Mater. Res. Part B: Appl. Biomater., 67B: 675–679, 2003.

30. Horch, R.E., Stark, G.B. ‘ Comparison of the effect of a collagen dressing and a polyurethane dressing on the healing of split thickness skin graft donor sites’, Scand. J. Plast. Reconstr. Hand. Surg., 32: 407–413, 1998.

31. Akita, S., Akino, K., Imaizumi T., Tanaka, K. ‘A polyurethane dressing is beneficial for split-thickness skin-graft donor wound healing’, Burns, 32: 447–451, 2006.

32. Ashley, F. ‘A new type of breast prosthesis’, Plast. Reconstr. Surg., 45(5): 421-425, 1970.

33. Capozzi, A. ‘Polyurethane-covered gel mammary implants’, Plast. Reconstr. Surg., 69: 904, 1982.

34. Hester, R., Bostwick, J., Cukic, J. ‘A 5-year experience with polyurethane-covered mammary prosthesis for treatment of capsular contracture, primary augmentation mammoplasty, and breast reconstruction’, Clin. Plast. Surg., 15(4): 569-575, 1988.

35. Smahel, J. ‘Tissue reactions to breast implants coated with polyurethane’, Plast. Reconst. Surg., 61(1): 80-88, 1987.

36. Barone, F., Perry, L., Keller, T., Maxell, P. 'The biomechanical and histopathologic effects of surface texturing with silicone and polyurethane in tissue implantation and expansion', Plast. Reconstr. Surg., 90(1): 77, 1992.

37. Pinchuk, L., 'A review of the biostability and carcinogeneric of polyurethanes in medicine and the new generation of biostable polyurethanes', J. Biomater. Sci. Polym. Ed., 6: 225-267, 1994.

38. Mathur, A.B., Collier, T.O., Kao, W.J., Wiggins, M., Schubert, M.A., Hiltner, A., Anderson, J.M. 'In vivo biocompatibility and biostability of modified polyurethanes', J. Biomed. Mater. Res., 36: 246–257, 1997.

39. Thakahara, A., Hergenrother, R.W., Coury, A.J., Cooper, SL. 'Effect of soft segment chemistry on the biostability of segmented polyurethanes. I In vitro oxidation', J. Biomed. Mater. Res., 25: 341–356, 1991.

40. Abraham, G.A., Marcos-Fernandez, A., San Roman, J. 'Bioresorbable poly(ester-ether urethane)s from L-lysine diisocyanate and triblock copolymers with different hydrophilic character', J. Biomed. Mater. Res., 76A: 729–736, 2006.

41. Williamson, M.R., Black, R., Kielty, C. 'PCL–PU composite vascular scaffold production for vascular tissue engineering: Attachment, proliferation and bioactivity of human vascular endothelial cells', Biomaterials, 27: 3608–3616, 2006.

42. Marcos-Fernandez A., Abraham G.A., Valentin, J.L., San Roman, J. 'Synthesis and characterization of biodegradable non-toxic poly(ester-urethane-urea)s based on poly(ε-caprolactone) and amino acid derivatives', Polymer, 47: 785–798, 2006.

43. Muh, E., Zimmermann, J., Kneser, U., Marquardt, J., M.ulhaupt, R., Stark, B. 'Lysineurethanedimethacrylate a novel generation of amino acid based monomers for bone cements and tissue repair', Biomaterials, 23: 2849–2854, 2002.

44. Bonzani, I.C., Adhikari, R., Houshyar, S., Mayadunne, R., Gunatillake, P., Stevens, M.M. 'Synthesis of two-component injectable polyurethanes for bone tissue engineering', Biomaterials, 28: 423-433, 2007.

45. Schwartz, C.J., Bahadur, S. 'Development and testing of a novel joint wear simulator and investigation of the viability of an elastomeric polyurethane for total-joint arthroplasty devices', Wear, 262(3): 331-339, 2007.

46. Gray, J. E., Norton, P. R., Alnouno, R., Marolda, C. L., Valvano, M. A., Griffiths, K. 'Biological efficacy of electroless-deposited silver on plasma activated polyurethane', Biomaterials, 24: 2759-2765, 2003.

47. Jain. P., Pradeep, T. 'Potential of silver nanoparticle-coated polyurethane foam as an antibacterial water filter', Biotechnol. Bioeng., 90: 59-63, 2005.

48. Joyce-Wohrmann, R.M., Hentschel, T., Münstedt, H. 'Thermoplastic silver-filled polyurethanes for antimicrobial catheters', Advanced Engineering Materials 2 (6): 380-386, 2000.

49. Kamışoğlu, K., Aksoy, E.A., Akata, B., Hasirci, N., Bac, N. 'Preparation and characterization of antibacterial zeolite - polyurethane composites', J.Appl. Polym. Sci., (article in press).

50. Ozdemir, Y., Hasirci, N. 'Surface modification of polyurethane membranes', Tech. Health Care, 10 (4): 316-319, 2002.

51. Sefton, M.V., Gemmell, C.H., Gorbet, M.B. 'What really is blood compatibility?' J. Biomater. Sci. Polymer Edn., 11(11): 1165–1182, 2000.

52. Kayirhan, N., Denizli, A., Hasirci, N. 'Adsorption of blood proteins on glow-discharge modified polyurethane membranes', J. Appl. Polym. Sci., 81: 1322-1332, 2001.

53. Brynda, E., Houska, M., Jirouskova, M., Dyr, J.E. 'Albumin and heparin multilayer coatings for blood-contacting medical devices', J. Biomed. Mater. Res., 51: 249-257, 2000.

54. Blomback, B., Hessel, B., Hogg, D., Therkildsen L. 'A two-step fibrinogen-fibrin transition in blood coagulation', Nature, 275: 501-515, 1978.

55. Gorbet, M. B., Sefton, M.V., 'Biomaterial-associated thrombosis: roles of coagulation factors, complement, platelets and leukocytes, Review', Biomaterials, 25: 5681–5703, 2004.

56. Rattray, A., Black, R.A., Rhodes, N.P. 'Platelet microparticle populations in whole blood exposed to laminar and turbulent flow in vitro', Int. J. Artif. Organs**,** 22 (6)**:** 455, 1999.

57. Brash, J. L. 'Role of plasma protein adsorption in the response of blood to foreign surfaces' in Blood Compatible Materials and Devices, Sharma C. P. et al. eds, Technomic, Lancaster, 3-24, 1991.

58. Vitte, J., Benoliel, A. M, Pierres, A., Bongrand, P. 'Is there a predictable relationship between surface physical-chemical properties and cell behaviour at the interface?', European Cells and Materials, 7: 52 – 63, 2004.

59. Andrade, J.D., Hlady, V. 'Plasma protein adsorption: The Big Twelvea' Annals of the New York Academy of Sciences, 516: 158, 1987.

60. Dockal, M., Carter, D.C., Ruker, F. 'The three recombinant domains of human serum albumin structural characterization and ligand binding properties', J. Biol. Chem., 274 (41): 29303–29310, 1999.

61. Wu, Y., Simonovsky, F.I., Ratner, B.D., Horbett, T.A. 'The role of adsorbed fibrinogen in platelet adhesion to polyurethane surfaces: A comparison of surface hydrophobicity, protein adsorption, monoclonal antibody binding, and platelet adhesion', J. Biomed. Mater. Res., 74A: 722–738, 2005.

62. Tzoneva, R., Groht, T., Altankov, G., Paul, D., 'Remodeling of fibrinogen by endothelial cells in dependence on fibronectin matrix assembely', J. Mater. Sci-Mater. M., 13: 1235-1244, 2002.

63. Harker, L.A., Hunt, P., Marzec, U.M., Kelly, A.B., Tomer, A., Hanson, S.R., Stead, R.B. 'Regulation of platelet production and function by megakaryocyte growth and development factor in nonhuman primates', Blood, 87 (5): 1833, 1996.

64. Grunkemeier, J.M., Tsai, W.B., McFarland, C.D., Horbett, T.A. 'The effect of adsorbed fibrinogen, fibronectin, von Willebrand factor and vitronectin on the procoagulant state of adherent platelets', Biomaterials, 21: 2243-2252, 2000.

65. Browne, M.M., Lubarsky, G.V., Davidson, M.R., Bradley, R.H. 'Protein adsorption onto polystyrene surfaces studied by XPS and AFM', Surf. Sci., 553: 155–167, 2004.

66. Sethuraman, A., Han, M., Kane, R. S., Belfort, G. 'Effect of surface wettability on the adhesion of proteins', Langmuir, 20: 7779-7788, 2004.

67. Kasemo, B. 'Biological surface science', Surf. Sci., 500: 656–677, 2002.

68. Holland, N.B., Marchant, R.E. 'Individual plasma proteins detected on rough biomaterials by phase imaging AFM', J. Biomed. Mater. Res., 51: 307–315, 2000.

69. Bae, J.S., Seo, E.J., Kang, I.K. 'Synthesis and characterization of heparinized polyurethanes using plasma glow discharge', Biomaterials, 20: 529- 537, 1999.

70. Michanetzis, G.P.A., Katsala, N., Missirlis, Y.F. 'Comparison of haemocompatibility improvement of four polymeric biomaterials by two heparinization techniques', Biomaterials, 24: 677–688, 2003.

71. Sigma Aldrich Product Information, 'Heparin Certificate; Heparin Sodium from Porcine Intestinal Mucosa', 1-4, 1996, USA.

72. Hirsh, J., Warkentin, T.E., Shaughnessy, S.G., Anand, S.S., Halperin, J.L., Raschke, R., Granger, C., Ohman, E.M., Dalen, J.E. 'Heparin and low molecular weight heparin mechanism of action, pharmacokinetics, dosing, monitoring, efficacy and safety', Chest, 119: 64-94, 2001.

73. Hirsh; J. 'Low molecular weight heparin for the treatment of venuos thromboembolism', Am. Heart. J., 135: 336-342, 1998.

74. Young, E., Venner, T., Ribau, J., Shaughnessy, S., Hirsh, J., Podor, T.J. 'The binding of unfractionated heparin and low molecular weight heparin to thrombin-activated human endothelial cells', Thromb. Res., 96: 373-381, 1999.

75. Serra, A., Esteve, J., Reventer, J.C., Lozano, M., Escolar, G., Ordinas, A. 'Differential effect of a low molecular weight heparin and unfractionated heparin on platelet interaction with the subendothelium under flow conditions', Thromb. Res., 87: 405-410, 1997.

76. Yeager, B.F., Pharm, D., Matheny, S.C. 'Low molecular weight heparin in outpatient treatment of DVT', Am. Fam. Physician, 59 (4): 1999.

77. Ito,Y., Sisido, M., Imanishi, Y. 'Synthesis and antithrombogenicity of polyetherurethaneureas containing quaternary ammonium groups in the side chains and the polymer/heparin complex'. J. Biomed. Mater. Res., 20:1017-1033, 1986.

78. Barbucci, R., Casini, G., Ferruti, P. 'Surface-grafted heparinizable materials', Polymer, 26:1349-1352, 1985.

79. Albanese, A., Barbucci, R., Belleville, J. 'In vitro biocompatibility evaluation of a heparinizable material based on polyurethane and poly(amido-amine) components', Biomaterials, 15:129-136, 1994.

80. Lin, W.C., Tseng, C.H., Yang, M.C. 'In-Vitro haemocompatibility evaluation of a thermoplastic polyurethane membrane with surface-immobilized water-soluble chitosan and heparin', Macromol. Biosci., 5: 1013–1021, 2005.

81. Kang, I.K., Kwon, O.H., Byun, KH. 'Surface modification of polyetherurethaneureas and their thrombogenicity', J Mater. Sci-Mater. M., 7: 135-140, 1996.

82. Kang, I.K, Kwon, O.H., Kim, M.K. 'In vitro blood compatibility of functional group-grafted and heparin-immobilized polyurethanes prepared by plasma glow discharge', Biomaterials, 18: 1099-1107, 1997.

83. Aksoy, E.A., Akata, B.A., Bac, N., Hasirci, N. 'Preparation and characterization of zeolite beta-polyurethane composite membranes', J. Appl. Polym. Sci., 104: 3378-3387, 2007.

84. Ozdemir, Y., Serbetci, K., Hasirci, N. 'Oxygen plasma modification of polyurethane membranes', J. Mat. Sci-Mater. M. 13: 1147-1152, 2002.

85. Ulubayram, K., Hasirci, N. 'Polyurethanes: effect of chemical composition on mechanical properties and oxygen permeability', Polymer, 33 (10): 2084-2088, 1992.

86. Hasirci, N., Aksoy, E.A. 'Synthesis and modifications of polyurethanes for biomedical purposes', High Perform. Polym., 19: 621-639, 2007.

87. Macomber, R.S. 'A Complete Introduction to Modern NMR Spectroscopy, John Wiley & Sons, New York, 283-284, 1998.

88. Su, C.Y., Lin, C.K., Lin, C.R., Lin, C.H. 'Polymerization-like grafting of thermoplastic polyurethane by microwave plasma treatment', Surf. Coat. Tech., 200: 3380-3384, 2006.

89. Yilgor, I., Yilgor, E. 'Hydrophilic polyurethaneurea membranes: influence of soft block composition on the water vapor permeation rates', Polymer, 40: 5575–5581, 1999.

90. Tavares, M.I.B., Mothe´, C.G., Arau´jo C.R. 'Solid-state nuclear magnetic resonance study of polyurethane/natural fibers composites', J. Appl. Polym. Sci., 85: 1465–1468, 2002.

91. Ishida, M., Yoshinaga, K., Horii, F. 'Solid-state 13C NMR analyses of the microphase-separated structure of polyurethane elastomer', Macromolecules, 29: 8824-8829, 1996.

92. Arau´jo, C.R., Pasa, V. M. D. 'Mechanical and thermal properties of polyurethane elastomers based on hydroxyl-terminated polybutadienes and biopitch', J. Appl. Polym. Sci., 88: 759–766, 2003.

93. Liu, H., Zheng, S. 'Polyurethane networks nanoreinforced by polyhedral oligomeric silsesquioxane', Macromol. Rapid. Commun., 26: 196, 2005.

94. Socrates, G. 'Infrared Characteristic Group Frequencies', John Wiley, Chichester, 1994.

95. Das, S., Cox, D.F., Wilkes, G.L., Klinedinst D.B., Yilgor, I, Yilgor, E., Beyer, F.L. 'Effect of symmetry and H-bond strength of hard segments on the structure-property relationships of segmented, non chain extended polyurethanes and polyureas', J. Macromol. Sci. B., 46: 853–875, 2007.

96. Garrett, J.T., Xu, R., Cho, J., Runt, J. 'Phase separation of diamine chain-extended poly(urethane) copolymers: FTIR spectroscopy and phase transitions', Polymer, 44: 2711–2719, 2003.

97. Crawford, D.M., Bass, R.G., Haas, T.W. 'Strain effects on thermal transitions and mechanical properties of thermoplastic polyurethane elastomers', Thermochim. Acta., 323: 53-63, 1998.

98. Crawford, D.M., Escarsega, J.A. 'Dynamic mechanical analysis of novel polyurethane coating for military applications', Thermochim. Acta., 357-358: 161-168, 2000.

99. Yi, J., Boyce, M.C., Lee, G.F., Balizer, E. 'Large deformation rate-dependent stress–strain behavior of polyurea and polyurethanes', Polymer, 47: 319–329, 2006.

100. Chuang, T.H., Yang, T.C.K., Chang, A.H, 'Dynamic mechanical studies of polyurethane composites filled with glass microfillers', Int. J. Polymer. Mater., 53 (5): 465-474, 2004.

101. Thomson, T. 'Polyurethanes as specialty chemicals: principles and applications', CRC Press LLC, Florida, 2005.

102. Ozcan, C., Hasirci, N. 'Evaluation of surface free energy for PMMA films', J. Appl. Polym. Sci., 108: 438–446, 2008.

103. Lopez-Perez, P.M., Marques, A.P., Silva, R.M.P, Pashkulevaab, I., Reis, R.L. 'Effect of chitosan membrane surface modification via plasma induced polymerization on the adhesion of osteoblast-like cells', J. Mater. Chem., 17: 4064–4071, 2007.

104. Ostuni, E., Chapman, R.G., Holmlin, R.E., Takayama, S., Whitesides, G.M. 'A survey of structure-property relationships of surfaces that resist the adsorption of protein', Langmuir, 17: 5605-5620, 2001.

105. Chen, Z., Zhang, R., Kodoma, M., Nakaya, T. 'Anticoagulant surface prepared by the heparinization of ionic polyurethane film', J. Appl. Polym. Sci., 76: 382-390, 2000.

106. Moreia, P.L., Wada, M.L.F., Novello, W.P. 'Importance of uniform heparin coating on biopolymers', Artif. Organs, 24 (3): 209-211, 2000.

107. Wang, A., Cao, T., Tang, H., Liang, X., Salley, S.O., Simon, K.Y. 'In vitro haemocompatibility and stability of two types of heparin-immobilized silicone surfaces', Colloid. Surface. B., 43: 245-255, 2005.

108. Du, Y.J., Brash, J.L., McClung, G., Berry, L.R., Klement, P., Chan, A.K.C. 'Protein adsorption on polyurethane catheters modified with a novel antithrombin-heparin covalent complex', J. Biomed. Mater. Res. Part A, 80: 216-225, 2007.

109. Park, K.D., Kim, W.G., Jacobs, H., Okano, T., Kim, S.W. 'Blood compatibility of SPUU-PEO-heparin graft copolymers', J. Biomed. Mater. Res., 26: 739-756, 1992.

110. Knetsch, M.L.W., Aldenhoff, Y.B.J., Koole, L.H. ‘The effect of high-density-lipoprotein on thrombus formation on and endothelial cell attachment to biomaterial surfaces’, Biomaterials, 27: 2813–2819, 2006.

111. Motta, A., Migliaresi, C., Lloyd, A.W., Denyer, S.P., Santin, M. ’Serum protein adsorption on silk fibroin fibers and films: surface optimization and binding strength’, J. Bioact. Compat. Pol., 17: 23-34, 2002.

112. Goodman, S.L. ‘Sheep, pig, and human platelet-material interactions with model cardiovascular biomaterials’, J. Biomed. Mater. Res., 32: 249-258, 1999.

113. Application Note No 108, ‘Surface Free Energy – Background, Calculation and Examples by Using Contact Angle Measurements’ KSV Instruments, Ltd, USA.

114. Rankl, M., Laib, S., Seeger, S. ‘Surface tension properties of surface-coatings for application in biodiagnostics determined by contact angle measurements’, Colloid. Surface. B., 30: 177-186, 2003.

115. Cantin, S., Bouteau, M., Benhabib, F., Perrot, F. ‘Surface free energy evaluation of well-ordered Langmuir–Blodgett surfaces comparison of different approaches’, Colloid. Surface. A., 276: 107–115, 2006.

APPENDIX A

GPC DISTRIBUTION PLOTS

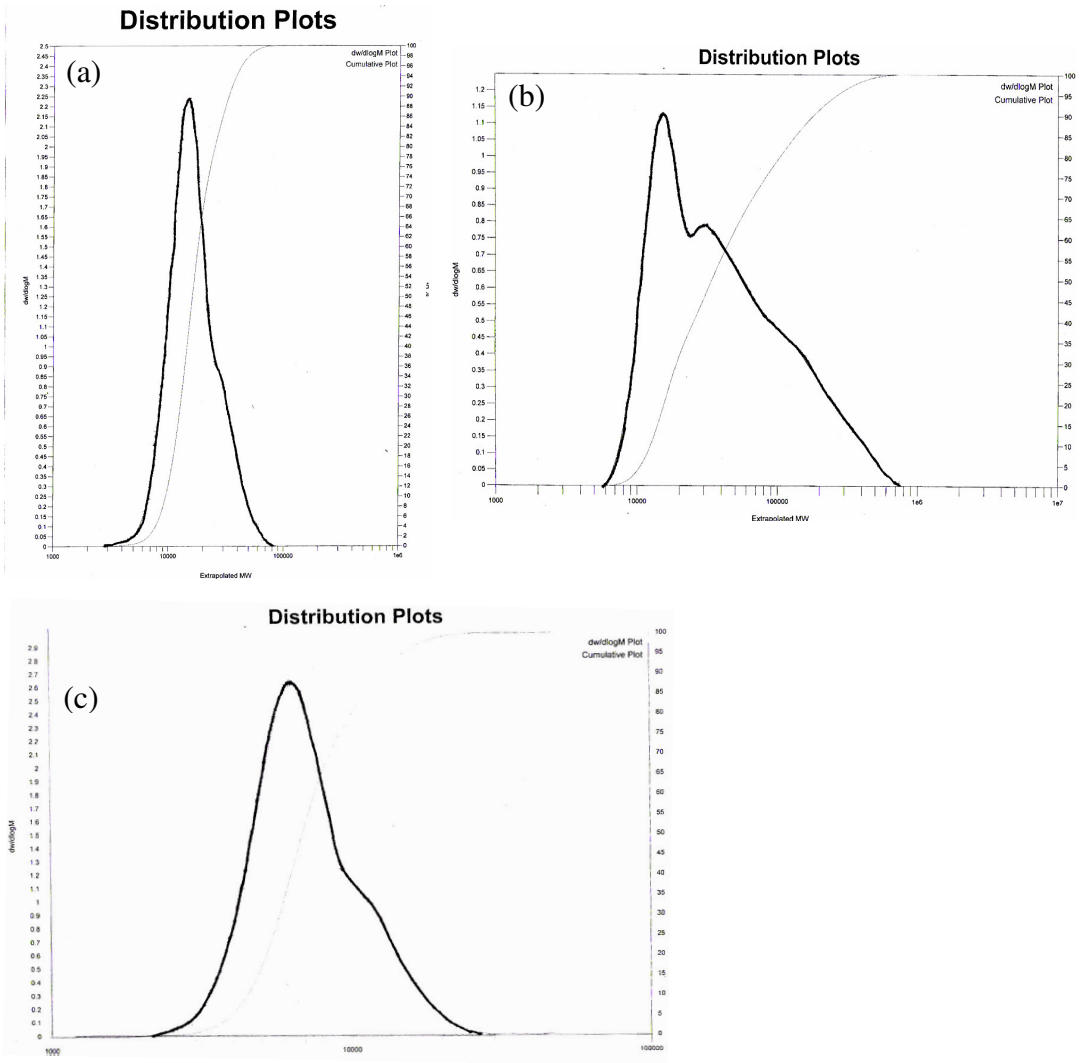

Figure 62 GPC molecular weight distribution plots of 8PU prepolymer (a) 6 h cured, (b) 12 h cured, (c) 18 h cured.

APPENDIX B

DMA CURVES OF PU FILMS

A.1 Storage Modulus Graphs of PU Films at Different Frequencies

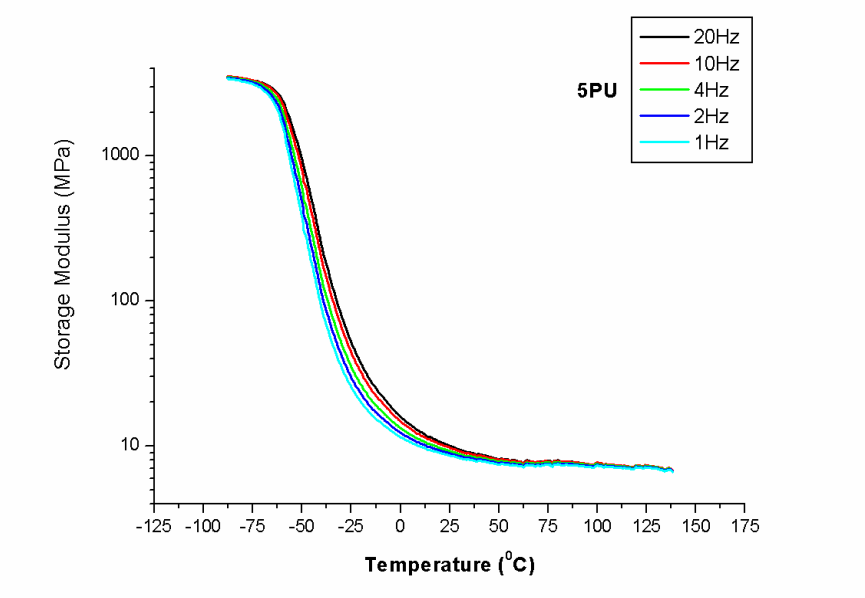

Figure 63 Storage modulus versus temperature curve of 5PU sample.

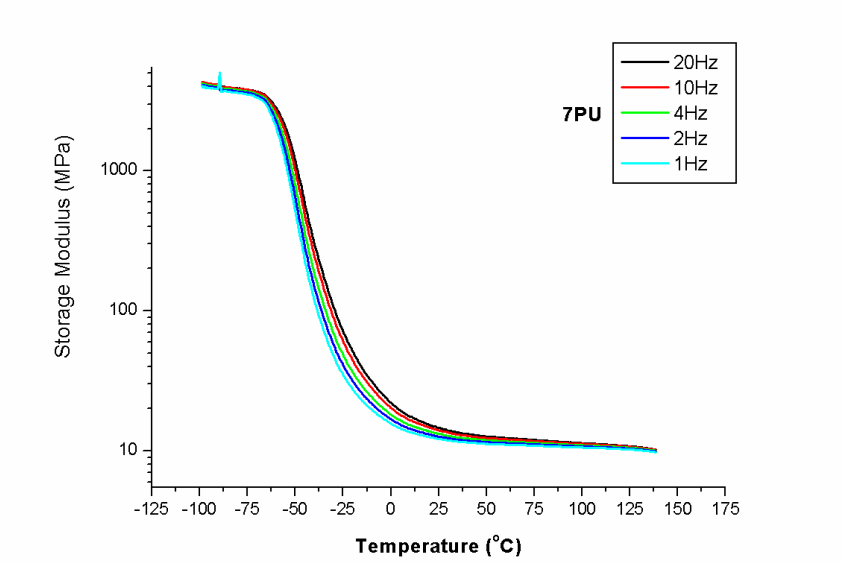

Figure 64 Storage modulus versus temperature curve of 7PU sample

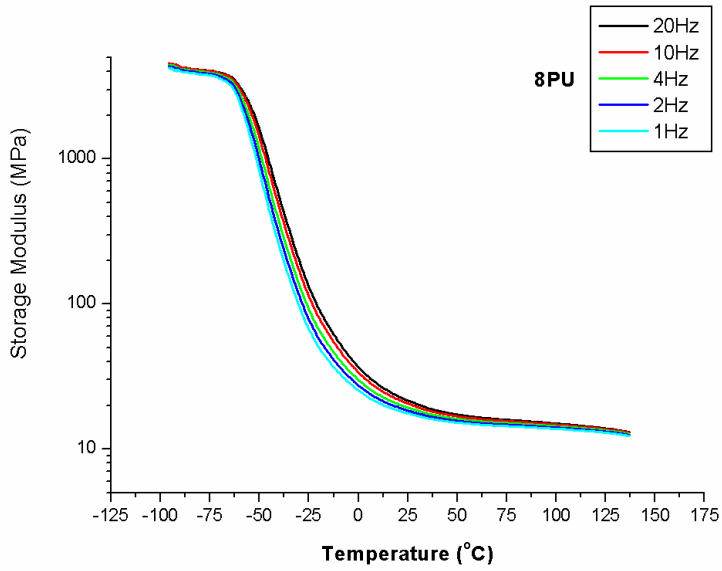

Figure 65 Storage modulus versus temperature curve of 8PU sample.

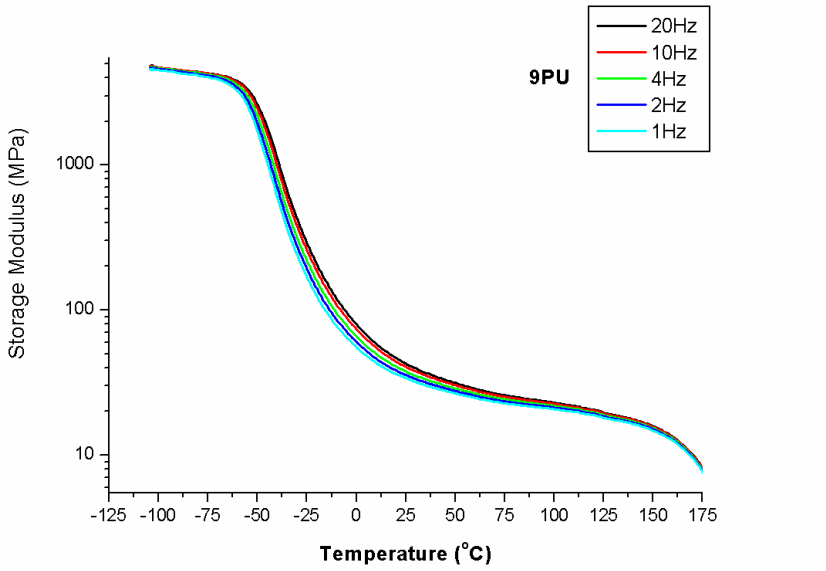

Figure 66 Storage modulus versus temperature curve of 9PU sample.

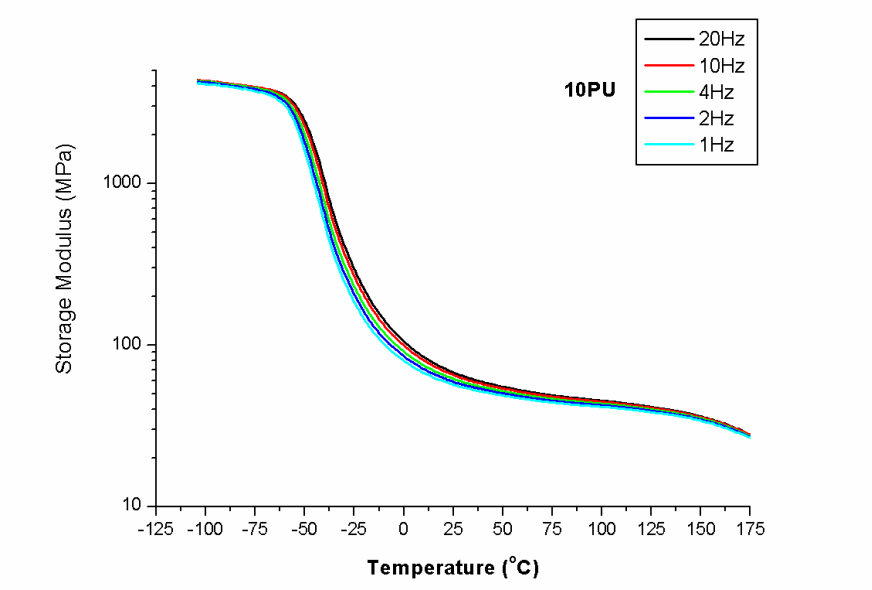

Figure 67 Storage modulus versus temperature curve of 10PU sample.

A.2 Loss Modulus Graphs of PU Films at Different Frequencies

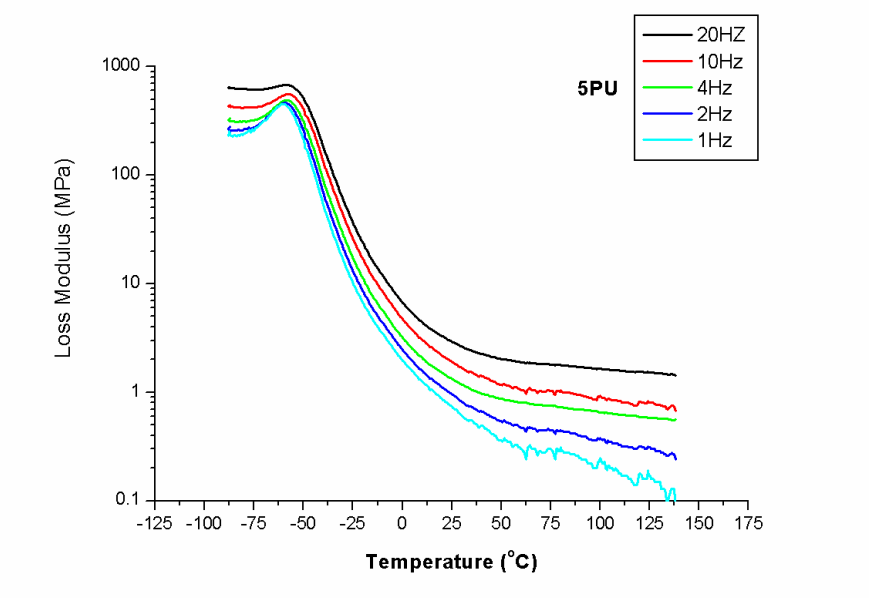

Figure 68 Loss modulus versus temperature curve of 5PU sample.

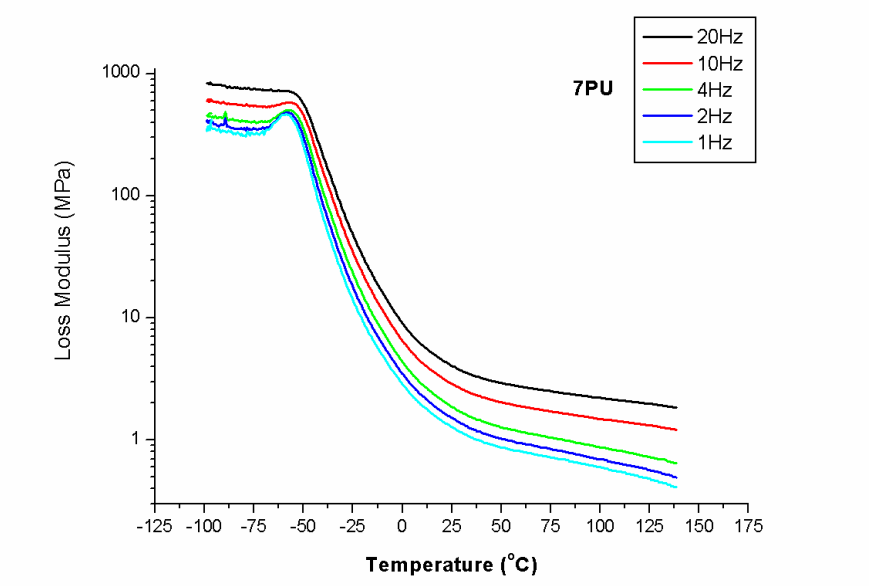

Figure 69 Loss modulus versus temperature curve of 7PU sample.

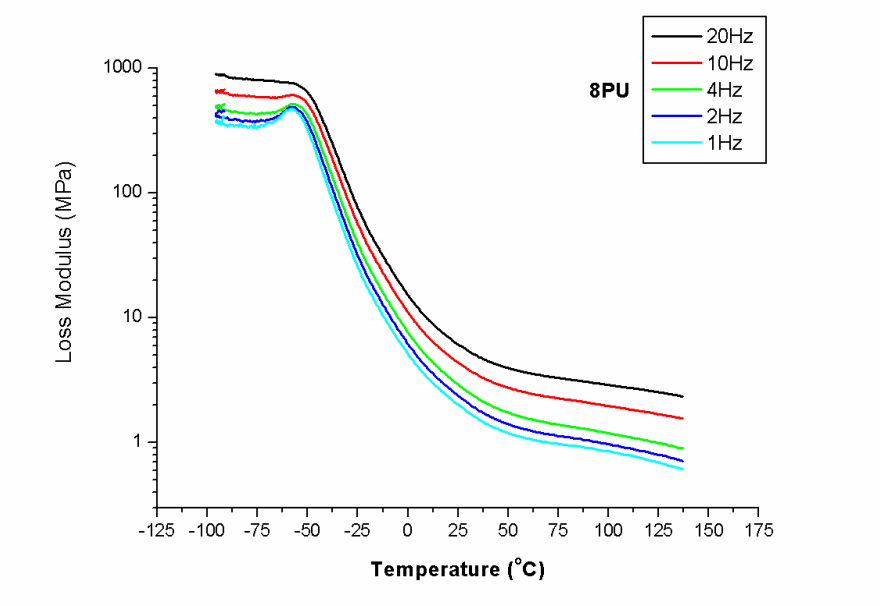

Figure 70 Loss modulus versus temperature curve of 8PU sample.

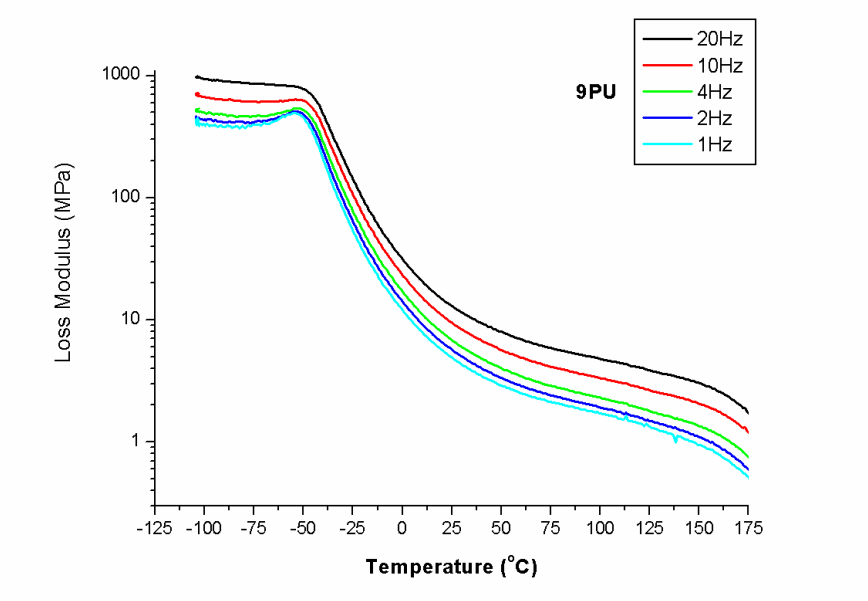

Figure 71 Loss modulus versus temperature curve of 9PU sample.

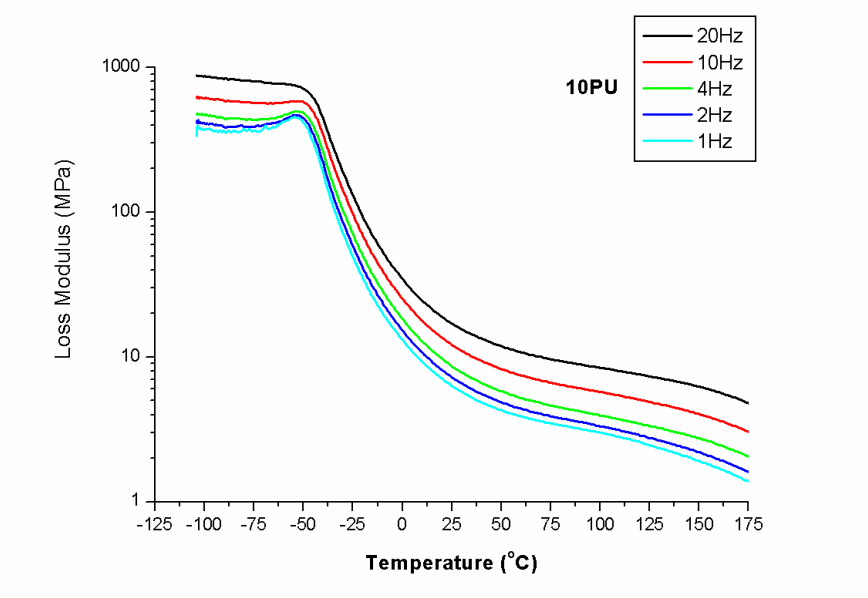

Figure 72 Loss modulus versus temperature curve of 10PU sample.

A.3 Tan Delta Graphs of PU Films at Different Frequencies

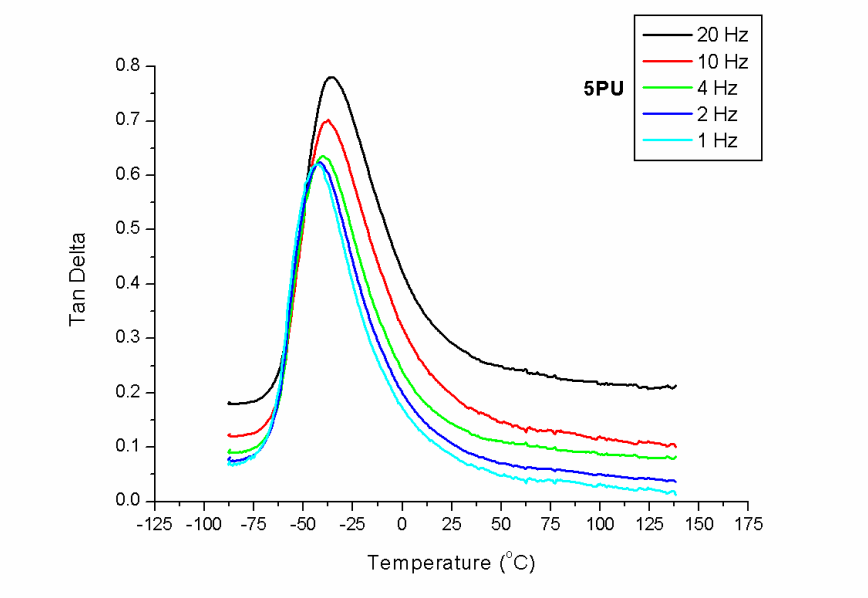

Figure 73 Tan delta versus temperature curve of 5PU sample.

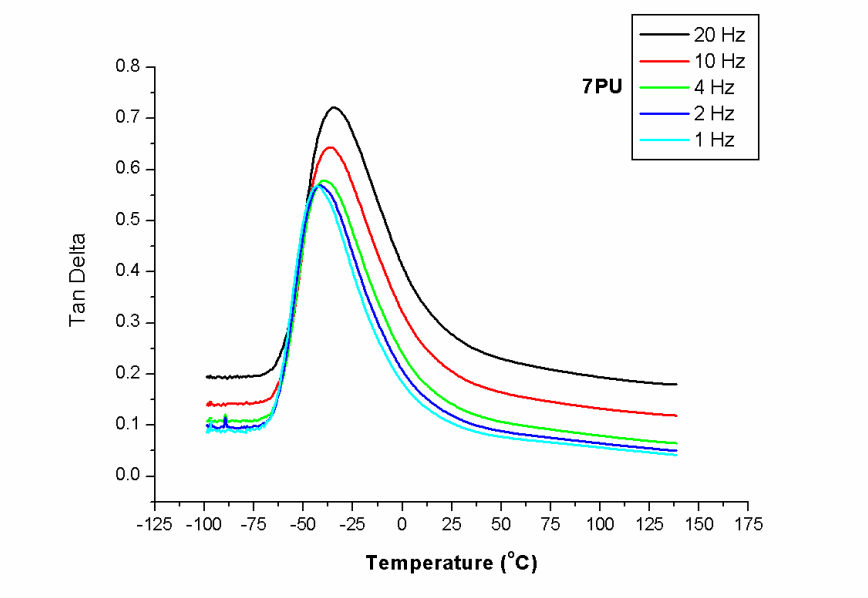

Figure 74 Tan delta versus temperature curve of 7PU sample

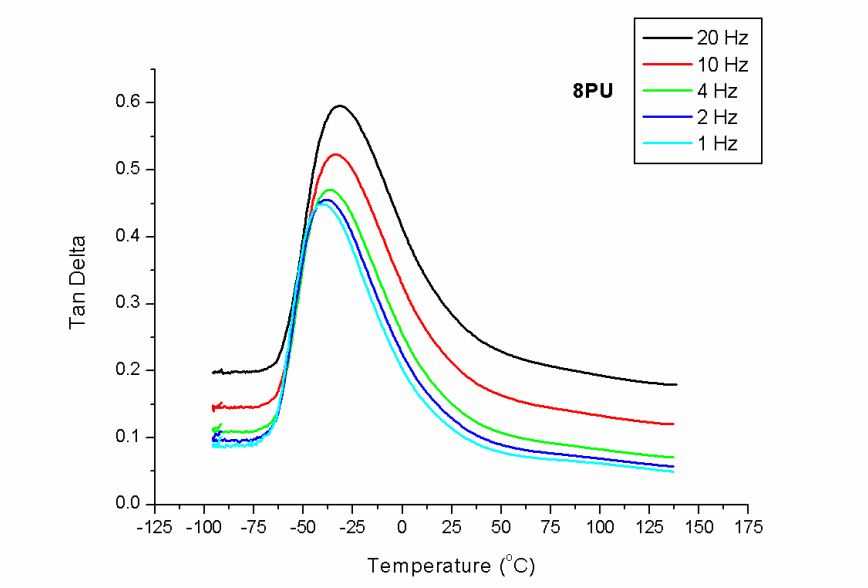

Figure 75 Tan delta versus temperature curve of 8PU sample.

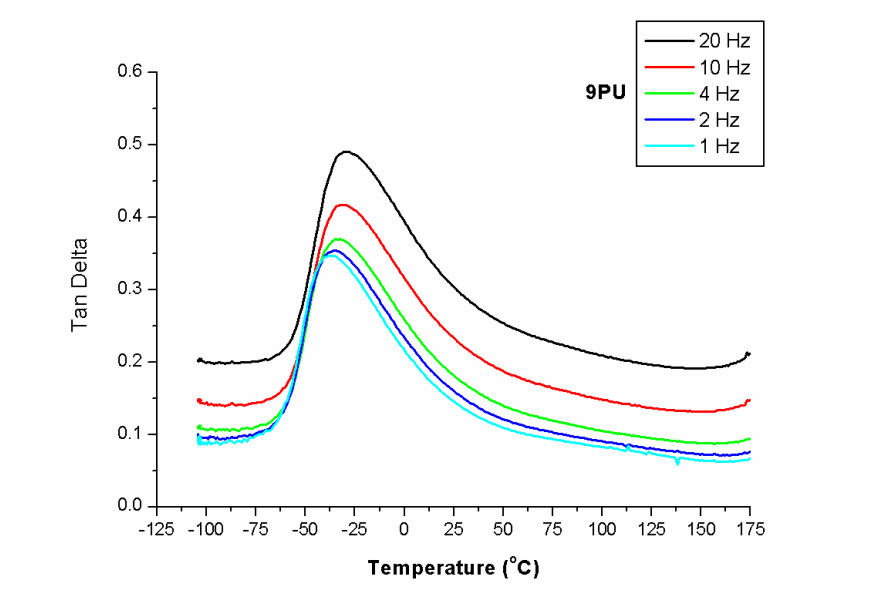

Figure 76 Tan delta versus temperature curve of 9PU sample.

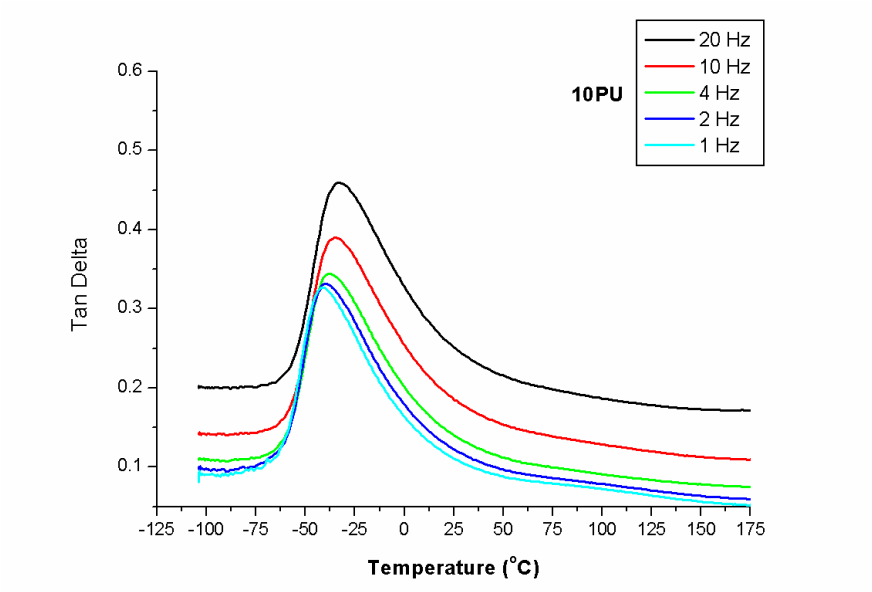

Figure 77 Tan delta versus temperature curve of 10PU sample.

Table 21 Tg values of all PU samples at different frequencies.

	Samples				
Frequency	5PU	7PU	8PU	9PU	10PU
1Hz	-43.08°C	-42.63°C	-40.94°C	-38.14°C	-41.63°C
2Hz	-41.58°C	-40.74°C	-38.73°C	-36.48°C	-39.31°C
4Hz	-39.96°C	-38.73°C	-36.9°C	-34.5°C	-37.17°C
10Hz	-37.49°C	-35.48°C	-33.27°C	-32.64°C	-34.25°C
20Hz	-35.65°C	-33.27°C	-31.19°C	-29.63°C	-32.04°C

APPENDIX C

TGA CURVES AND FIRST DERIVATIVES OF PU FILMS

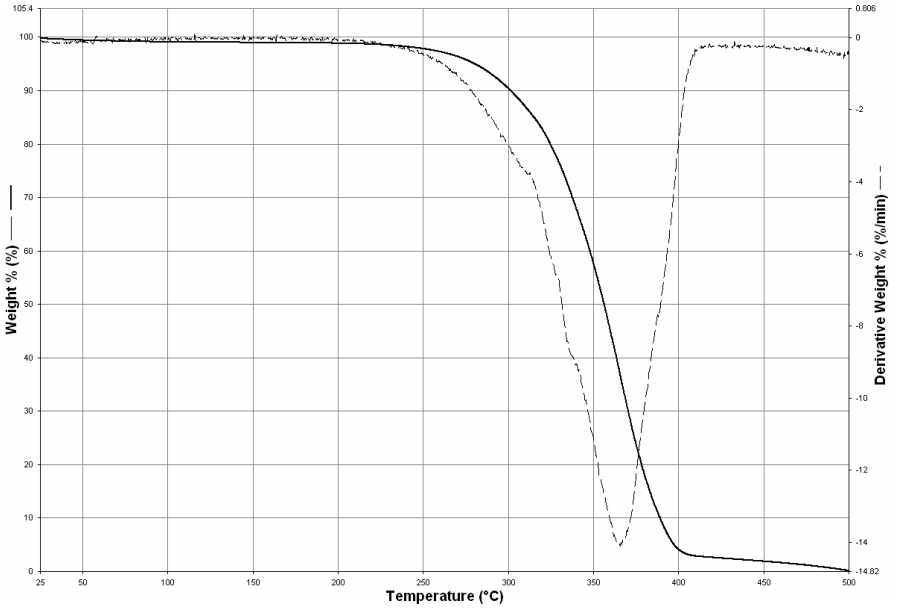

Figure 78 TGA curve of 5PU sample.

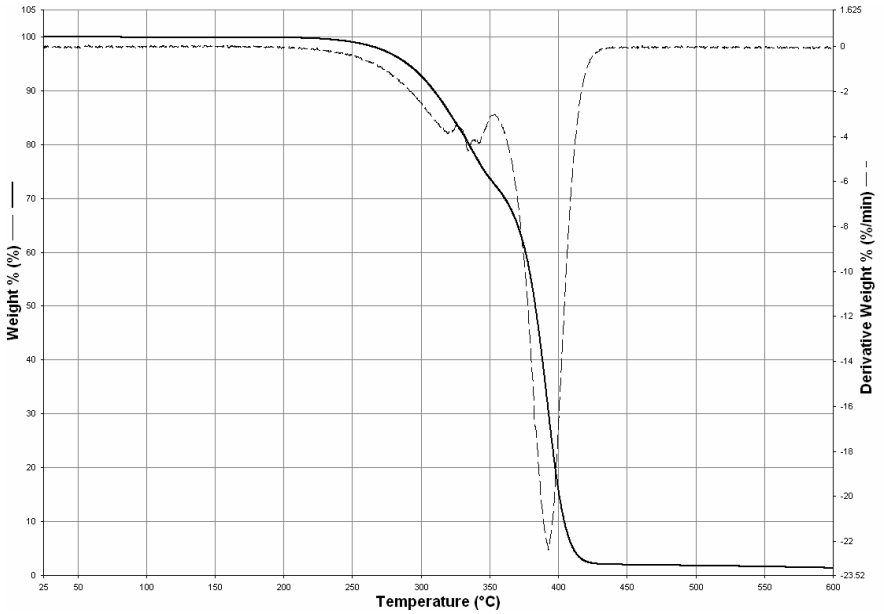

Figure 79 TGA curve of 8PU sample.

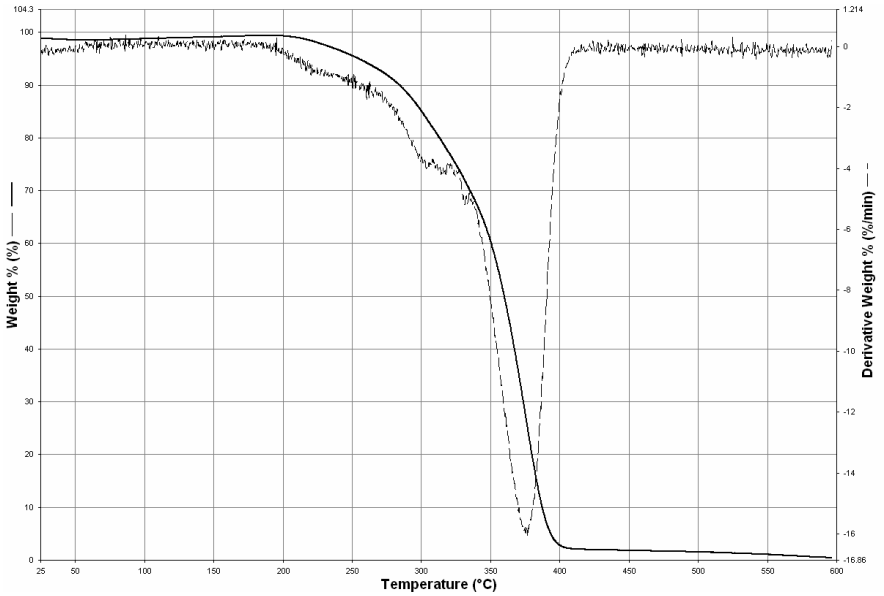

Figure 80 TGA curve of 10PU sample.

APPENDIX D

SURFACE FREE ENERGY CALCULATIONS

D.1 Surface Free Energy Formulas

Contact angle, is a quantitative measure of the wetting of a solid by a liquid. It is defined geometrically as the angle formed by a liquid at the three phase boundary where a liquid, gas and solid intersect is shown in Figure 81. In this figure vector A shows γsl, which is the interfacial tension between solid and liquid, vector B shows γlv, which is the interfacial tension between liquid and vapor and vector C shows γsv, which is the interfacial tension between solid and vapor.

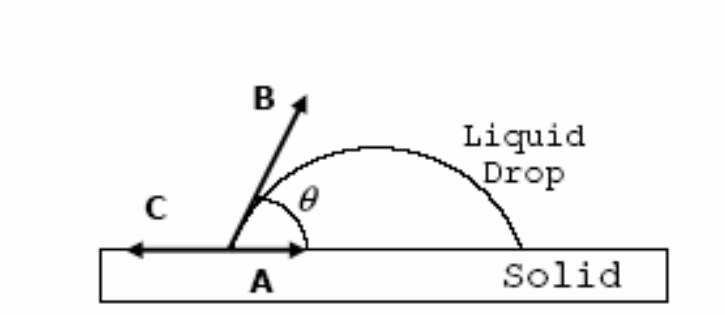

Figure 81 SFE vectors at equilibrium and contact angle.

If water drops are used, contact angle values give information about the hydrophilicity and hydrophobicity of the solid surface.

Surface Free Energy (SFE) has polar (γs^p) and dispersive (γs^d) components which give information about the polar or apolar character of the surface. Their summation givethe total SFE (γs^{Tot}) as shown:

$$\gamma s^{Tot} = \gamma s^p + \gamma s^d \quad \text{.....(D.1)}$$

In addition these polar constituents also have acidic and basic components which give more detailed information about the character of the surface. Different approaches are used for determining the energy of solid substrates.

Zisman Approach: Zisman plot, is build where the surface tension of the test liquids is plotted on the X-axis, and the cosine of the corresponding contact angle on the Y-axis. The extrapolation of the cos θ vs γ curve to cos θ = 1 (corresponding to the zero contact angle, or the complete wetting limit) gives the value of the critical surface energy of the material tested. A series of homologous nonpolar liquids of differing surface tensions a graph of cosθ vs γ is produced (Figure 82) [113].

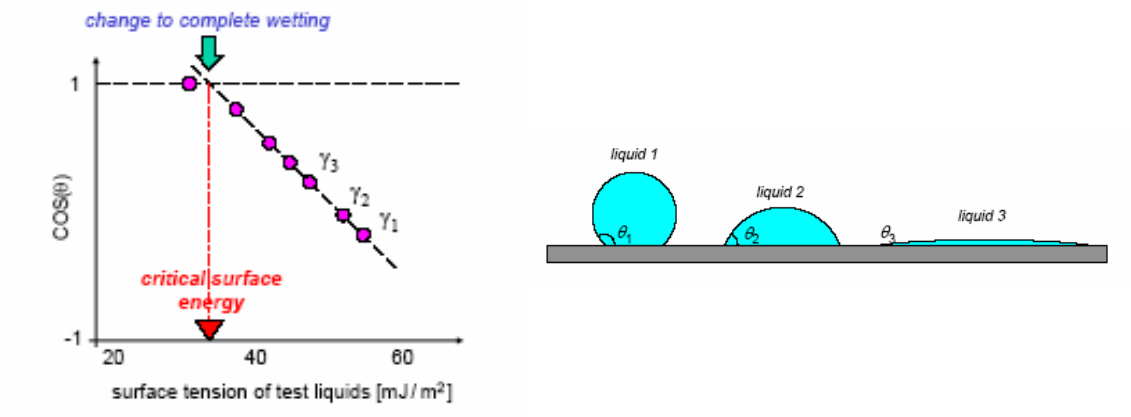

Figure 82 Determination of the critical surface energy of solids.

Geometric Mean (OWRK) Approach: This approach divides the surface energy into two components, dispersive and polar, and uses a geometric mean approach to combine their contributions. The resulting equation when combined with Young's equation yields (Fowkes approach) [113-115]:

$$\gamma_l (1+ \cos\theta) = 2[(\gamma_l^p \gamma_s^p)^{1/2} + (\gamma_l^d \gamma_s^d)^{1/2}] \quad \text{.....(D.2)}$$

This equation was rearranged as by Owens and Wendt to yield:

$$\gamma_l (1+ \cos\theta) / (\gamma_l^d)^{1/2} = (\gamma_s^p)^{1/2} [(\gamma_l^p)^{1/2}/(\gamma_l^d)^{1/2}] + (\gamma_s^d)^{1/2} \quad \text{.....(D.3)}$$

where θ is the contact angle, γ_l is liquid surface tension and γ_s is the solid surface tension, or free energy. The addition of d and p in the superscripts refer to the dispersive and polar components of each.

The form of the equation is of the type y = mx + b. The graph $(\gamma_l^p)^{1/2}/(\gamma_l^d)^{1/2}$ versus $(1/2)\gamma_l (1+ \cos\theta) / (\gamma_l^d)^{1/2}$ is plotted. The slope is $(\gamma_s^p)^{1/2}$ and the y-intercept is $(\gamma_s^d)^{1/2}$. The total free surface energy is merely the sum of its two component forces [113, 115].

Harmonic Mean (Wu) Approach: This method utilizes a similar approach but uses a harmonic mean equation to sum the dispersive and polar contributions. Contact angles against two liquids with known values of γ^d and γ^p are measured. The values for each experiment are put into the following equation;

$$(1 + \cos\theta)\gamma_l = 4(\gamma_l^d \gamma_s^d / \gamma_l^d + \gamma_s^d + \gamma_l^p \gamma_s^p / \gamma_l^p + \gamma_s^p) \quad \text{.....(D.4)}$$

where γ refers to surface tension (surface free energy), the subscripts l and s refer to liquid and solid, and the superscripts d and p refer to dispersive and polar components. The two equations with two unknowns and are solved for γ_s^d and γ_s^p .Total surface energy and surface energy components derived using the harmonic mean equation [113-115].

Acid-Base Approach: Contact angles against at least three liquids with known values of γd, γ+ and γ- are measured. The values for each experiment are put into the following equation:

$$0.5(1 + \cos\theta)\gamma_l = (\gamma_s^{LW} \gamma_l^{LW})^{1/2} + (\gamma_s^{-} \gamma_l^{+})^{1/2} + (\gamma_s^{+} \gamma_l^{-})^{1/2} \quad \text{(D.5)}$$

where γ refers to surface tension (surface free energy), the subscripts l and s refer to liquid and solid, and the superscripts d, + and - refers to dispersive, acid and base components. The three equations with three unknowns and is solved for γ_s^{d}, γ_s^{+} and γ_s^{-}. The total surface free energy of the solid is then given by [113-115]:

$$\gamma_s = \gamma_s^{LW} + \gamma_s^{AB}, \text{ where } \gamma_s^{AB} = 2(\gamma_s^{+} \gamma_s^{-})^{1/2} \quad \text{(D.6)}$$

Total surface energy, its dispersive and polar components, as well as the acid and base adhesion parameters are obtained.

D.2 Acidic, Basic Components of Test Liquids

Table 22 Surface tension parameters (acidic and basic components) of test liquids.

	Total SFE	Lifshitz–Van der Waals component SFE	Acid-Base intreaction	Acidic component SFE	Basic component SFE
Liquid	γ_L (mJ/m^2)	γ_L^{LW} (mJ/m^2)	γ_L^{AB} (mJ/m^2)	γ_L^{+} (mJ/m^2)	γ_L^{-} (mJ/m^2)
Water	72.8	21.8	51	25.5	25.5
Formamide	58.00	39	19	2.28	39.6
Bromonaphtalene	44.4	44.4	0.00	0.00	0.00
Dimethyl sulfoxide	44	36	8	0.5	32

The data is obtained from literature [114-115].

D.3 Dispersive, Polar Components Test Liquids

Table 23 Surface tension parameters (dispersive and polar components) of test liquids.

	Total SFE	Dispersive component SFE	Polar component SFE
Liquid	γ_L (mJ/m^2)	γ_L^{d} (mJ/m^2)	γ_L^{p} (mJ/m^2)
Water	72.80	21.8	51
Formamide	58.2	39.5	18.7
Bromonaphtalene	44.4	44.0	0
Dimethyl sulfoxide	44	36	8

The data is obtained from literature [114-115].

D.4 Manual SFE Calculations using OWRK Geometric Mean Approach:

PU sample

Slope $=(\gamma_s^p)^{1/2} = 2.2258$, $\gamma_s^p = 4.95$

Y-intercept $= (\gamma_s^d)^{1/2} = 6.2638$, $\gamma_s^d = 39.235$

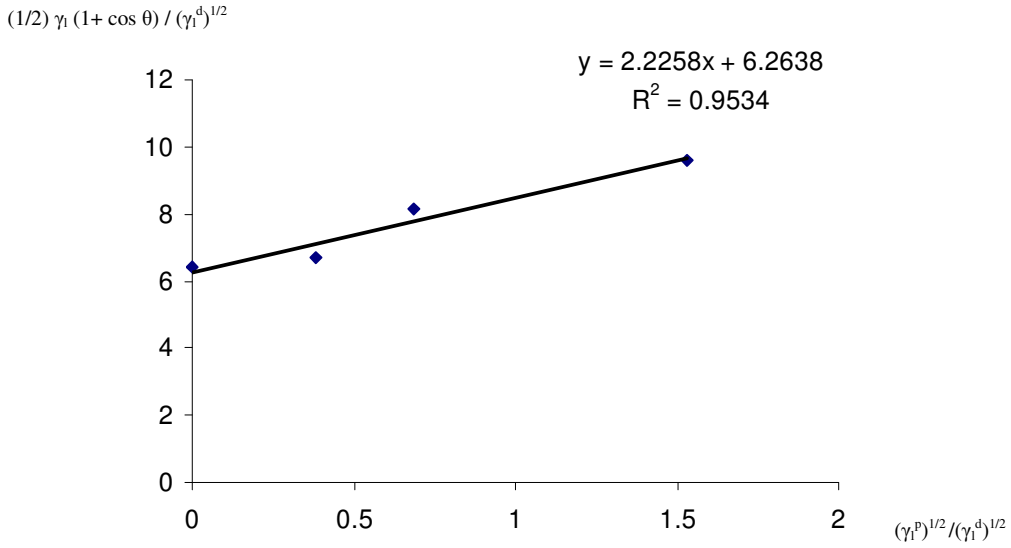

Figure 83 Fits of contact angle data of 8PU sample using OWRK approach.

PU-LMWH sample

Slope $=(\gamma_s^p)^{1/2} = 5.584$, $\gamma_s^p = 31.18$

Y-intercept $= (\gamma_s^d)^{1/2} = 5.1057$, $\gamma_s^d = 26.067$

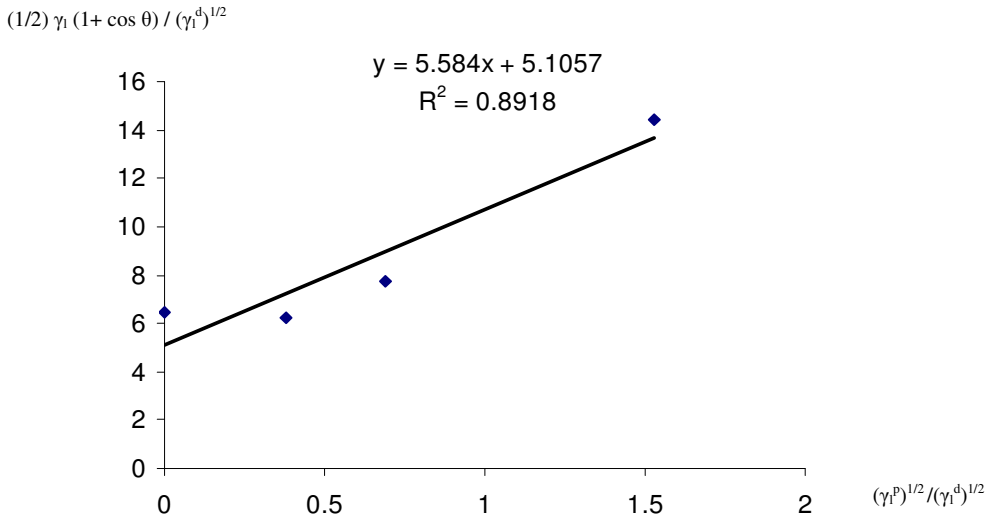

Figure 84 Fits of contact angle data of PU-LMWH sample using OWRK approach.

PU-UFH sample

Slope $=(\gamma_s^p)^{1/2} = 2.2258$, $\gamma_s^p = 4.95$

Y-intercept $= (\gamma_s^d)^{1/2} = 6.2638$, $\gamma_s^d = 39.235$

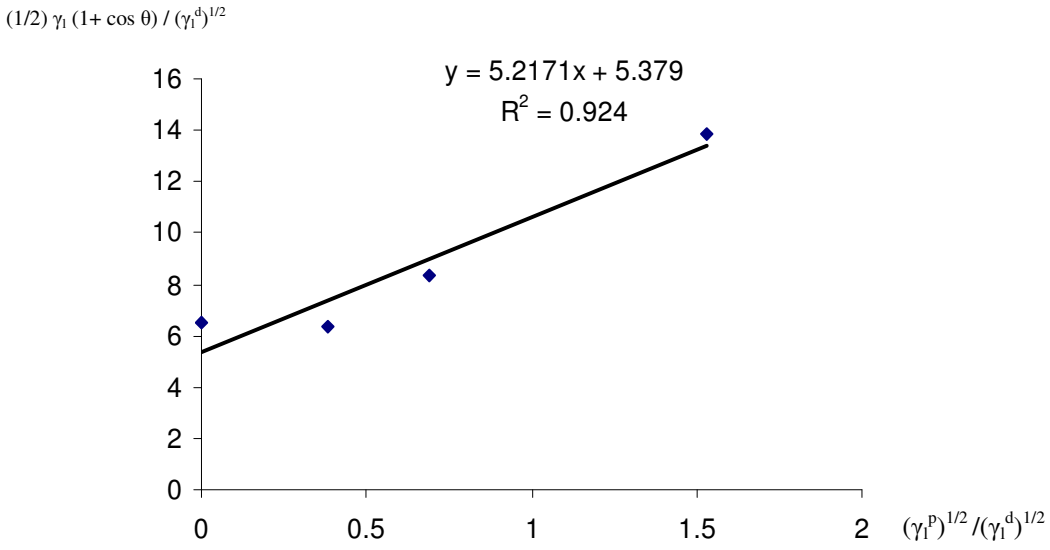

Figure 85 Fits of contact angle data of PU-UFH sample using OWRK approach.

Table 24 Surface free energy and its components calculated by OWRK method manually.

	OWRK Total SFE	OWRK Dispersive component SFE	OWRK Polar component SFE
Sample	γ_s (mN/m)	γ_s^d (mN/m)	γ_s^p (mN/m)
8PU	44.19	39.24	4.95
PU-LMWH	57.25	26.07	31.18
PU-UFH	55.51	28.29	27.22

D.5 Manual SFE Calculations using Acid-Base Approach:

Table 25 Surface free energy and its components calculated by AB method manually.

	Acid Base Total SFE	Acid Base Lifshitz–Van der Waals component SFE	Acid Base Acid-Base intreaction	Acid Base Square root of acidic component SFE	Acid Base Square root of basic component SFE
Sample	γ_s (mN/m)	γ_s^{LW} (mN/m)	γ_s^{AB} (mN/m)	γ_s^+ (mN/m)	γ_s^- (mN/m)
8PU	45.33	40.96	4.37	1.82	2.62
PU-LMWH	51.05	42.04	9.01	0.64	7.04
PU-UFH	47.91	41.92	5.99	0.41	7.32

APPENDIX E

AFM IMAGES OF OXYGEN PLASMA TREATED PU

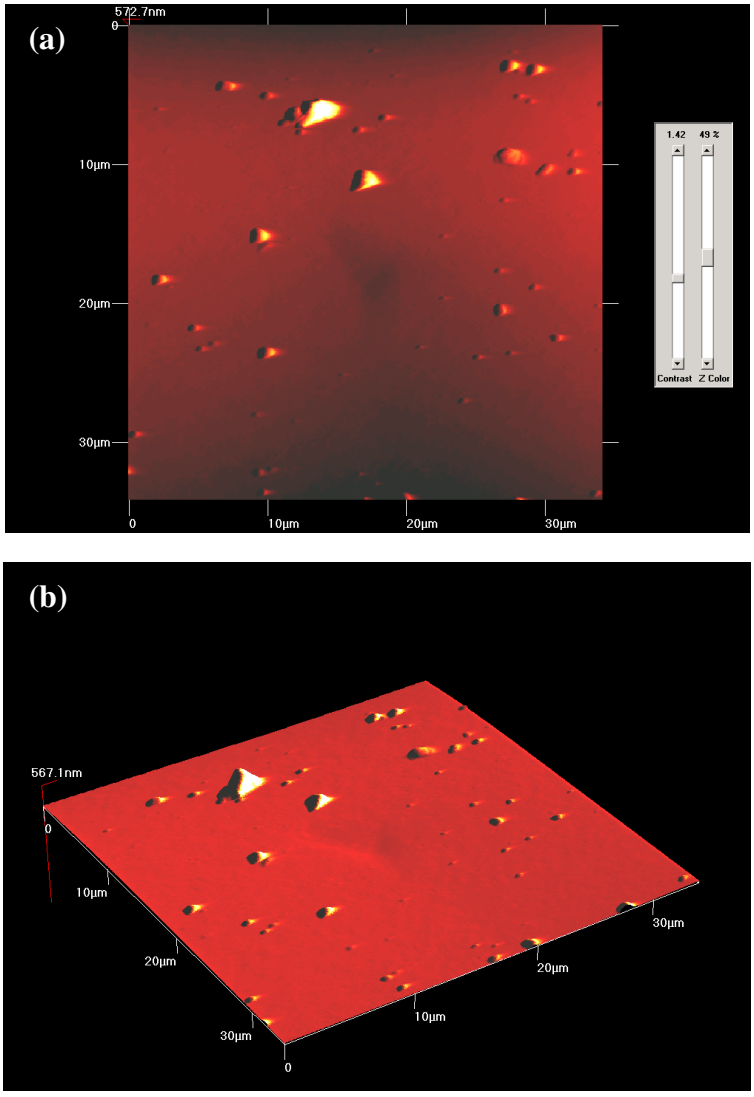

Figure 86 AFM images of oxygen plasma treated PU surface in non-contact mode (a) 2D image (b) 3D image. The scan size 30 µm x 30 µm.

APPENDIX F

ELECTROPHORESIS PROFILE OF CONTACTING PLASMA (PPP)

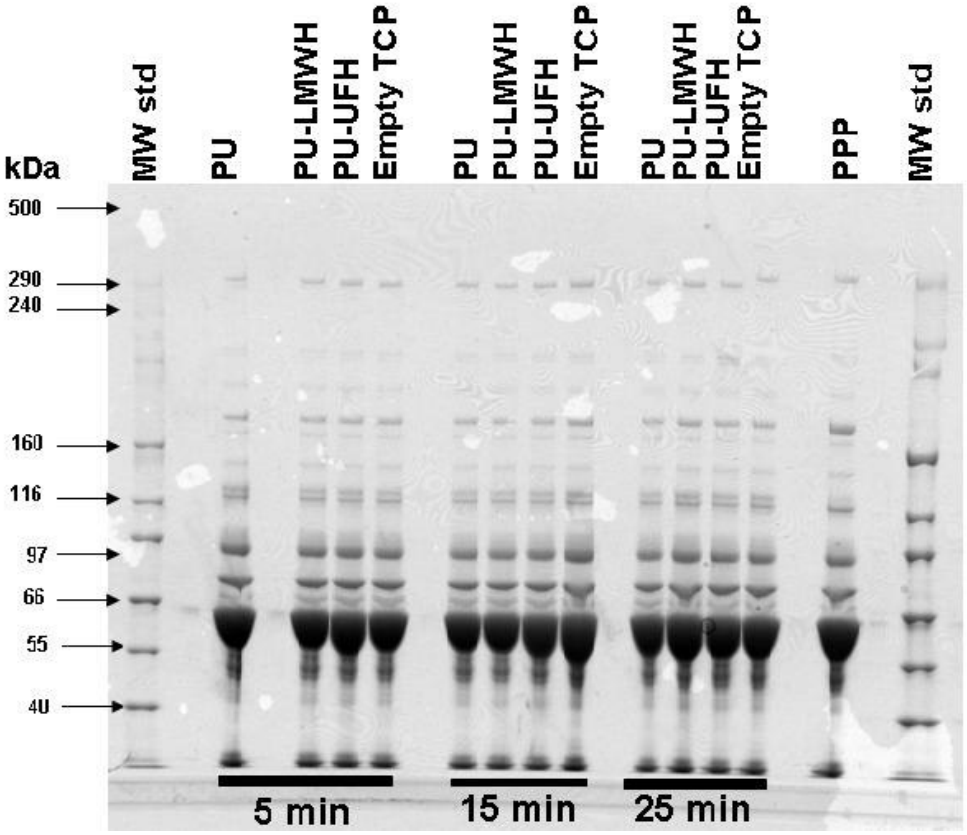

Figure 87 Electrophoresis profile of contacting plasma (PPP).

APPENDIX G

SEM OF SURFACES WITHOUT PRP INCUBATION

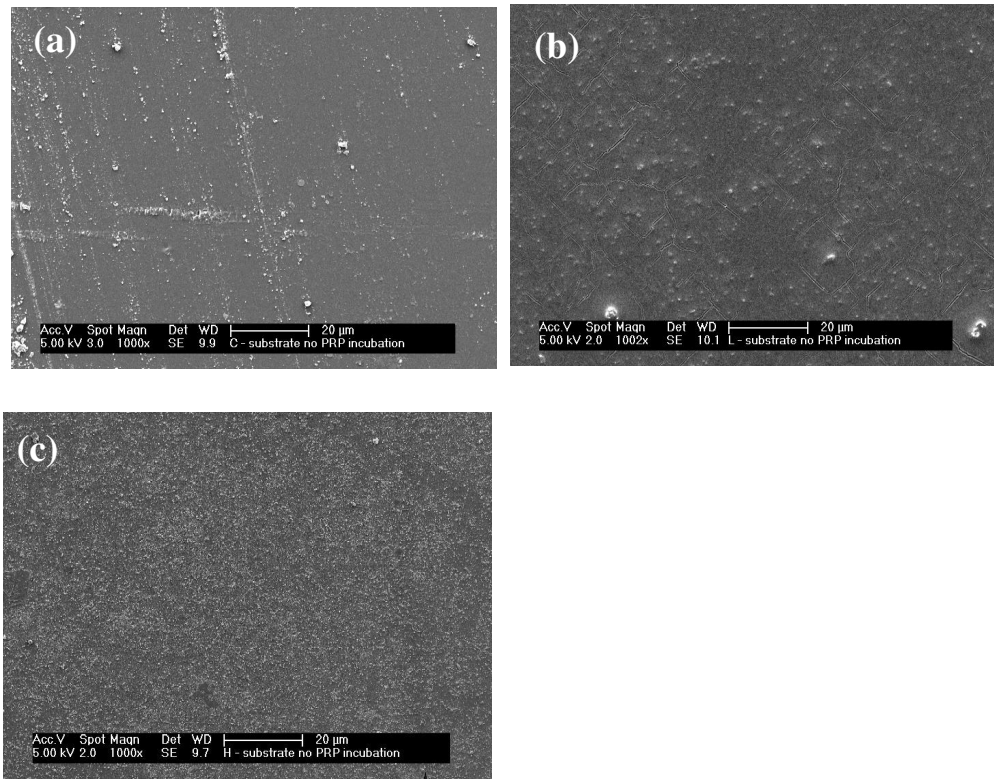

Figure 88 SEM of surfaces without incubation with PRP (a) PU, (b) PU-LMWH, (c) PU-UFH.

CURRICULUM VITAE

PERSONAL INFORMATION

Surname, Name: Aksoy, Eda Ayşe

Nationality: Turkish (T.C.)

Date and Place of Birth: 28 November 1976, Ankara

Marital Status: Single

Phone: +90 312 210 64 40

Fax: +90 312 210 64 25

E-mail: edaayse@metu.edu.tr

EDUCATION

Degree	Institution	Year of Graduation
MS	METU Chemistry Department	2001
BS	Hacettepe University	1998
High School	Yükseliş College	1994

WORK EXPERIENCE

Year	Place	Enrollment
2001-	METU Central Laboratory	Research Associate

FOREIGN LANGUAGES: Advanced English

PUBLICATIONS

1. Aksoy, E.A., Akata, B., Bac, N., Hasirci, N. 'Preparation and Characterization of Zeolite Beta–Polyurethane Composite Membranes', Journal of Applied Polymer Science, 104: 3378–3387, 2007.

2. Hasirci, N., Aksoy, E.A. 'Synthesis and Modifications of Polyurethanes for Biomedical Purposes', High Performance Polymers, 19; 621-637, 2007.

3. Kamışoğlu, K., Aksoy, E.A., Akata, B., Hasirci, N., Bac, N. 'Preparation and Characterization of Antibacterial Zeolite - Polyurethane Composites', Journal of Applied Polymer Science, (article in press).

4. Aksoy, E.A., Hasirci, V., Hasirci, N. 'Surface Modification of Polyurethanes with Covalent Immobilization of Heparin', Macromolecular Symposia, (article in press).

5. Aksoy, E.A., Motta, A., Fedel, M., Migliaresi, C., Hasirci,V., Hasirci, N. 'Plasma Protein Adsorption and Platelet Adhesion on Heparin-Immobilized Polyurethane Films', Journal of Bioactive and Compatible Polymers (article in press).